UNIVERSITY OF CALIFORNIA, SAN DIEGO

Investigation of Substrate Phosphorylation by and Subcellular Localization of SR Protein Kinase 1

A thesis submitted in partial satisfaction of the

requirements for the degree Master of Science

in

Biology

by

Kayla Giang

Committee in charge:

Professor Gourisankar Ghosh, Chair
Professor Joseph Noel, Co-Chair
Professor Maho Niwa

2008

The Thesis of Kayla Giang is approved, and it is acceptable in quality and form for publication on microfilm and electronically:

_____

_____
Co-Chair

_____
Chair

University of California, San Diego

2008

Table of Contents

List of Figures

List of Tables

ACKNOWLEDGEMENTS

I would like to thank my thesis advisor, Prof. Gourisankar Ghosh, for being the best professor.

I also would like to thank Dr. Mukherjee for being a wonderful labmate. She is always a resourceful person for me.

I thank Dr. Ngo for his wonderful mentorship during my undergraduate years.

I thank Dr. Cho and Nhat Huynh for being great team members in Splicing project.

I also would like to thank Dr. Chakrabarti and Dr. Zhong for teaching me Indirect Immunofluorescence and providing me necessary materials to conduct immunofluorescence experiments.

I would like to thank Olga Savinova for her advice and critical comments to my project.

I would like to thank Erika Mathes for teaching me Baculovirus and tissue culture techniques.

I would like to thank the past and current members of the lab for their scientific suggestions and invaluable supports: Jessica Ho, Randy Lukasiewicz, Rashmi Talwar, Amanda Fusco, and Tom Huxford.

Thanks to Kim Huynh, and Eriko Shimada, Dustyn Miller, and Walter Woo for always being my great young friends and keeping the lab lively and fun to work in. Every members of this lab has made a positive contribution to my learning.

Chapter 3 is, in part, a reprint of material as it appears in Molecular Cell, 2008, 29, 563-576, Ngo, J.C., Giang, K., Chakrabarti, S., Ma, C.T., Huynh, N., Hagopian, J.C., Dorrestein, P. C., Fu, X.D., Adams, J.A., and Ghosh, G.. The thesis author was the second author of this publication.

VITA

2006 B. S., University of California, San Diego

2008 M. S., University of California, San Diego

PUBLICATIONS

Cho S, Chakrabarti S, Huynh N, Giang N, Ghosh G. (2008) Multi-site ASF/SF2 RS2 Domain is an Exonic Splicing Enhancer (ESE) Recognition Switch. In Preparation.

Ngo JC, Giang K., Chakrabarti S, Ma C, Huynh N, Hagopian J, Dorrestein P, Fu XD, Adams J, Ghosh G. (2008) A Sliding docking interaction is essential for sequential and processive phosphorylation of an SR protein by SR protein kinase 1. Mol Cell, *29*, 563-76.

Ngo, J. C., Gullingsrud, J., Giang, K., Yeh, M. J., Fu, X. D., Adams, J. A., McCammon, J. A., and Ghosh, G. (2007). SR protein kinase 1 is resilient to inactivation. Structure *15*, 123-133.

ABSTRACT OF THE THESIS

Investigation of Substrate Phosphorylation by and Subcellular Localization of SR Protein Kinase 1

by

Kayla Giang

Master of Science in Biology
University of California, San Diego, 2008

Professor Gourisankar Ghosh, Chair
Professor Joseph Noel, Co-Chair

In eukaryotic organisms, mRNA synthesis requires splicing to remove non-coding introns. Two types of splicing events are constitutive and alternative. The serine-arginine (SR) protein and SR-protein kinase (SRPK) families are the two protein families necessary for alternative splicing. SR-proteins are characterized by N-terminal RNA recognition motif and C-terminal RS domain. In the cytoplasm, SRPK1, one of the SRPK family kinases, processively phosphorylates the RS in ASF/SF2, a well-studied SR-protein. The various phosphorylated forms of SR-proteins play critical role in alternative splicing. The

focus of my thesis work is how SRPK1 processively phosphorylates ASF/SF2 and what structural elements in SRPK1 regulate its subcellular localization.

X-ray structures of the SRPK1:ASF/SF2 complex allowed us to propose two possible docking motifs in ASF/SF2: the C-terminal end of RRM and the N'-terminal RS. Using chemical cross-linking experiments, I have demonstrated that ASF/SF2 indeed possesses two docking motifs that mediate in sequential and phosphorylation-dependent manner. These experiments further established the C to N-terminal directionality of ASF/SF2 phosphorylation.

I have further investigated the mechanism of how SRPK1 is distributed in cells. My experiments supported the existence of SRPK1 as a dimer and that the dimerization of SRPK1 needs its spacer domain as well as the C-terminal end. However, I found dimerization not to be the only factor in the regulation of cellular distribution of SRPK1. I have further shown that another splicing-related kinase family, Clk/Sty, which is exclusively nuclear, interacts with SRPK1 in vivo. It is likely that interactions with Clk/Sty may regulate the compartmentalization of SRPK1.

CHAPTER I

INTRODUCTION

A. The Essence of Splicing:

A largely unexplained structural feature common to metazoan genomes is the presence of vast amount of nonprotein-coding DNA (Britten and Davidson 1969; Taft and Mattick 2007). About 95% of haploid genomes in multicellular eukaryotes are found in noncoding regions (Zuckerkandl 2002). This noncoding DNA feature is accordingly seen in messenger RNA, suggesting that its removal is an important regulation in gene expression. The process of removing the non-coding sequences is called splicing. Splicing requires the spliceosome and considerable progress has been made in the understanding of spliceosome assembly (Chaira & Palandjian, 1997; Burge et al., 1999). The spliceosome comprises of five small nuclear ribonucleoprotein particles (snRNPs), designated U1, U2, U4, U5, and U6, and a large number of non-snRNP proteins. The snRNP components act together in a stepwise manner to splice the coding sequences called exons (Figure 1.1). snRNP recognizes specific sites in pre-mRNA for their assembling, rearrangement, and catalysis (Maeder & Guthrie 2008). Besides snRNPs, non-snRNPs are also involved in assembly and regulation of splicing. One of the non-snRNP families is Serine-Arginine (SR) protein family, which has direct function in splicing reactions. SR proteins engage the general splicing machinery to recognize specific splice sites (Graveley 2000). Two major splicing events are constitutive and alternative splicing; SR proteins are found to facilitate the splicing machinery in both of these events (Wu U Maniatis, 1993). Constitutive splicing involves in bringing

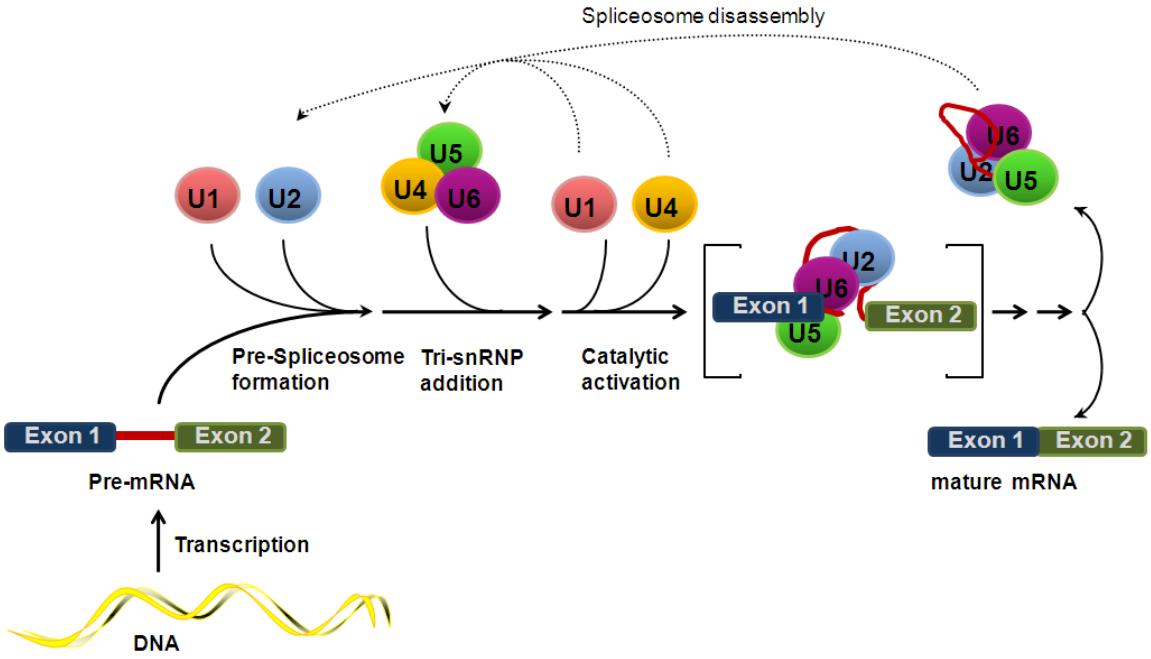

Figure 1.1: Splicing, an overview (modified from Maeder & Guthrie 2008)**.** The spliceosome comprises mainly of small nuclear ribonucleoproteins (snRNPs), designated U1, U2, U4, U5, and U6. The U1 first binds to the pre-mRNA 5'-splice site and subsequently U2 binds pre-mRNA. The binding of U1 and U2 to pre-mRNA generates the pre-spliceosome. Tri-snRNP complex, which contains of U4, U5, and U6, is then recruited to the pre-spliceosome, and the splicing of pre-mRNA is ready to be catalyzed to completion. After mature messenger RNA is generated, snRNP components disassemble and are recycled for the next splicing.

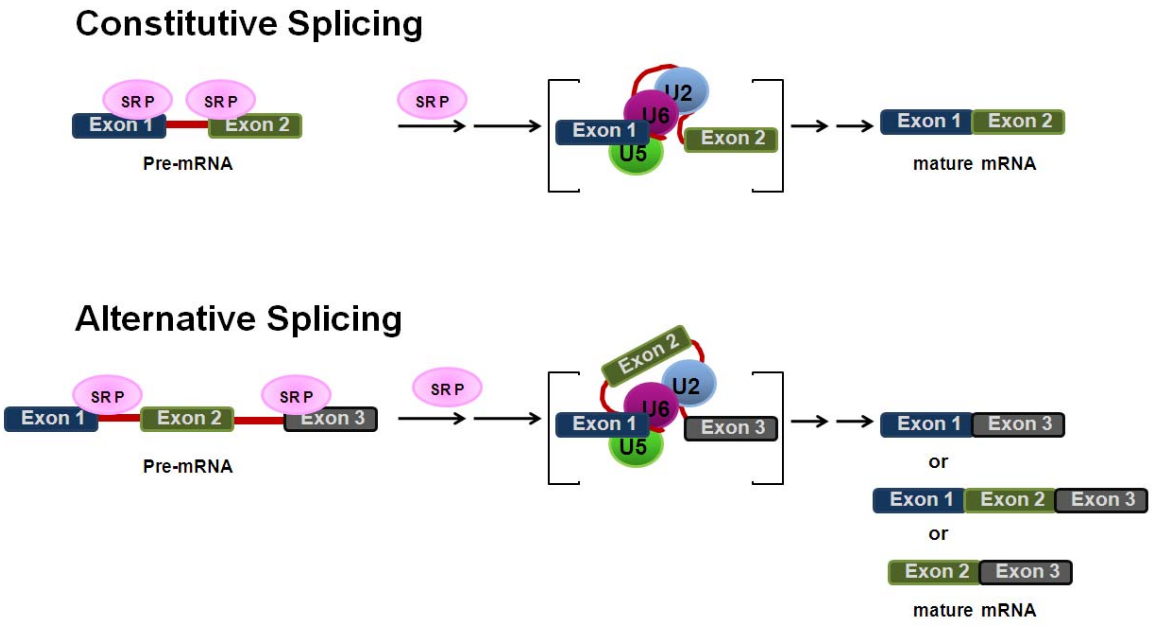

Figure 1.2: SR proteins regulate the two major splicing events. SR proteins are involved in 3'-splice site selection to facilitate the ligation of adjacent exons in constitutive splicing. In alternative splicing, SR proteins regulate 5'-splice site selections and recruitment of spliceosome to generate different versions of mature mRNAs.

consecutive exons together into the final mRNA transcript and SR proteins play a key role in 3' splice site selection to enhance the splicing of adjacent exons (Lavigueur et al., 1993; Sun et al., 1993; Tian & Maniatis, 1993). Distant exons nevertheless can also be brought together under the facilitation of SR proteins and this splicing process is called the alternative splicing. Different lengths and versions of mature mRNA are produced based on the 5'-splice site selection and recruitment of snRNPs. Thus, splicing not only mediates removal of noncoding sequences but also generates different mature mRNA transcripts for gene expression, resolving the problem of low amount of coding sequences in genes.

B. SR Proteins:

Serine-Arginine (SR) proteins are a family of non-snRNP (small nuclear ribonucleoprotein particle) splicing factors involved in constitutive and alternative splicing. They are also known to have diverse roles in RNA metabolism, such as mRNA export, RNA stability, and translation (Zahler et al., 1993; Fu, 1995; Manley and Tacke, 1996; Graveley, 2000; Sanford et al., 2004; Huang and Steitz, 2005; Lin et al., 2005). SR proteins are highly conserved throughout eukaryotes, comprising of the RNA-recognition motifs (RRM) and an RS domain at the amino- and carboxyl-termini, respectively (Valcarcel & Green 1996). The RS domain consists of multiple Arginine-Serine dipeptide repeats, in which serine residues are extensively phosphorylated (Zahler et al., 1993). The phosphorylation of SR proteins affects their protein-protein interactions and

intracellular localization and trafficking (Xiao and Manley, 1997, Fu, 1995, Zahler et al., 1993) (Figure 1.4). Many evidences show that the phosphorylation state (un-, hypo- and hyperphosphorylation) of SR proteins play an important role in RNA metabolism including alternative splicing of pre-mRNA (Duncan et al., 1997; Prasad et al., 1999).

C. SR Protein Kinases:

The RS domain of SR proteins are phosphorylated by several reported proteins including SR protein kinase (SRPKs) (Gui et al., 1994, Kuroyanagi et al., 1998; Wang et al., 1998), Cdc2-like kinases (Clks; Ben-David et al. 1991; Howell et al., 1991; Johnson and Smith, 1991), pre-mRNA processing 4 (PRP4, (Alahari et al., 1993), topoisomerase I (Rossi et al., 1996) and dual-specificity tyrosine-regulated kinases (DYRKs, Alvarez et al., 2003; de Graaf et al., 2004). SRPK1 is the first SR kinase purified and cloned on the basis of its ability to phosphorylate SR proteins *in vitro* and localizes to cytoplasm (Gui et al., 1994). Two other structurally related proteins, SRPK2 and SRPK3, are also identified to phosphorylate an SR protein, splicing factor 2/alternative splicing factor (SF2/ASF; Kuroyanagi et al., 1998; Wang et al., 1998; Nakagawa et al., 2005).

D. Domain Architecture of SRPKs

The kinase core domain of SRPKs is highly similar to all other protein

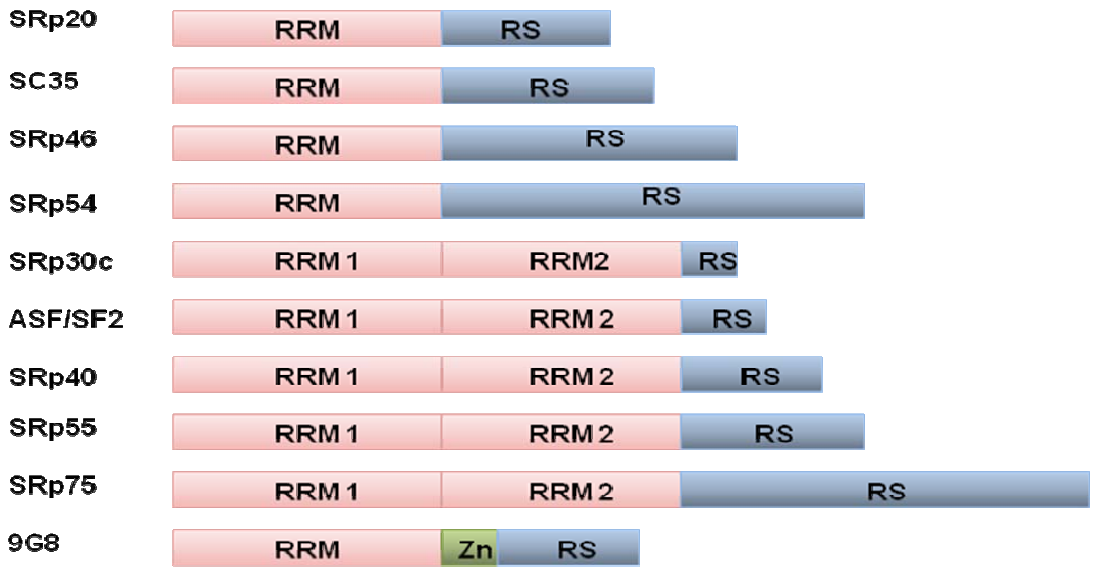

Figure 1.3: Schematic Organization of SR proteins: SR proteins are characterized by N-terminal RNA-recognition motifs (RRM) and C-terminal Arginine-Serine (RS) dipeptides. The SR protein 9G8 contains Zn knuckle domain between RRM and RS domain.

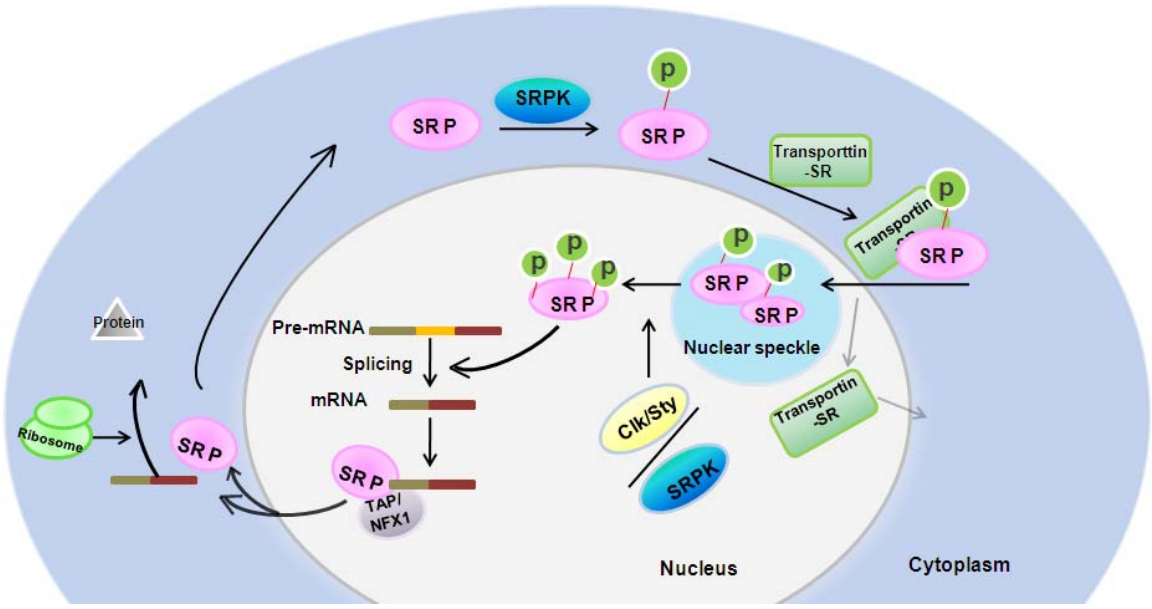

Figure 1.4: Intracellular localization and trafficking of SR proteins: A generalized view. Hypophosphorylated SR proteins (SR P) migrate to the nucleus through interactions with transportin-SR proteins and localizes to nuclear speckles. Upon splicing signal, SR proteins are hyperphosphorylated and recruited to the splicing site where they mediate splice site selection and recruitment of spliceosome. Some SR proteins also assist mRNA cystoplasmic export through interaction with TAP/NFX1.

kinases both in terms of retaining signature sequence feature and in length. However, SRPKs also possess several unusual structural features: in the primary sequence the kinase domain of SRPKs is separated by the long spacer which loops out of the kinase core in the three dimensional structure (Figure 1.5). Functional importance of the spacer is unknown. The removal of the spacer in SRPK1 has little effect on the kinase activity, but triggers the nuclear translocation of kinases and consequently induces aggregation of splicing factors in the nucleus (Ding et al., 2006). In addition, SRPKs also contain long N-terminal extensions, the precise function of which remains unknown. The yeast counterpart of SRPK1, Sky1p, also contains a long C-terminal extension which is absent in mammalian kinases. Sky1p phosphorylates SR proteins with high specificity although surprisingly no obvious SR proteins are identified in the completely sequenced yeast genome (Colwill et al., 1996a; Colwill et al., 1996b; Nolen et al., 2001; Zahler, 2001).

E. Structural Studies on SRPKs

Sky1p is the first SR protein kinase structure to be solved followed by that of SRPK1 protein (Nolen et al., 2001; Ngo et al., 2005). Both the structures adopt similar fold like other protein kinases- the N-terminal small lobe composed primarily of β-strands and the C-terminal large lobe, which is mostly helical (Huse and Kuriyan, 2002; (Johnson et al., 2003; Nolen et al., 2001, Ngo et al., 2005) (Figure 1.6 & 1.7). However, they have unique structural features that may

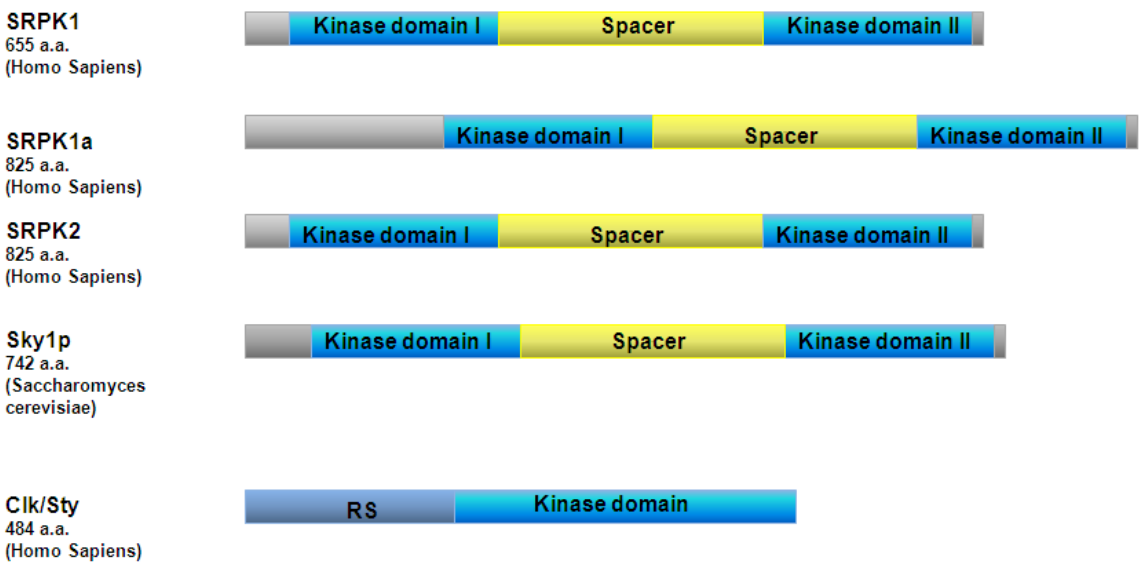

Figure 1.5: Schematic diagram of SR protein Kinase family and Clk/sty. SRPK shares the same feature of a spacer domain separating the kinase domain in the primary sequence. Sky1p, SRPK counterpart in yeast, has similar domain organization with the SRPK family. Clk/Sty contains an RS domain and a kinase domain at the amino- and carboxyl-termini, respectively.

explain how these two proteins remain constitutively active. In Sky1p, the C-terminal tail position itself underneath the activation loop and maintains the active conformation of the kinase by direct interaction. In SRPK1, the activation loop maintain active state without any specific intraprotein interactions but through indirect mechanism where distal parts play important roles.

The biological importance of SRPK family has been recognized by its role in restrictive phosphorylation of SR proteins and by its subcellular distribution. Cytoplasmic SRPK1 activates nuclear translocation of cytoplasmic SR proteins in a phosphorylation dependent manner. Recent studies on the subcellular localization of SRPKs have revealed their physiologic role in cell cycle – SRPK1 and 2 are found to be more populated in the nucleus at the G_2-M boundary (Ding et al., 2006; Jang et al., 2008). The functional role of SRPKs in the nucleus is further investigated and SRPKs are observed to be cofractionated with U1-70K, an SR-related splicing factor and a component of U1 snRNP (Mathew et al., 2008). SiRNA and RNAi against the expression of SRPK family *in vivo* show reduction in cell viability, suggesting the role of SRPK for cell survival (Hayes et al., 2006; Mathew et al., 2008). However, the mechanisms of SRPK- substrate interactions, SRPK subcellular localization, and regulation of their catalytic activity remain unclear.

F. Coordinated Function of Clk/Sty and SRPK Families

The Clk/Sty family kinases, consisting of four members (Clk1/sty and

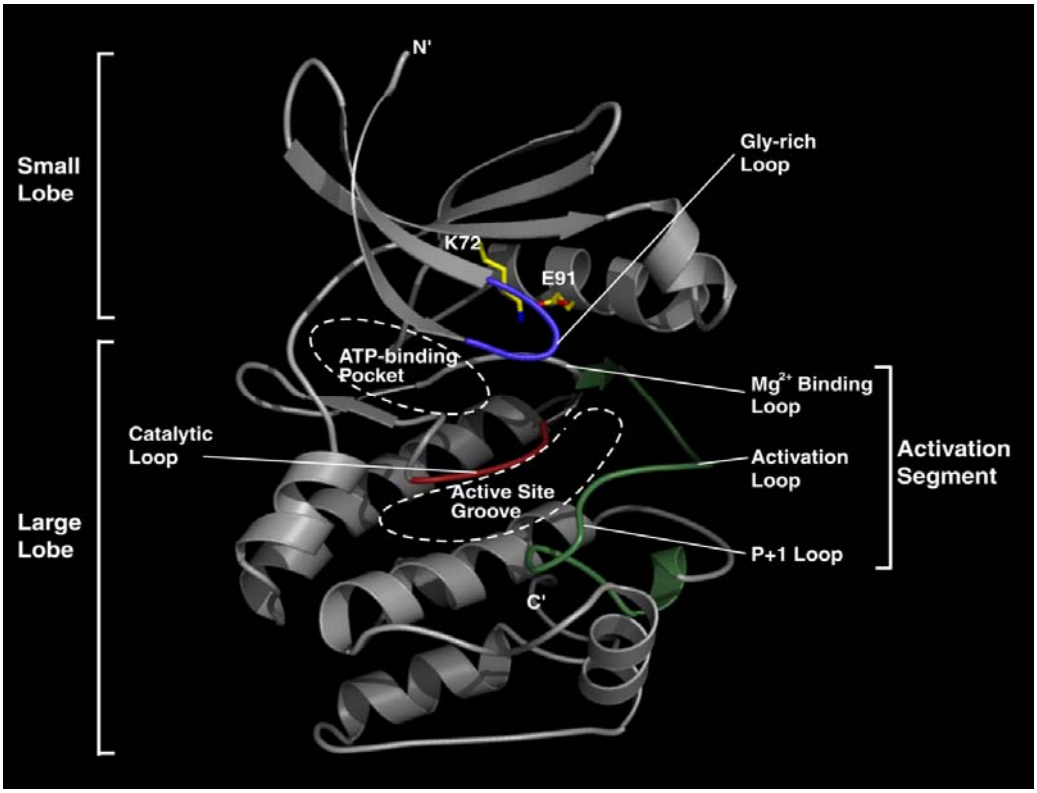

Figure 1.6: An overview of a kinase fold, ribbon diagram of PKA (1ATP.pdb) (Knighton et al., 1991a, Dr. Ngo's 2006 thesis). The catalytic subunit of a kinase is characterized by two lobes. The smaller lobe is dominant by a β-sheet consisting of five antiparrallel β-strands. The only region of helix in this lobe lies between β-strands 3 and 4. The first three strands plus the C –helix that interact directly with the ATP. Mammalian kinase has the amino-terminal glycine myristoylated (Carr et al 1982) and this acyl group is very likely important for stabilizing the protein (Slice & Taylor 1899, Yonemoto et al 1991). The large lobe is primarily comprised of helices. Between the two lobes is a cleft, where catalysis occurs. The single region of β-structure in the large lobe lies at the surface of the cleft and most of the important residues for catalysis connect to these β-strands. The activation segment in the cleft region is comprised of Mg^{2+}binding loop of the small lobe, the activation loop of the large lobe, and the P+1 site in the activation loop to mediate in the position of the substrate (Taylor et al., 1992).

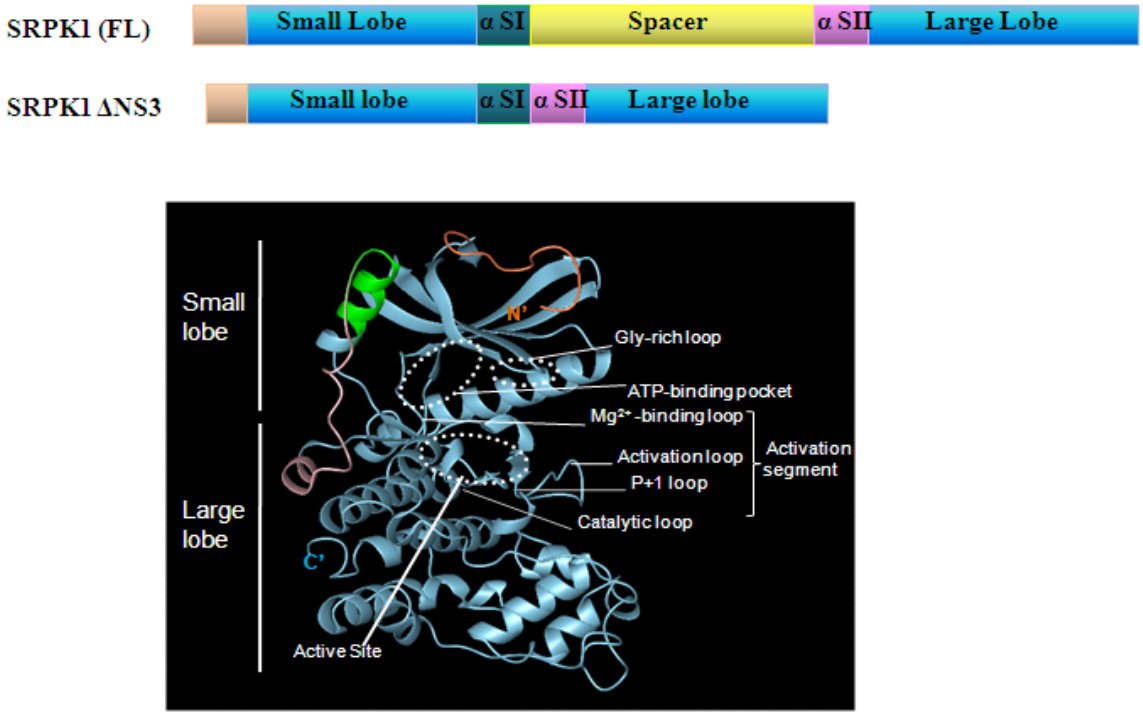

Figure 1.7: An overview of the kinase core of SRPK1 (1WAK.pdb): The crystal structure of the kinase core of SRPK1 was solved by Ngo et al[2005] . The kinase core of SRPK1 is folded into two lobes similar to other protein kinases. The N-terminal small lope is composed primarily of β-strands and C-terminal large lobe, which is highly α-helical. The cleft between the two lobes adopts the catalytic structure formed by the activation segment and ATP-binding pocket. One notable feature in SRPK1 is the spacer region that bifurcates the kinase domain in the primary sequence loops out of the kinase core structure.

Clk2-4), is known to be dual-specificity kinases that autophosphorylate Ser, Thr, and Tyr residues in over-expression systems and *in vitro* (Ben-David et al., 1991; Howell et al., 1991). Clk/Sty contains an N-terminal RS domain and a C-terminal kinase domain (Graveley, 2000). The RS domain contains a putative nuclear localization signal that determines its nuclear localization and is also found to interact in yeast two-hybrid assays with several SR proteins, including ASF/SF2, via this domain (Howell et al., 1991; Prasad et al., 1999). Many evidences show that when over-expressed in mammalian cells, inactive Clk mutants localizes to the nuclear speckles, whereas the wild-type ClKs distribute throughout the nucleus and cause the nuclear speckles to dissolve (Colwill et al., 1996a; Duncan et al., 1998). Both SRPK1 and Clk/Sty also known to act in a concerted manner in regulating SR proteins. SRPK1 phosphorylates N-terminal half of the RS domain in ASF/SF2 while Clk/Sty phosphorylates the rest of the RS domain (Aubol et al., 2003; Ngo et al., 2005; Velazquez-Dones et al., 2005; Ma et al., 2008). Both hyper- and hypophosphorylation states of SR protein inhibit SR protein splicing activity, repressing constitutive splicing and switching the alternative splice site selection (Prasad et al., 1999). Together, SR protein kinases function as potent regulators of SR proteins and the insight into what regulates these kinases would add another level of understanding about the complexity of control in gene expression.

G. Substrate Specificity of Protein Kinases from Docking Interactions

Substrate specificity of enzymes is primarily defined by the stereochemical complementarity between the active site of the kinase and its substrate. Although protein kinases do possess preferred target phosphorylation sequence, they often recognize their targets through interactions that occur outside of their active site (Figure1.8). They use variety of structural and mechanical elements to mediate interaction with their specific substrates. Therefore, substrate recognition by protein kinases can be studied at two levels: the interaction at the active site and the interaction at the site distal from the active site (Figure 1.9). Interactions at the active site required specific modules as mentioned earlier such as the phosphorylation of one or more residues in the activation loop, the binding of regulator factors, and/or the orientation of the substrate segment bound to the active site. These requirements are nevertheless not stringent enough as they are primarily configured to perform phosphoryl transfer. The distal sites apart from the active sites have been recognized in many protein kinases such as the Src, Abl, Hck, Csk, MAPK. Kinase and substrate interactions at the distal site increase the level of substrate specificity and kinase regulation that are required *in vivo*. The distal sites can be divided into two structural elements: the recognition domain and the docking groove. The recognition domain, separate from the catalytic domain, are often used to establish links with other signaling protein partners (Remenyi et al., 2006). The example for this is the Src homology (SH) domains in Src that enables Src to interact with many downstream signaling proteins (Frame et al., 2001). On the other hand, kinase domains can also acquire surface grooves- referred to as

docking sites – that are capable of establishing specific connections via small peptide motifs residing in interacting partners (Remenyi et al., 2006). It plays an important role in targeting catalytic domains to particular substrates, partners, and locations. The example for this is the docking of the mitogen-activated protein kinase (MAPK). Structural, biochemical, and genetic data have all shown that the docking motifs from interacting proteins are necessary for MAPK to bind and phosphorylate its targets (Remenyi et al., 2006). Thus, the docking interaction can govern protein association as well as influence the kinase activity through allosteric mechanisms.

Structures of Sky1 and SRPK1 suggest that docking interactions in these kinases are conserved. The nature of docking interactions in these kinases is different from those in other kinase systems. In both SRPK1 and Sky1p, docking interaction is electrostatic in nature whereas in other cases both polar and hyhrophobic interactions help stabilize the complex.

H. Focus of study

Direct interactions between the SRPK family members and their substrates, SR proteins, not only generate hypo-phosphorylated SR proteins but also play a key role in regulation of the subcellular localization of SR proteins. Since the various phosphorylated forms of SR proteins display unique subcellular localizations and functional activities, this suggests that the SRPK family

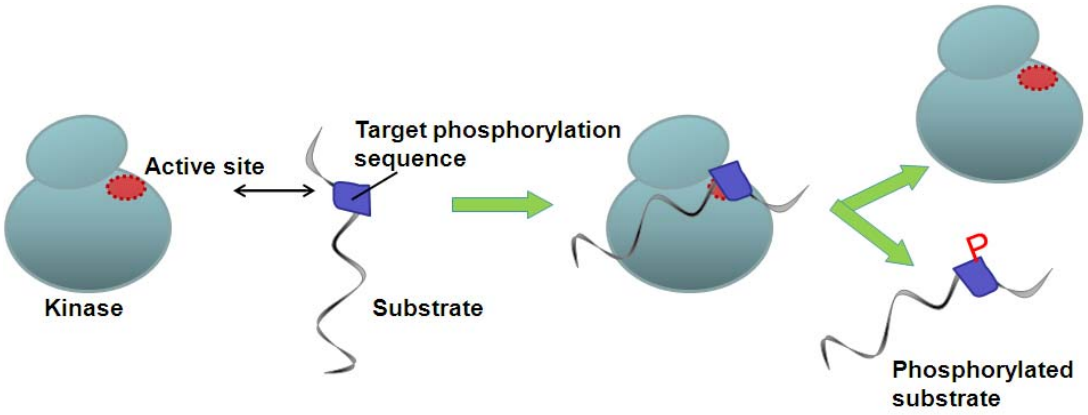

Figure 1.8: Substrate specificity at the kinase active site. The kinase can identify its target substrate by the target phosphorylation sequence. The active site of a kinase is usually charge complementary to the phosphorylation sequence in its specific substrate.

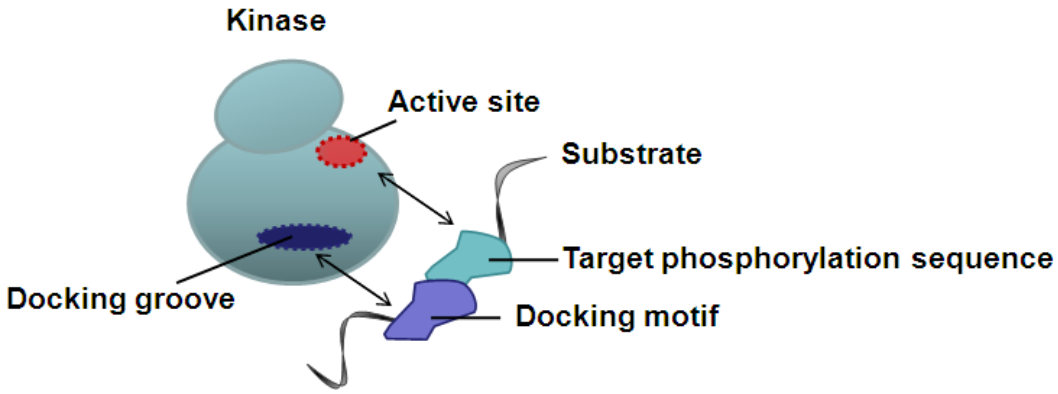

Figure 1.9: Substrate recognition by docking interactions. The general features of the substrate recognition distal from the active site. The substrate possesses a docking motif that recognizes the kinase docking groove. The interaction between kinase and substrate is regulated via docking.

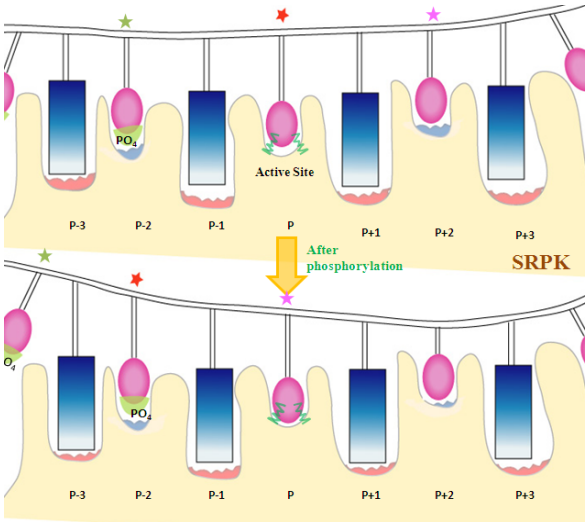

Figure 1.10: Model for the consecutive phosphorylation at the active site of SRPK1 (adapted from Zahler et al. 2001). The substrate binding pocket at P-3, P-1, P+1 and P+3 positions in SRPK1 has surface charge that can accommodate Arg residues in the substrate. The pocket P-2 is positively charged that can interact with the negatively charged residue such as a phosphoserine. Serine in the active site, P position, is labeled with red star. Serine, in the P+2 site is labeled with a pink star. After phosphorylation of the serine at the P position, the substrate transitions along the catalytic site such that the new phosphoserine reside to the P-2 site and the serine labeled with pink star displace the P position. The transitioning of the substrate and the electrostatic interactions at the active site allow the next serine in the substrate to be phosphorylated.

members are the cytoplasmic regulators of SR proteins. The interactions between the well-characterized kinase and substrate, SRPK1 and ASF/SF2, do not require phosphorylation by upstream kinases but are shown to depend on the docking interaction. The X-ray structural studies showed that SRPK1 possesses a docking groove within the large lobe of the kinase core, which specifically interact with two motifs in ASF/SF2. Whether these two motifs in ASF/SF2 serve as the docking sites for SRPK1 or mediate the processive phosphorylation by SRPK1 is not clear by x-ray structural studies. Our aim is to establish the molecular basis of the processive phosphorylation by SRPK1 by chemical cysteine crosslinking assays. Since SRPK family members are found abundant in the cytoplasm while SR proteins localize mostly in the nucleus, the mechanism of cytoplasmic retention of SRPK1 is still unknown. In this thesis, I have characterized some features of the retention elements in SRPK1 that render the kinase cytoplasmic stability and subcellular localization.

CHAPTER II

MATERIALS AND METHODS

A. Preparation of recombinant DNA

Primers were designed to anneal the 5' and 3' sites of the gene of interest (see Appendix for the list of primers). Polymerase Chain Reaction (PCR) was performed to amplify the gene of interest using the designed primers. The amplified gene was double digested by specific restriction enzymes (NEB); the same restriction enzymes were also used to digest DNA vector of interest, namely pET 15b, pET 11a, pGEX4T2, pCMV, pβActin, or pFast-HTA. Both the digested vector and the gene were purified using gel extraction kit (Qiagen or Pioneer) before ligation. The ligated vector with the gene of interest was used for transformation in JM-109 or DH5α strain of E.coli. At least five single colonies were chosen for inoculation for 16 hours, followed by plasmid purification using plasmid extraction kit (Qiagen or Pioneer). The plasmid with the gene interest was then subjected to double digestion by specific restriction enzymes to see the release of the gene of interest. The positive clones were then selected for transformation in BL-21(DE3) to check protein expression. The plasmid with the over-expression of the desired construct of protein was sent for sequencing at (Cancer Center or Eton).

B. Mutagenesis of ASF/SF2 and SRPK1

Primers were designed to carry the designed mutation and the mutagenesis procedure was done according to Strategene Mutagenesis Protocol. After the

positive clone was obtained; the procedure is similar to the subcloning of plasmid.

C. Expression and purification of recombinant proteins

1. His-ΔNS3:

E. coli BL21 (DE3) cells were transformed with pET15b ΔNS3 were cultured in 2L LB media (containing 200ug/ul Ampicilin) at 37^{o}C to an OD_{600} of 0.3 and induced with 0.1mM IPTG overnight at 25^{o}C. The cells were harvested at 5500rpm Beckman centrifugation or Sorvall centrifuge using GLA-8.1 rotor. The cell pellet was then resuspended in 100ml of Lysis buffer that contains 50 mM KCl, 20 mM MES pH 6.5, 10% Glycerol, 1 mM DTT, and 1 mM PMSF. The cells were lysed by sonication at 9x90% during cycles for 5 x30". This was followed by centrifugation at 13000-14000 rpm (Sorvall centrifugation SS-34 rotor) for one hour. The supernatant was loaded onto the pre-equilibrated 30 ml Q-sepharose column (Amersham). The column was washed with three column volume of Lysis buffer. The flow through of Q-column was brought to 500mM KCl using buffer of 3M KCl, 1mM DTT, and 20mM MES pH 6.5. The sample was then loaded onto Nickel NTA agarose column (Invitrogen) at 4^{o}C. The column was washed twice with the lysis buffer that had 25 mM Imidazole added. The protein was then eluted off the column by the elution buffer (the lysis buffer supplemented with 300 mM Imidazole). The purity of the elutions was checked

by SDS-PAGE analysis. A typical yield for this protein preparation is 15 mg/ml and the total protein yield is 150 mg per 2 liter culture.

* His-ΔNS3 was provided by Dr. Ngo.

2. His-SRPK1(FL) [N-terminus His tagged] and His-SRPK1(FL) [C-terminus His tagged]

Method 1:

E. coli BL21 (DE3) cells were transformed with PRSETb-SRPK1(FL) for N-terminus His-tagged SRPK1 or pET 11a-SRPK1 for C-terminus His-tagged SRPK1. The cells were cultured in 2 L LB media (containing 200ug/ul Ampicilin) at 37^{o}C to an OD_{600} of 0.25 and induced with 0.2 mM IPTG overnight at 25^{0}C. The cells were harvested by centrifugation as mentioned in previous section. The cell pellet was then resuspended in 100ml of Lysis buffer that contains 50 mM KCl, 20 mM Capso pH 9.5, 10% Glycerol, 1mM DTT, and 1 mM PMSF. The cells were lysed by sonication and the cellular fractions were cleared by centrifugation at high speed (13000-14000 rpm) for one hour. The supernatant was loaded onto the pre-equlibrated Q-sepharose column (Amersham) and the column was then washed with 3 column volume of lysis buffer. The flow through of Q-sepharose column was loaded onto the pre-equilibrated S-sehparose column (Amersham). The column was wash with 3 column volume of Lysis buffer. The flow through of S-sepharose column was brought to 500 mM KCl using 3 M KCl, 20 mM Capso pH 9.5, and 1 mM DTT before being loaded to

Nickel NTA agarose column (Invitrogen). Here it should be noted that Ni-NTA resin from Invitrogen can tolerate upto 5 mM DTT. The column was washed twice with the lysis buffer that had 25 mM Imidazole added. The protein was then eluted off the column by the elution buffer (the lysis buffer supplemented with 300 mM Imidazole). The purity of the elutions was checked by SDS-PAGE analysis. The desired elutions were then pooled together for concentration using Centriprep-30 (Milipore) and loaded onto a 16/20 Superdex 200 size-exclusion column, pre-equilibrated with the buffer that contains 500 mM KCl, 20 mM Capso pH 9.5, 5% Glycerol, and 1 mM DTT. The peak fractions were evaluated by SDS-Page analysis and the fractions of the desired peak are pooled for concentration. A typical yield for this protein preparation is 2 mg/ml and the total protein amount is 10 mg per 2 L culture.

Method 2:

The preparation of bacterial culture and cell lysate is identical to that mentioned in method 1 except that lysis buffer is composed of 50 mM KCl, 20 mM Tris pH 7.5, 1 mM DTT, 10% Glycerol. The cell lysate was loaded onto Q-Sepharose column (Amersham) and the flow-through solutions from the load and wash were combined and the salt concentration of the solution was brought to 500 mM KCl using high salt buffer (3 M KCl, 20 mM Tris pH 7.5, and 1 mM DTT). The sample was loaded onto the Nickel NTA agarose column (Invitrogen). The column was washed twice with the lysis buffer that had 25mM Imidazole added. The protein was then eluted from the column by the elution buffer (the lysis buffer

supplemented with 300 mM Imidazole). The purity of the elutions was checked by SDS-PAGE analysis. The elutions of SRPK1 were combined and brought to 2 M of Ammonium sulfate (AS), followed by high speed centrifugation to remove precipitates. The soluble fraction was loaded onto the phenyl-sepharose 5ml-column (preequilibrated in 2 M Ammonium Sulfate, 20 mM Tris pH 7.5, 1 mM DTT, 5% Glycerol). The column was run at the gradient of 2 M to 50 mM AS. SRPK1 elutes at the conductance of 45 mS/cm, that corresponds to 800 mM of monoatomic salt. The purity of SRPK1 was analyzed by SDS-PAGE analysis. The yield for this protein preparation is 2 mg/ml and the total protein amount is 5 mg per 2 L culture.

* SRPK1(FL) in pRSET was provided by Dr. Chakrabarti.

3. His-SRPK1 in insect cells

E. coli DH10 Bac competent cells were transposed with pFast HTA-SRPK1(FL). Ten white colonies were selected for inoculation in 2 ml of Luria Broth that contains 500 ug Kanamycin, 14 ug Genamycin , and 20 ug Tetracycline. The bacmid DNA from each culture was extracted by plasmid purification Kit (Qiagen). The insert gene of SRPK1(FL) in bacmid DNA was then confirmed by DNA sequencing. The expression of the positive plasmid was used for transfection in SF9 cells using CellFectin reagent (Invitrogen). The P1 virus from cell culture medium was collected at 72 hours post-transfection and stored in dark at 4^{o}C. The cell monolayer was lysed for the expression of His-SRPK1(FL).

The expression of His-SRPK1(FL) was confirmed by Western Blot analysis against His antibody (Catalog SC-8036; Santa Cruz Biotechnology) and against SRPK1 antibody (Catalog no. 61172; BD Transduction Laboratories, Lexington, KY). 100 ul of P1 virus was then used to transfect SF9 cells to generate P2 virus after 72 hours and the expression of His-SRPK1(FL) was also checked by Western blot. Similarly, P3 virus was generated. A 500-ml culture of 2.0 x 10^6 of SF9 cells per milliter was transfected with P3 virus for large scale expression and grown in suspension with gentle shaking at 25^{o}C for 72 hours. The cells were harvested by centrifugation at 500 rpm (Sorvall). The cell pellet was then resuspended and incubated for 2 hours in 50 ml of Lysis buffer that contains 50 mM KCl, 20 mM Tris pH 7.5, 10 %Glycerol, 5 mM βME, 1 mM PMSF, 0.1% Triton X-100, and 100ul of ΣPIC. The cells were lysed by sonication and the cellular fractions were cleared by centrifugation at high speed (13000-14000 rpm) for one hour as previously mentioned. The supernatant was loaded onto the pre-equilibrated 30-ml Q sepharose column (Amersham). The column was washed with 10 ml of lysis buffer. The flow through solutions from the load and the wash were combined and the salt concentration of the combined solution was brought to 500 mM KCl. The solution was then loaded onto the pre-equlibrated Nickel NTA agarose column (Invitrogen) at 4^{o}C. The column was washed twice with the lysis buffer that had 40 mM Imidazole added. The protein was then eluted off the column by the elution buffer (the lysis buffer supplemented with 300 mM Imidazole). The purity of the elutions was checked by SDS-PAGE analysis. The

yield for this protein preparation is 0.4mg/ml and the total protein amount is 2 mg per 500 ml culture.

4. GST-SRPK1 (FL)

E. coli BL21 (DE3) cells transformed with pGEX4T2-SRPK1(FL) were cultured in 2 L LB media (containing 200ug/ul Ampicilin) at 37^{o}C to an OD_{600} of 0.25 and induced with 0.2 mM IPTG overnight at 25^{o}C. The cells were harvested by centrifugation. The cell pellet was resuspended in 100 ml of Lysis buffer that contains 300 mM KCl, 50mM Hepes pH 7.0, 10% Glycerol, 1 mM $MgCl_2$, 2 mM DTT, and 1 mM PMSF. The cells were lysed by sonication and the cellular fractions were cleared by centrifugation at high speed (13000-14000 rpm) for one hour at 4^{o}C. The supernatant was loaded onto the pre-equilibrated 2-ml GST column (GE Healthcare) at 4^{o}C. The column was washed with 100 ml of lysis buffer. The protein was then eluted off the column by the elution buffer (the lysis buffer supplemented with 15 mM reduced glutathione). The purity of the elutions was checked by SDS-PAGE analysis. The desired elutions were then pooled together for concentration and loaded onto a 16/20 Superdex 200 size-exclusion column, pre-equilibrated with the buffer that contains 300 mM NaCl, 20 mM Hepes pH 7.5, 5% Glycerol, and 1 mM DTT. The peak fractions were evaluated by SDS-Page analysis and the fractions of the desired peak are pooled for concentration. A typical yield for this protein preparation is 2 mg/ml and the total protein amount is 20 mg. A typical yield for this protein preparation is 1.5 mg/ml

and the total protein amount is 5 mg per 2 L culture. The protein was aliquoted and flash frozen.

5. His-SRPK1 (71-655) or ΔN70

E. coli BL21 (DE3) cells were transformed with PRSETb-SRPK1(71-655). Single colony was cultured in 2 L LB media (containing 200 ug/ul Ampicilin) at 37^{o}C to an OD_{600} of 0.25 and induced with 0.2 mM IPTG overnight at 25*C. The cells were harvested by centrifugation. The cell pellet was then resuspended in 100 ml of lysis buffer that contains 500 mM KCl, 20 mM MES pH 6.5, 10% Glycerol, 1 mM DTT, and 1 mM PMSF. The cells were lysed by sonication and the cellular fractions were cleared by centrifugation at high speed (13000-14000 rpm) for one hour. The supernatant was loaded onto the pre-equlibrated 3-ml Nickel-NTA agarose column (Invitrogen) at 4^{o}C. The column was washed twice with the lysis buffer that had 25 mM Imidazole added. The protein was then eluted off the column by the elution buffer (the lysis buffer supplemented with 300 mM Imidazole). The purity of the elutions was checked by SDS-PAGE analysis. A typical yield for this protein preparation is 2mg/ml and the total protein amount is 20 mg per 2 L culture.

* His-SRPK1 Δ70 was provided by Dr. Fu.

6. His-SRPK1 (226-491) or His-Spacer

E. coli BL21 (DE3) cells were transformed with pET24a-SRPK1(226-491). Single colony was cultured in 2 L LB media (containing 200 ug/ul Ampicilin) at 37^{o}C to an OD_{600} of 0.25 and induced with 0.2 mM IPTG overnight at 25^{o}C. The cells were harvested by centrifugation. The cell pellet was then resuspended in 100 ml of lysis buffer that contains 500 mM KCl, 20 mM Capso pH 9.5, 10% Glycerol, 1 mM DTT, and 1 mM PMSF. The cells were lysed by sonication and the cellular fractions were cleared by centrifugation at high speed (13000-14000 rpm) for one hour. The supernatant was loaded onto the pre-equlibrated 3-ml Nickel-NTA agarose column (Invitrogen) at 4^{o}C. The column was washed twice with the lysis buffer that had 25 mM Imidazole added. The protein was then eluted off the column by the elution buffer (the lysis buffer supplemented with 300 mM Imidazole). The purity of the elutions was checked by SDS-PAGE analysis. A typical yield for this protein preparation is 2mg/ml and the total protein amount is 20 mg per 2 L culture.

* His-SRPK1 (226-491) was provided by Dr. Fu.

7. GST-SRPK1 (226-491) or GST-Spacer

E. coli BL21 (DE3) cells transformed with pGEX4T2-Spacer were cultured in 2 L LB media (containing 200ug/ul Ampicilin) at 37^{o}C to an OD_{600} of 0.25 and induced with 0.2 mM IPTG overnight at 25^{o}C. The cells were harvested by centrifugation. The cell pellet was resuspended in 100 ml of Lysis buffer that contains 400 mM KCl, 50mM Tris pH 7.5, 10% Glycerol, 1 mM DTT, and 1 mM PMSF. The cells were lysed by sonication and the cellular fractions were

cleared by centrifugation at high speed (13000-14000 rpm) for one hour at 4^0C. The supernatant was loaded onto the pre-equilibrated 2-ml GST column (GE Healthcare) at 4^oC. The column was washed with 100 ml of lysis buffer. The protein was then eluted off the column by the elution buffer (the lysis buffer supplemented with 15 mM reduced glutathione). The purity of the elutions was checked by SDS-PAGE analysis. The desired elutions were then pooled together for concentration and loaded onto a 16/20 Superdex 200 size-exclusion column, pre-equilibrated with the buffer that contains 400 mM NaCl, 20 mM Tris pH 7.5, 5% Glycerol, and 1 mM DTT. The peak fractions were evaluated by SDS-Page analysis and the fractions of the desired peak are pooled for concentration. A typical yield for this protein preparation is 2 mg/ml and the total protein amount is 10 mg. A typical yield for this protein preparation is 1.5 mg/ml and the total protein amount is 5 mg per 2 L culture. The protein was aliquoted and flash frozen.

* GST-SRPK1 (226-491) was provided by Dr. Fu.

8. His-ASF/SF2 (105-248)

The cells were harvested by centrifugation. The cell pellet was then resuspended and incubated for 2 hours in 50 ml of lysis buffer that contains 50 mM KCl, 20 mM Tris pH 7.5, 20% Glycerol, and 6 M urea. The cells were lysed by sonication and the cellular fractions were cleared by centrifugation at high speed (13000-14000 rpm) for one hour. The supernatant was loaded onto the pre-

equilibrated Q sepharose column (Amersham). The column was washed with 100 ml of lysis buffer. The flow through solutions from the load and the wash were combined and the salt concentration of the combined solution was brought to 500 mM KCl. The solution was then loaded onto the pre-equlibrated Nickel NTA agarose column (Invitrogen). The column was washed twice with the lysis buffer that had 40 mM Imidazole added. The protein was then eluted off the column by the elution buffer (the lysis buffer supplemented with 300 mM Imidazole). The purity of the elutions was checked by SDS-PAGE analysis. The yield for this protein preparation is 8 mg/ml and the total protein amount is 30 mg per 2 L culture. The protein was aliquoted and flash frozen.

* His-ASF/SF2(FI) pET19 and His-ASF/SF2 (105-248) pET15b are provided by Dr. Cho and Dr. Ngo, respectively.

D. Refolding SRPK1 and ASF/SF2 complex or Spacer and SRPK1(1-70) complex

SRPK1 and ASF/SF2 were mixed in the ratio 1:1 or 1:2 respectively and diluted to 0.3mg/ml using denaturing buffer (500 mM KCl, 20 mM Tris pH 7.5, 2 mM DTT, 10% Glycerol, 1 mM $MgCl_2$, and 6 M Urea). The complex were incubated on stirring at 4^{o}C for 40 minutes, followed by two times dialysis in refolding buffer (500 mM KCl, 20 mM Tris pH 7.5, 2 mM DTT, 1 mM $MgCl_2$ and 20% Glycerol). The third dialysis takes place in high pH buffer of 500 mM KCl, 20 mM Capso pH 9.5, 1 mM DTT, 1 mM $MgCl_2$, and 5% Glycerol. The refolded complex was

concentrated to 3 mg/ml and load onto a 16/20 Superdex 200 size-exclusion column, pre-equilibrated with the buffer that contains 500 mM KCl, 20 mM Capso pH 9.5, 5% Glycerol, and 1mM DTT. The peak fractions were evaluated by SDS-Page analysis and the fractions of the desired peak are pooled for concentration. A typical yield for this protein preparation is 2mg/ml and the total protein amount is 10 mg per 50mg of protein mixture.

E. *In vitro* kinase assays

4 μM of SRPK1 and 40 μM of full length ASF/SF2 were mixed in kinase buffer (50 mM Tris pH 7.5, 10 mM $MgCl_2$, 1 mg/ml BSA, and 1 mM DTT) for 5 minute at 25^{o}C. The reaction was inititated with 200 μM of cold ATP and trace amount of γ^{32} ATP. The reaction was allowed to proceed for a specific time and quenched by 4X SDS dye. Phosphorylated protein was detected by autoradiography.

F. Limited Chymotrypsin Digestion

Full length SRPK1was diluted to 1 mg/ml using Digestion buffer (100 mM NaCl, 20 mM Tris pH 8.5, 1 mM DTT). Chymotrypsin was added to full length SRPK1 at 1:2500 digestion ratio to start the digestion reaction. Aliquots of the reaction were removed at specific time-points and analyzed by SDS-PAGE.

G. GST Pulldown Assays

1:1 ratio of SRPK1constructs were incubated at 4^0C for 30 minutes. The mixture was then incubated in 15 ul GST resin (GE Healthcare), pre-equilibrated in Binding buffer (150 mM NaCl, 25 mM Tris pH 7.5, 0.5% Triton X-100, and 1 mM DTT) for 1 hour. The protein resin suspension was washed three times with Binding buffer. The soluble fraction of the mixture was analyzed by SDS-PAGE for protein binding. GST protein was used as a negative control.

H. Co-immunoprecipitation (Co-IP) assays

HEK-293T cells were co-transfected with two plasmids of different SRPK1 constructs or SRPK1 and Clk/Sty, using Lipofectamine 2000 (Invitrogen). After 24-hour postransfection, cells were lysed using Binding buffer (150 mM NaCl, 50 mM Tris pH 8.0, 0.1% SDS, 1% NP-40, 1 mM DTT, 1 mM PMSF, and ΣPIC). Bradford assay was performed to determine total protein concentration and 1 mg of protein lystate was used for co-IP. The protein lysate was pre-cleared with 20 ul of pre-equlibrated protein G slurry, followed by centrifugation to separate the soluble and resin-bound fractions. The soluble fraction was incubated with 1ul of antibody specific to one of the transfected constructs at 4^oC for 3 hours before 35ul of pre-equilibrated protein G slurry was added to the soluble sample for another 3 hours of incubation at 4^oC. The sample was spun down at 4200 g force for 1 minutes, followed by two times washing with Wash buffer (1x PBS and 0.5% Triton X-100). The sample was then incubated in 4x SDS dye at 100^oC for

5 minutes. Centrifugation at high speed was done to separate the soluble fraction from the resin. The soluble fraction was analyzed by Western blot.

I. Indirect immunefluorescence assays

HeLa cells were plated onto poly-lysine coated glass coverslips 12-24 hours prior to transfection. SRPK1 constructs were either singly transfected or co-transfected with ASF/SF2 or Clk/Sty using Lipofectamine 2000 (Invitrogen). After 24-48 hours post transfection, cells were fixed by 4% paraformaldehyde for 15 minutes, followed by permeabilization using 0.1% TritonX-100 for 15 minutes. Cells were blocked with 1% BSA before staining with the primary antibody specific for the transfected protein for 1 hour. To prevent nonspecific binding, cells were washed six times with 0.1% BSA 1x PBS. Cells were then stained with fluorescent-conjugated secondary antibody for another 1 hour, followed by overnight incubation in a mounting solution containing 4,6-diamidino-2-phenylindole (DAPI) (vectashield; Vector Laboratories, Burlingame, CA). Cells were analyzed under a Zeiss Axiophot microscope and images acquired with a Hamamatsu ORCA-ER digital camera with Improvision OpenLab 3.1.5 software.

J. Nuclear and Cytoplasmic Fractionation (modified Protocol from Han & Braiser 1997)

HEK-293T cells were cultured in DMEM supplemented with 10% fetal bovin serum and 1X PSG. Cells were then transferred to cold eppendorf tubes. Cells were pelleted and resuspended in cytoplamic lysis buffer that contains 320 mM Sucrose, 5 mM MgCl2, 10 mM Hepes 7.5, 1% Triton X-100. Cellular nuclei were separated from the cytoplasmic lysate after centrifugation at 500 g for 5 minutes. Nuclei were washed twice and then resuspended in Nuclear lysis buffer that contains 10 mM Hepes 7.9, 25% Glycerol, 420 mM NaCl, 1.5 mM $MgCl_2$, 0.2 mM EDTA, and 0.5 mM DTT. The nuclei mixture was then freeze-thawed three times at liquid nitrogen temperature and 37^{o}C water. Nuclei lysate was then collected after centrifugation at 16000g for 5 minutes. The efficiency of fractionation was evaluated by western blot against tubulin or IκBα for the cytoplasmic fraction and against ASF/SF2 or Histone for that of the nucleus.

K. Chemical Crosslinking Experiment on SRPK1-ASF/SF2 complex

The foremost step in crosslinking assays is to ensure the absence of any background crosslinked complexes by removing possible surface-exposed cysteines. Cysteine 68 of the kinase ΔNS3 was found on the surface based on the crystal structure of ΔNS1 and the one of the complex of ΔNS3-ASF/SF2 (courtesy of Dr. Ngo) and thus was mutated to serine. ASF/SF2 (105-248)-His had C148 mutated to serine. Thus, the complex of ΔNS3 C68S and ASF/SF2 (105-248) C148S was treated as the no crosslinking background. This surface cystein-free background also served as the template for additional mutations in

docking interaction sites on ΔNS3 and ASF/SF2. For ΔNS3, two independent cysteine mutations, W88C and K604C, were created in the C68S background. For ASF/SF2, all four cysteine mutations,Q135C, K193C, R204C, and Y226C, were created in the C148S background. All mutants were made by using mutagenic oligonucleotides and confirmed by DNA sequencing. Mutant proteins were expressed and purified by using methods as described earlier for the wild-type complex. Each protein complex was diluted to 2 mg/ml using buffer containing 500 mM NaCl, 5 mM Tris pH 7.5, 5% Glycerol, and 10 mM DTT. After the complexes were incubated on ice for 1 hour, they were exchanged with the crosslinking buffer (500 mM NaCl, 5 mM Tris pH7.5, and 5% Glycerol) using desalting spin columns (Pierce). The protein complexes were further diluted to 0.4mg/ml with crosslinking buffer in order to be used for the following reactions: (1) 0.03 mM BMB (Pierce), (2) 0.03 mM BMB + 10 μM (or 50 μM) ATP or 50 uM ADP + 4 mM $MgCl_2$, (3) 0.03 mM BMB + 4 mM $MgCl_2$, (4) 10 mM DTT + DMSO (equal volume with the amount of BMB added in the reaction 1-3), and (5) DMSO. The reactions were carried out at 4^0C. Equal-volume aliquots (reaction 1-4) were removed at each time point and quenched by 4x reducing SDS dye. The reaction 5 was quenched by 4X nonreducing SDS dye. The reactions were resolved by SDS-PAGE and analyzed by Coomassie blue staining

L. Circular Dichroism of SRPK1 constructs

5 μM of SRPK1 was prepared in 100 mM NaCl and 20 mM Tris pH 7.5 before being applied to Circular Dichroism spectrophotometer (Model 202, Howard Hughes Medical Institutes). The secondary structure signature of SRPK1 was recorded from 250nm – 200 nm wavelength.

M. H/D exchange and mass spectrometry of full length SRPK1

100 μM of SRPK1 was incubated in H_2O or D_2O at room temperature. At a specific time-point, the incubation was quenched by Quench solution (10 μl of 100 μM SRPK1 and 90 μl of 0.1% TFA, pH 2.0), followed by peptic digestion at 4^oC. The digested sample was applied to MS/MS spectrometry (Perspective Biosystem) for peptide analysis. The spectrometry analysis is calibrated by standard peptides (MH^+: 1296.6853, 2093.0867, 2465.1989, and 3657.9294). The peptides of particular mass were then identified by MS Nonspecific program (Prospector, UCSF) and the peptide sequence was further confirmed by MALDI TOF/TOF analyzer (Applied Biosystem). H/D exchange at a specific mass envelope was aligned by Data Explorer program.

CHAPTER III

DOCKING INTERACTION BETWEEN SRPK1 & ASF/SF2

A. Introduction:

2.4 Å X-ray crystal structure of a complex of SRPK1 and a 9 mer peptide derived from Npl3p led to the discovery of the docking groove of SRPK1 and the docking motif in ASF/SF2 (Ngo et al., 2005). The docking groove of the kinase is located in the bottom of the kinase primarily constituted by an insert, helix αG and the loop between helix αF and αG. The groove is also highly negatively charged which is prone to interact with a positively charged peptide. The docking motif in ASF/SF2 was shown to be the sequence R^{191}VKVDGPR^{197}, which was thought to be located between the RRM and RS domains. Direct interactions between the docking groove of SRPK1 and the docking motif in ASF/SF2 showed to govern the mode of phosphorylation of ASF/SF2. A docking groove mutant of SRPK1 binds to ASF/SF2 weakly and displays distributive mode of phosphorylation on ASF/SF2. Also, when the docking motif in ASF/SF2 was deleted, more serines in the RS domain of ASF/SF2 were phosphorylated by SRPK1, indicating the role of the docking motif in restricting the phosphorylation event to the N-terminal part of the RS domain of ASF/SF2. This restricted mode of phosphorylation by SRPK1 also agrees with the previous study that showed SRPK1 phosphorylates approximately half the sites in the RS domain in a processive manner *in vitro* (Aubol et al., 2003). It was concluded that this restricted mode of phosphorylation by SRPK1 generates the hypophosphorylated state of ASF/SF2 while CLK/Sty phosphorylates the rest of the RS domain to generate the hyperphosphorylated state of ASF/SF2.

Our laboratory has completed a second crystal structure of the complex between SRPK1 and ASF/SF2. This structure showed that docking groove of the kinase binds to the RS domain (residues 201-210), instead of the RVKVDGPR (residues 191-197), as determined by biochemical experiments. It was hypothesized that the kinase binds to both docking motifs of the substrate but during different times of phosphorylation. A sliding mode of phosphorylation would justify this docking interaction event: whether the docking at the RRM docking motif or the N-terminal RS docking motif in ASF/SF2 occurs first to regulate the processive phosphorylation by SRPK1 and direction of phosphoryl transfer to the RS domain (C'-to-N' termini or N'-to-C' termini in ASF/SF2). One of the ways to test the above hypothesis is to use chemical cross-linking assay. This assay relies on the spatial proximity between two cysteines; when in close proximity, a crosslinker will form a disulfide bridge between the two cysteines. If ASF/SF2 binds to the docking groove of SRPK1 at two sites, both the cysteines in the docking sites of ASF/SF2 will be able to crosslink with the cysteines in the SRPK1.

B. Results:

1. Strategy for cysteine chemical crosslinking

SRPK1 binds to ASF/SF2 with an unusual high affinity (K_d= 25- 50nM) for

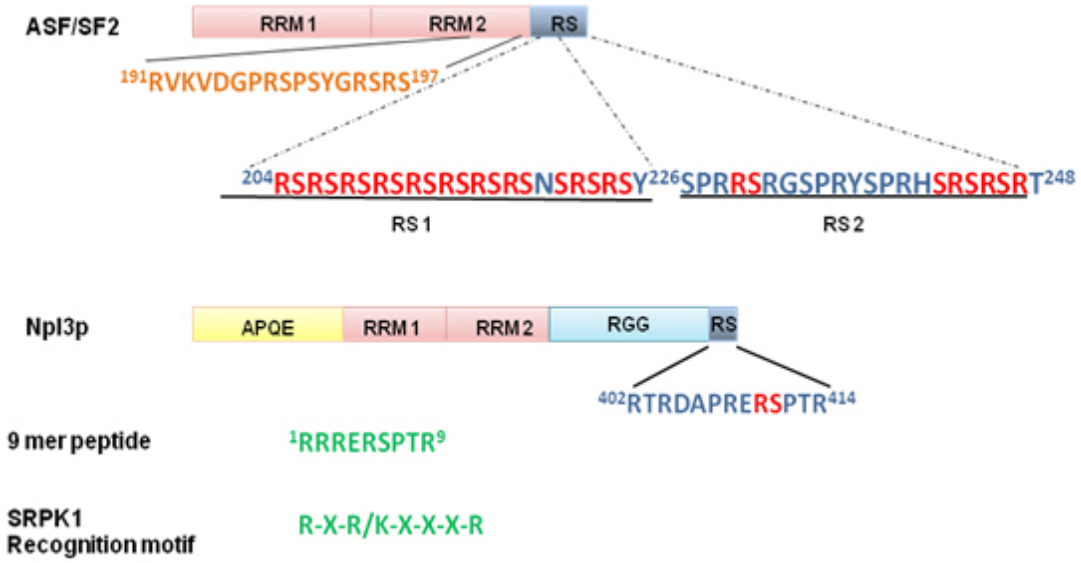

Figure 3.1: Docking motif in ASF/SF2. (Top) Domain organization of ASF/SF2: ASF/SF2 contains two N'-terminal RRM domains followed by an RS domain. The RS domain can be divided into two subdomains: RS1 contains ten RS dipeptides in tandem and RS2 has multiple discontinuous RS dipeptides. Npl3p, an SR-like protein in yeast, contains only one RS dipeptide at the C-terminus and is phosphoyrlated by Sky1p. (Below Npl3) 9 mer peptide was synthesized based on the single phosphorylation site on Npl3 (S411 being the P site serine). The peptide binds to SRPK1 docking groove (Ngo et al., 2005). This peptide sequence suggests the sequence of SRPK1 recognition motif, which has sequence homology to the C'-terminal end of the RRM2 in ASF/SF2 (residues 191-197).

A) N-terminal RS and SRPK1 B) C-terminal RRM2 and SRPK1

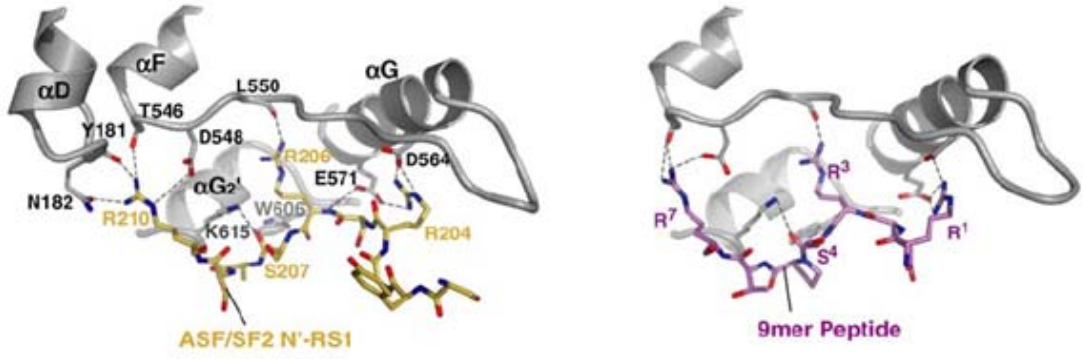

Figure 3.2: X-ray structures of SRPK1:ASF/SF2 docking interactions (Ngo et al., 2008). The RS peptide from ASF/SF2 binds to the SRPK1 docking groove in an extended conformation. A) The docking peptide extends from residue 201 to 210. Residues R204, R206, S207, and R210 of the substrate and Y181, N182, T546, D548, T546, D548, L550, E571, D564, W606, and K615 of the kinase are involved in the binding interaction. B) A 9-mer peptide, derived from the docking phosphorylation site of the yeast SR-like protein Npl3p, is involved in similar interactions with the kinase-docking groove, as described previously (Ngo et al., 2005). Hydrogen bonds are depicted by dotted lines.

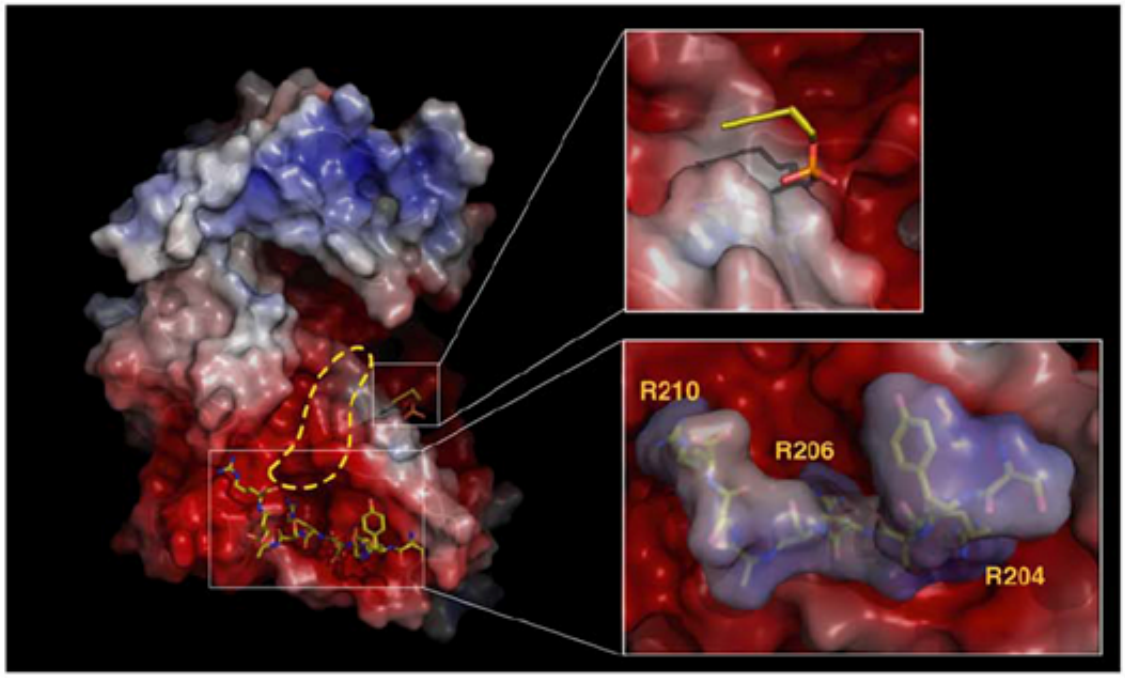

Figure 3.3: Substrate binding at the docking site is electrostatic in nature (Ngo et al.,2008). High negative potential within the docking groove (depicted by red) and positive potential of the N'-RS (depicted by blue) confirms that the docking interaction is predominantly electrostatic. Extension of the high negative charge potential to the active site implies that the rest of the highly basic peptide extends along this path.

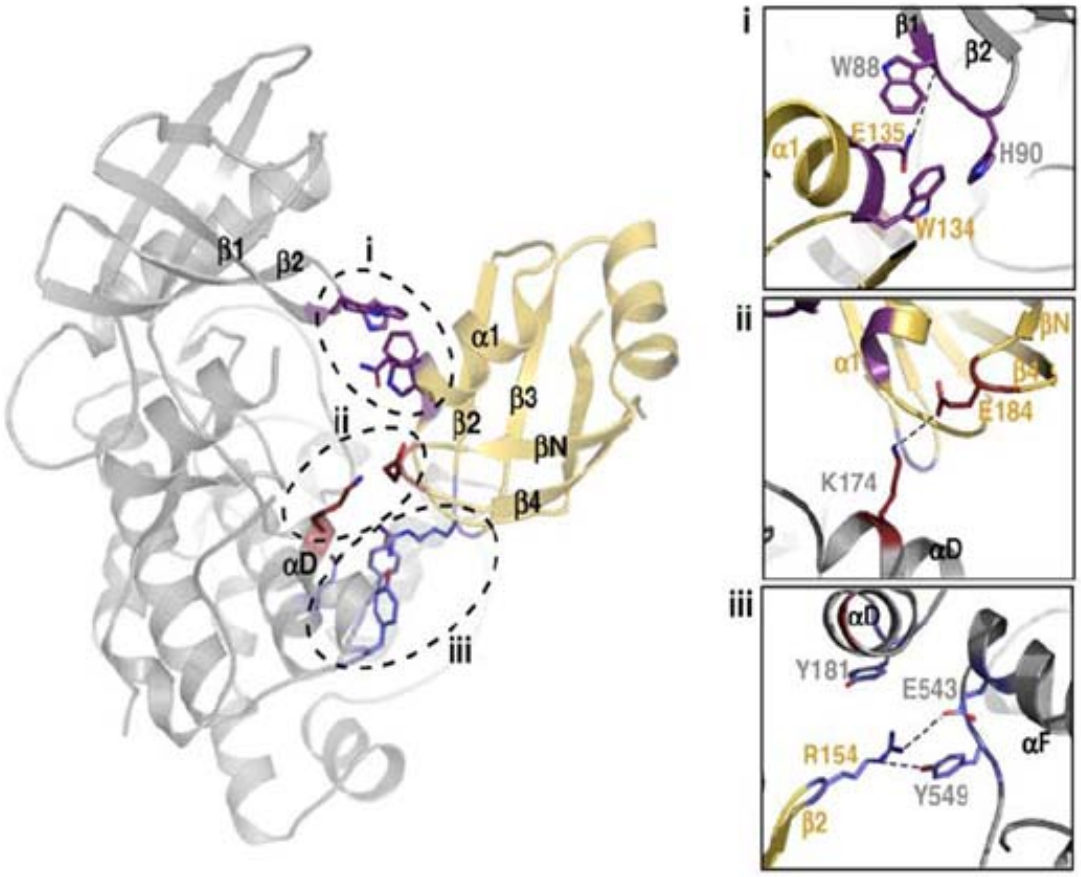

Figure 3.4: Interactions between RRM2 of ASF/SF2 and SRPK1 (Ngo et al., 2008). The three finger-like projections from RRM2 are marked dotted ovals (left). Important residues involved in the interactions between each of the fingers and the kinase are shown in detail in the insert (right). Residue of W88 in the kinase and Q135 in ASF/SF2 are used to generate positive control of the chemical crosslinking assay.

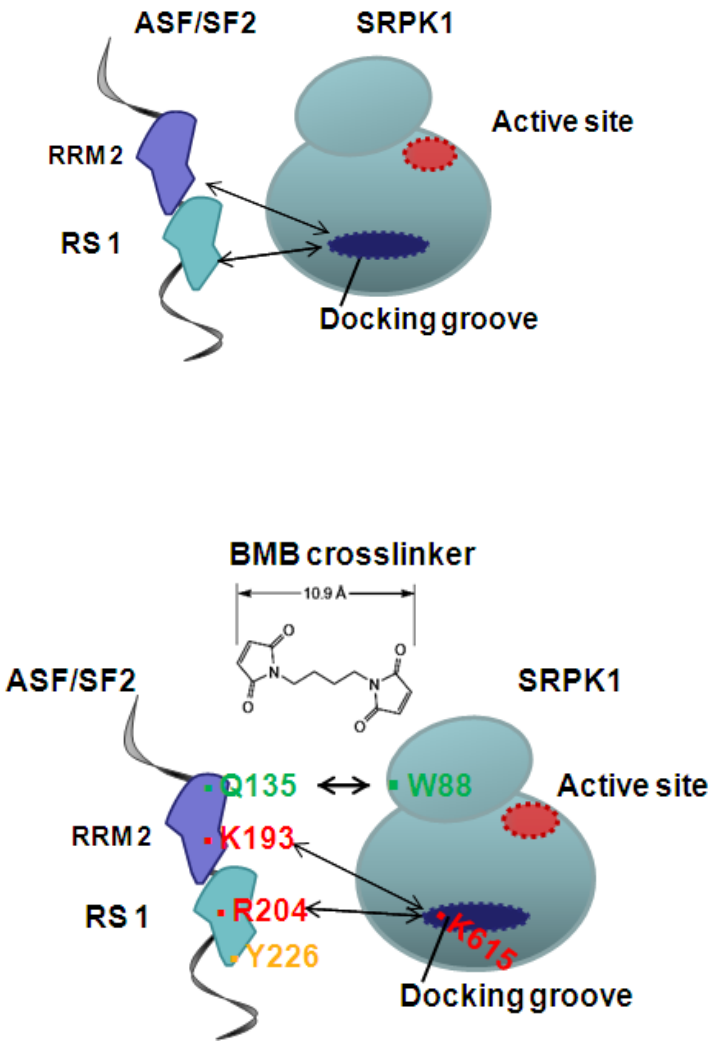

Figure 3.5: Proposed model for docking interactions between SRPK1 and ASF/SF2. Strategic cysteine mutations are designed according to X-ray structural studies (Figure 3.2-3.4). ASF/SF2 Q135 is shown to interact with SRPK1 W88; thus, the mutations at these sites (in Green) can generate a positive control for chemical cysteine crosslinking assay. ASF/SF2 K193 (in Red) resides within the vicinity of the docking motif identified by SRPK1. ASF/SF2 R204 (in Red) is shown to interact with the docking groove of SRPK1 and it resides at the beginning of the N'-terminal end of the RS1 domain. Double-head arrows indicate where the crosslinker form disulfide bridge. The chemical crosslinker, Bismaleimide (BMB), is drawn in molecular atom (Thermo Scientific).

a kinase-substrate pair (Aubol et al., 2003; Ding et al., 2006). Such high affinity suggests that SRPK1 can rescue ASF/SF2 from precipitation out of solution by binding to ASF/SF2 and enhance its solubility in the complex form. To obtain the native form of ASF/SF2, which is known to be aggregated in solution, I purified ASF/SF2 from *E. coli* under the denaturing condition and then refolded with SRPK1ΔNS3 and the complex is isolated. I made cysteine mutations at strategic positions in both SRPK1 ΔNS3 and ASF/SF2 to allow cysteine cross-lining to occur. The complex between the Cys-mutant proteins was purified in a similar manner as described for the wild type complex (Chapter 2). The cross-linked complexes in chemical crosslinking assays were resolved by SDS-PAGE to clarify if both docking events between SRPK1 and ASF/SF2 were possible.

My laboratory's x-ray structure of SRPK1:ASF/SF2 complex showed that the N-terminal RS domain of ASF/SF2, S^{201}YGRSRSRSR^{210}, interacts with the docking groove of SRPK1 with R204 being one of the charged residues ion-pairing to the acidic residues of SRPK1 (Figure 3.1-3.3). Thus, R204C in ASF/SF2 was generated for the study of the docking site at the N-terminal RS domain. Similarly, K193, being one of the sites for interaction with SRPK1 as previously identified in Ngo et al.[2005] was mutated to cysteine to examine the docking site at the C-terminal of the RRM2 (Figure 3.1-3.3). In the kinase-substrate bound form, K604 of SRPK1 is located near the docking groove and in the proximity that can crosslink with residues in the docking motif of ASF/SF2; thus SRPK1 [K604C] was used to form complex with ASF/SF2 [R204C] or

[K193C]. The ASF/SF2 C204-SRPK1 C604 cross-link would prove initial docking interaction whereas ASF/SF2 C193-SRPK1 C604 cross-link would prove late docking interaction. To prevent aberrant crosslinking of the complex, all other surface cysteines were mutated to generate a surface cysteine-free kinase and substrate, SRPK1 [C63S] and ASF/SF2 [C148S], respectively. Also, to verify the chemically cross-linked complex in SDS-PAGE gels, we made a complex of SRPK1 [C63C & W88C] and ASF/SF2 [C148S & Q135C] as the positive control for the crosslinking experiment (Figure 3.5). W88 and Q135 do not participate in the docking interaction but are implicated in the overall stabilization of the complex; for this reason, the cysteine mutations at these sites was expected to generate a tight complex for the crosslinking study as seen in Figure 3.9.

2. ASF/SF2 slides along the SRPK1 during phosphorylation:

As shown in Figure 3.9, both R204C and K193C in ASF/SF2 could crosslink to K604 in SRPK1. Yet, the amounts of the crosslinked complex based on these docking motifs in ASF/SF2 are not the same, suggesting that these docking motifs exhibit some mechanistic difference in the mode of docking interactions. K193C in ASF/SF2 cross-linked to SRPK1 more in the presence of ATP (Figure 3.10). K193 constitutes the very end of the C-terminus of the RRM2 domain, which adopts the canonical RRM fold comprising of beta sheets and two α helices. Such fold indicated that K193 is occluded from docking interaction

A)

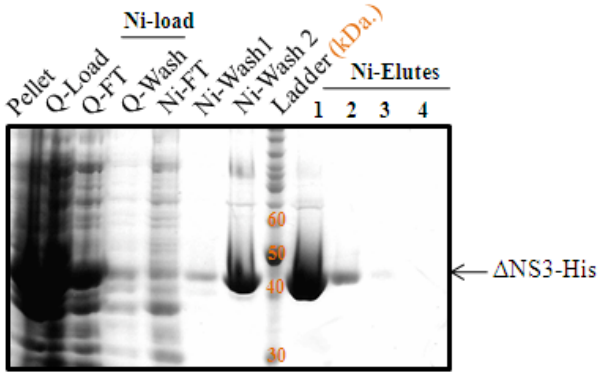

B)

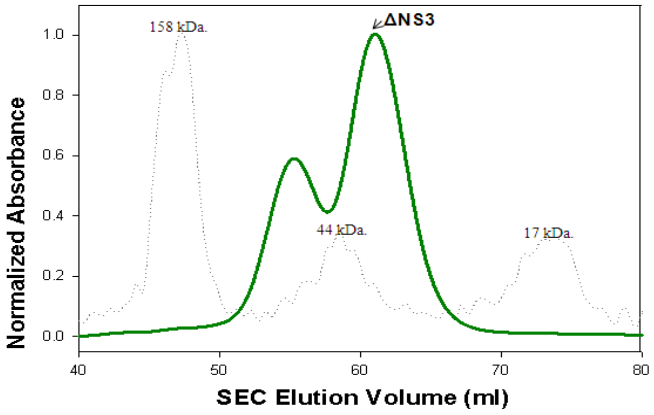

C)

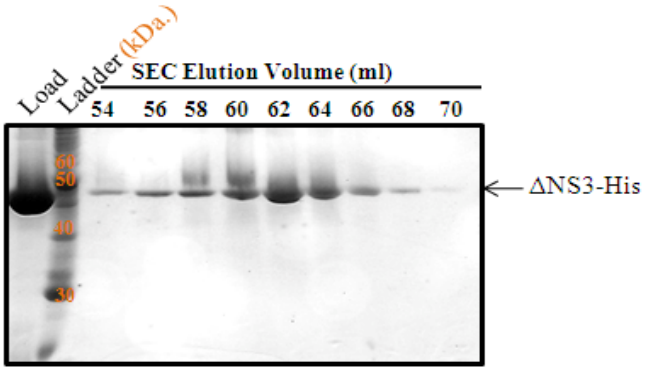

Figure 3.6: Purification of ΔNS3 mutant constructs. ΔNS3 [C63S & W88C] and ΔNS3[C63S & Q135C] are purified from the same method using Q-sepharse column, Nickel-NTA column and size-exclusion chromatography (Hiprep-Supedex75).

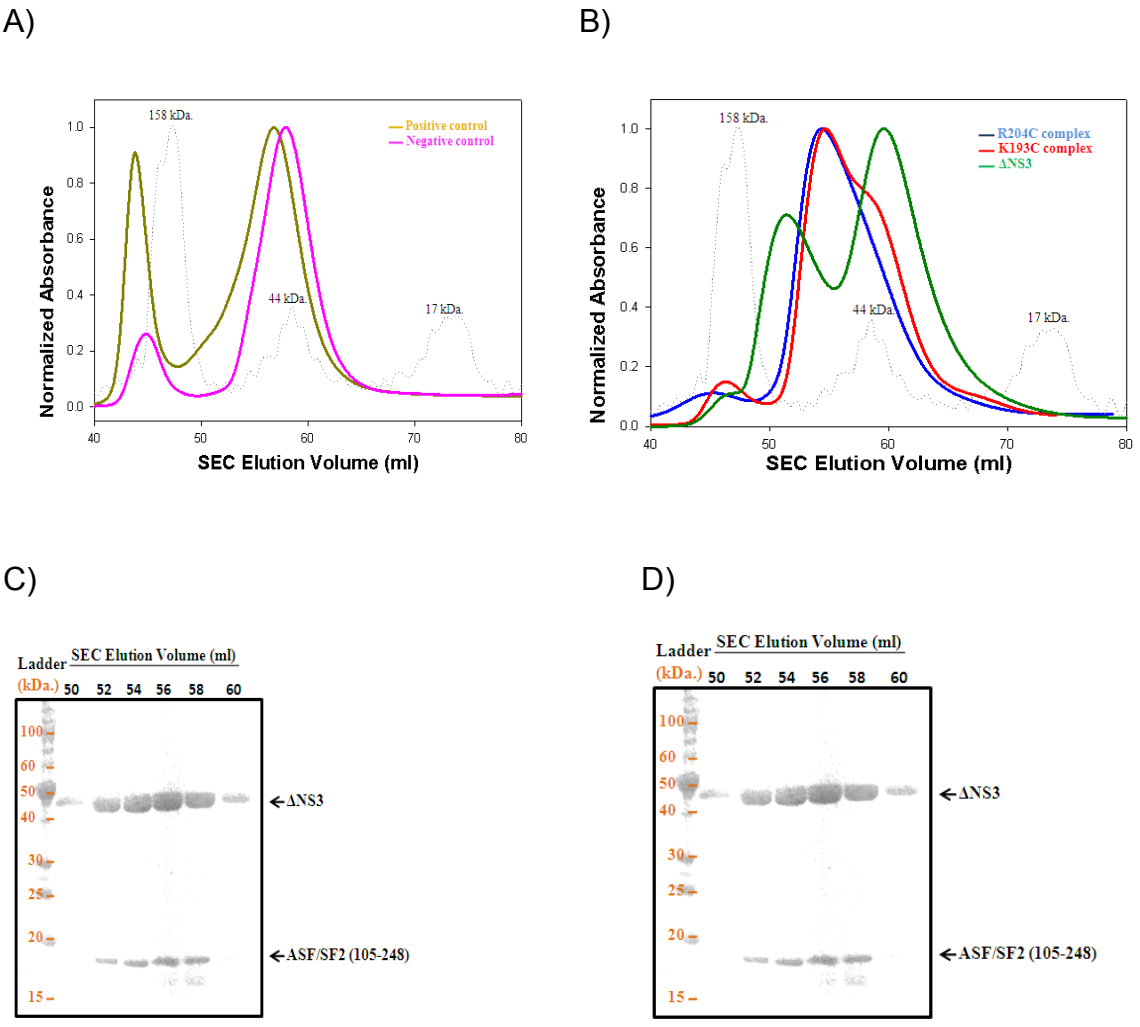

Figure 3.7: Preparation of ΔNS3:ASF/SF2 (105-248) mutants. A) Size-exclusion chromatography of refolded complex of ΔNS3:ASF/SF2 (105-248) mutants: ΔNS3 is purified independently as shown in figure 4; the expected molecular weight of the complex (61.96 kDa by ProPagram) is observed in the right range of the standard; ASFSF2 construct is purified in 6 M Urea passing from Q-sepharose to Nickel-NTA column. The kinase and substrate were refolded together. The positive control is ΔNS3 [C63S & W88C]:ASF/SF2 (105-248) [C148S & Q135C]. The negative control is ΔNS3 [C63S]:ASF/SF2 (105-248) [C148S]. B) (left) Kinase and subtrate are purified independently. (Right) Refolded complex size-exclusion peak in part A is analyzed by SDS-PAGE. C) Kinase activity is not altered by cysteine mutation. D) Docking interaction between kinase and substrate is not altered by cysteine mutation.

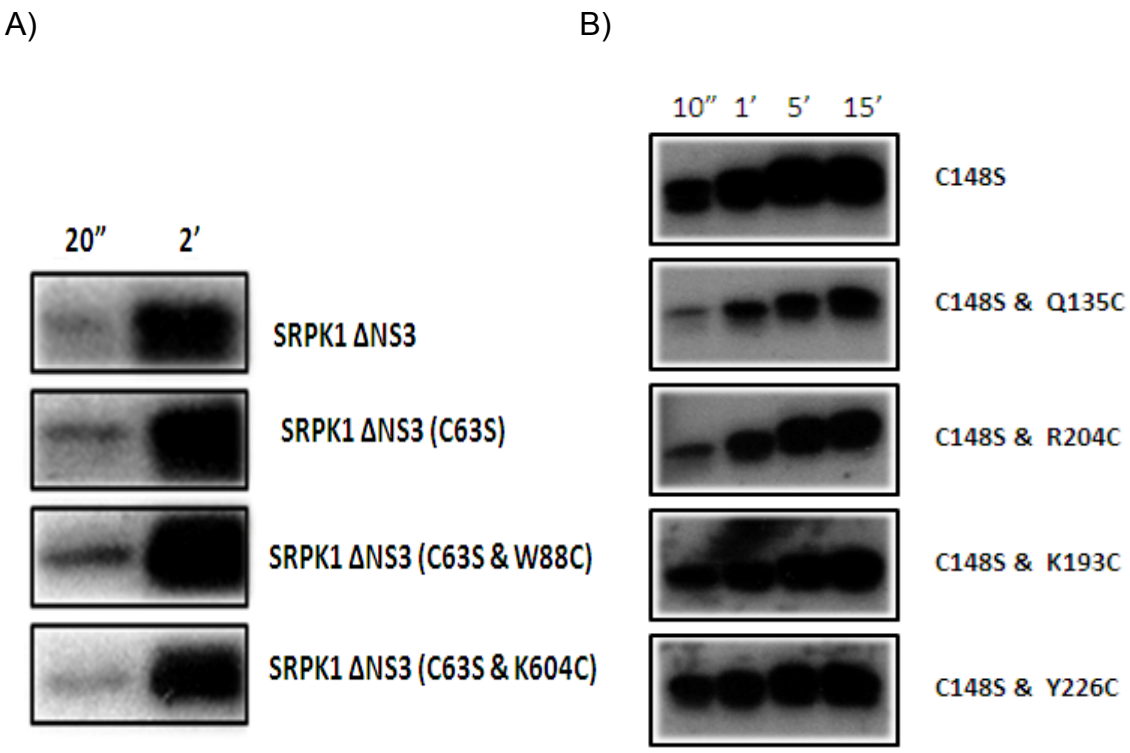

Figure 3.8: Kinase assays of ΔNS3:ASF/SF2 (105-248) mutants. A) Kinase assay was carried out to test the kinase activity of the kinase mutants: ΔNS3 [C63S], ΔNS3 [C63S & W88C], and ΔNS3 [C63S & K604C]. Kinase mutants show comparable kinase activity to full length ASF/SF2. ASF/SF2 was purified by Dr. Cho. B) Kinase assays were conducted to test the kinase activity of the complex mutants. The complex mutants show similar kinase activity. The mutation sites do not affect complex formation or the kinase activity.

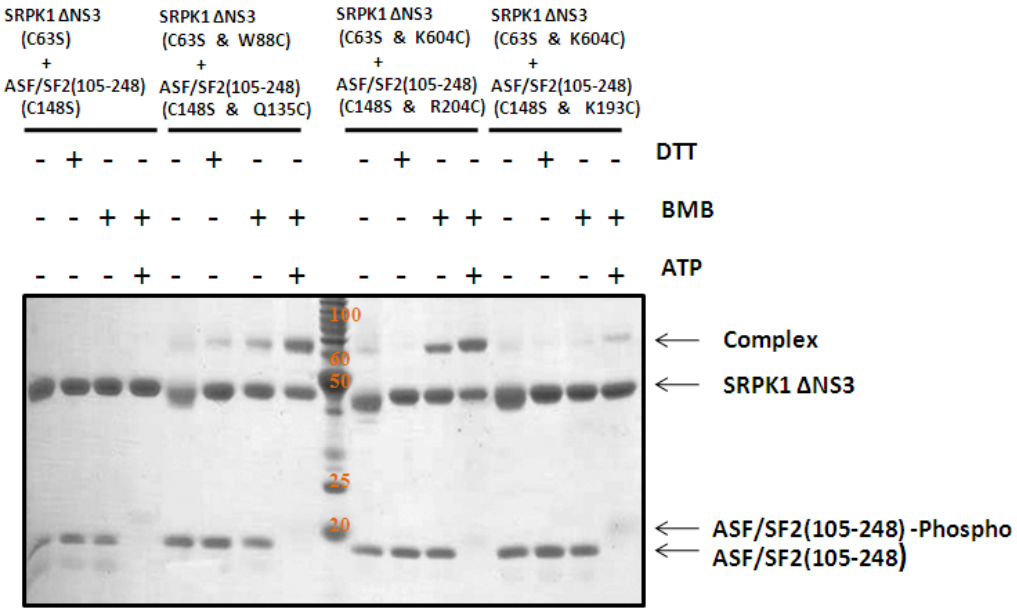

Figure 3.9: Phosphorylation of ASF/SF2 RS1 domain by SRPK is regulated by docking interaction. The first set (left) is the negative control in which the kinase and substrate have cystein-free surface and docking interface. The next set is the positive control, in which the interacting site between kinase and substrate is mutated to cysteine residues. The interacting site comprises of kinase W88 and substrate Q135. The two docking interactions are the last two sets after benchmark ladder.

A)

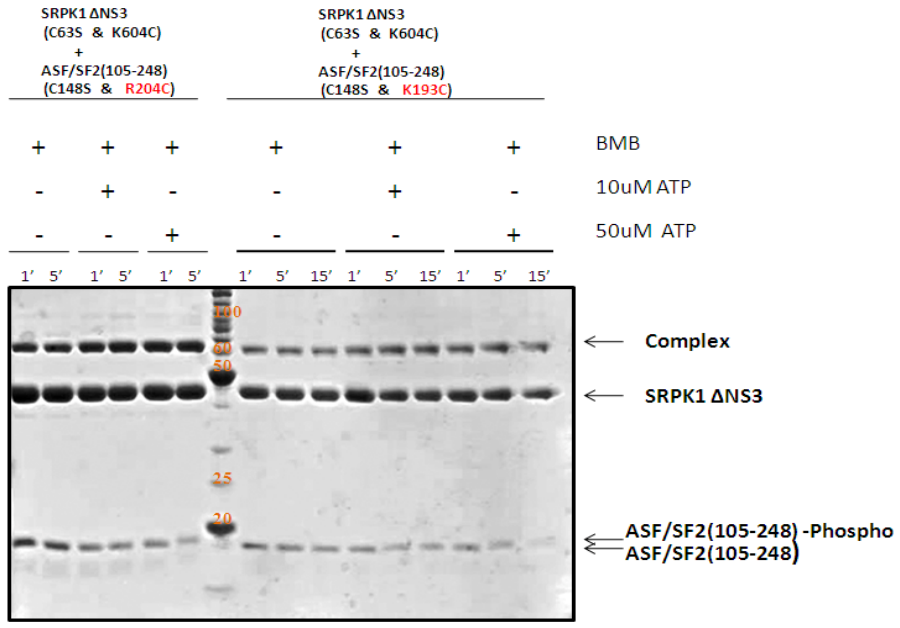

B)

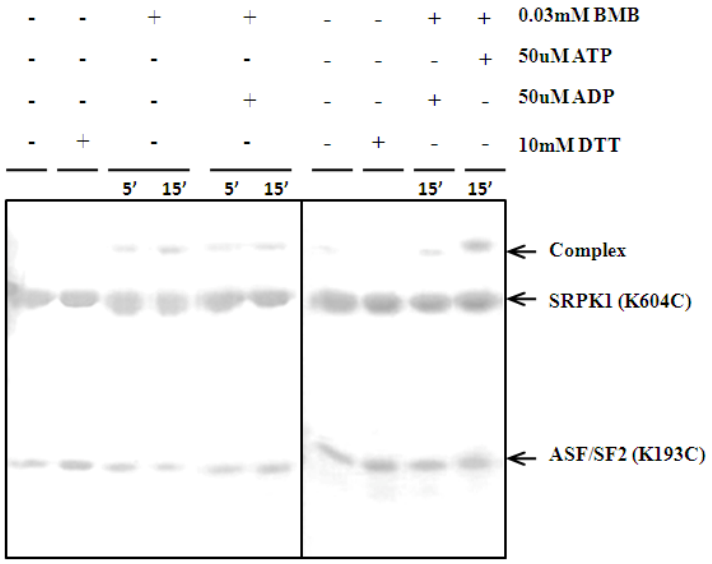

Figure 3.10: Disulfide crosslinking experiments indicate that ASF/SF2 possesses two docking motifs but each of the motifs interacts with the kinase-docking groove at different ATP constraints. Limited amount of ATP was used to improve the amount of the crosslinked complex. The efficient crosslinking between K193C and K604C requires the phospho priming of the substrate.

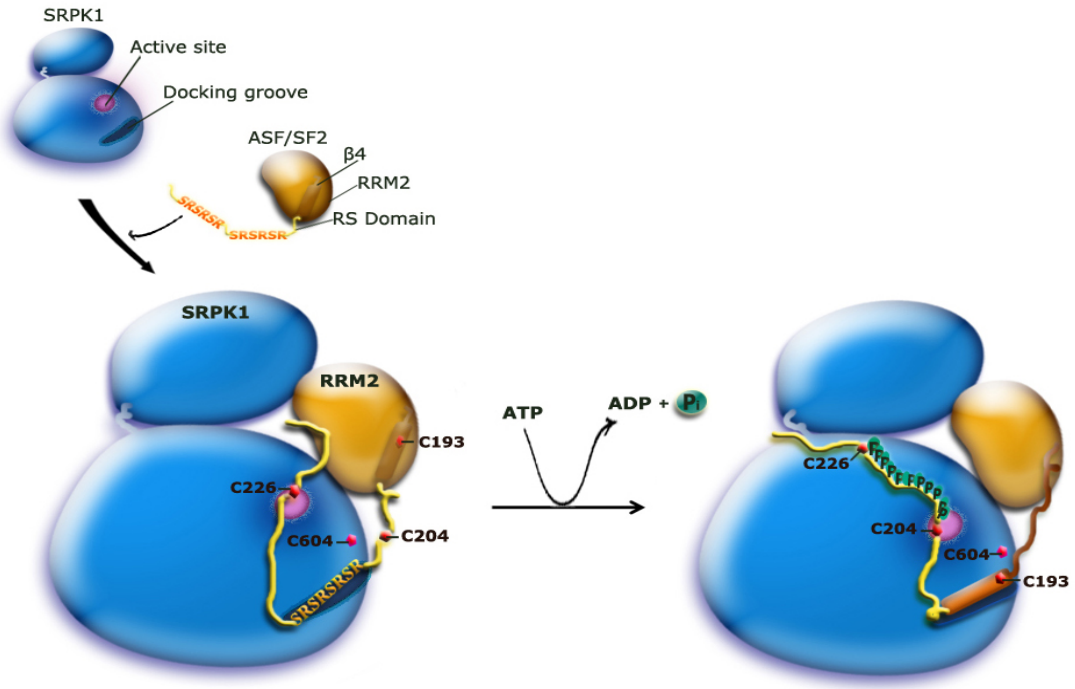

Figure 3.11: Proposed model for docking interactions between SRPK1 and ASF/SF2. N'-RS docking motif interacts to the docking groove first to generate primed substrate for the C'-RRM docking motif to unfold from the RRM and occupy the kinase docking groove.

unless the β4 strand that K193 belongs to unfolds from the RRM fold and moves to the docking groove in SRPK1. As mentioned earlier that the affinity binding of the complex is at 50 nM and SRPK1 protein as being a processive kinase, how ASF/SF2 manages to dissociate during the course of phosphorylation and switch to the alternative docking motif in the RRM2 confirmed our hypothesis that the alternative docking motif in ASF/SF2 is needed for completion of phosphorylation in the RS1 domain and this motif only come into picture upon substrate-primed phosphorylation. To examine this hypothesis, we studied the K193 crosslinked complex in the presence of limited amount of ATP and ADP. As seen in Figure 3.9, complete phosphorylation at high amount of ATP caused ASF/SF2 [C148S, K193C] to dissociate from SRPK1 [C63S, K604C] before the crosslink reaction occurred. The substrate might possibly lose affinity with progressive phosphorylation. We figured that partial phosphorylation of the RS 1 domain would be enough to prime the unfolding of the β4 strand and allow the alternative site to be in close proximity to crosslink to the K604 in SRPK1. In 50 uM ATP, partial phosphorylation occurred and we were able to observe the crosslinked complex of SRPK1 [C63S, K604C] and ASF/SF2 [C148S, K193C], which we could not observe at 2 mM ATP or 50uM ADP (Figure 3.9). Thus, we conclude that ASF/SF2 possesses two docking motifs and these motifs allow the substrate to translocate from the kinase-docking groove to the active site in a sequential manner during catalysis (Figure 3.10-3.13).

C. Discussion:

The result of the chemical cross-linking experiment described above showed the expected interaction-based on our previous studies the two motifs were able to crosslink to the docking groove in SRPK1. The second docking motif (β4) in the RRM2 was found to be phosphorylation dependent, suggesting its interaction with the kinase during the completion of phosphorylation in the RS domain. Thus, the chemical cross-linking experiment under the condition of limited ATP allowed us to confirm that the unfolding of the β4 from the RRM facilitated the second docking motif to move to the kinase docking groove during the course of catalysis. During the time when β4 binds to the kinase groove, N-terminal serines of RS1 undergo phosphorylation. Therefore, the cross-linking experiments also confirmed the direction of catalysis occurring from the C-terminus to the N-terminus of the RRM2.

Our collaborator, Dr. Adams, conducted circular dichroism (CD) on the complex of SRPK1 and ASF/SF2. The CD result provided the secondary structure signature structure of ASF/SF2 over the course of catalysis and revealed the impact of nucleotide on the β sheet signature in ASF/SF2, supporting our data about the unfolding of β4 strand from the β sheet of the RRM.

All the experiments described here provided insight into the mechanism of interaction between kinase and substrate. SRPK1 recognizes the RS motif first and then the RRM motif without dissociation of the substrate during catalysis.

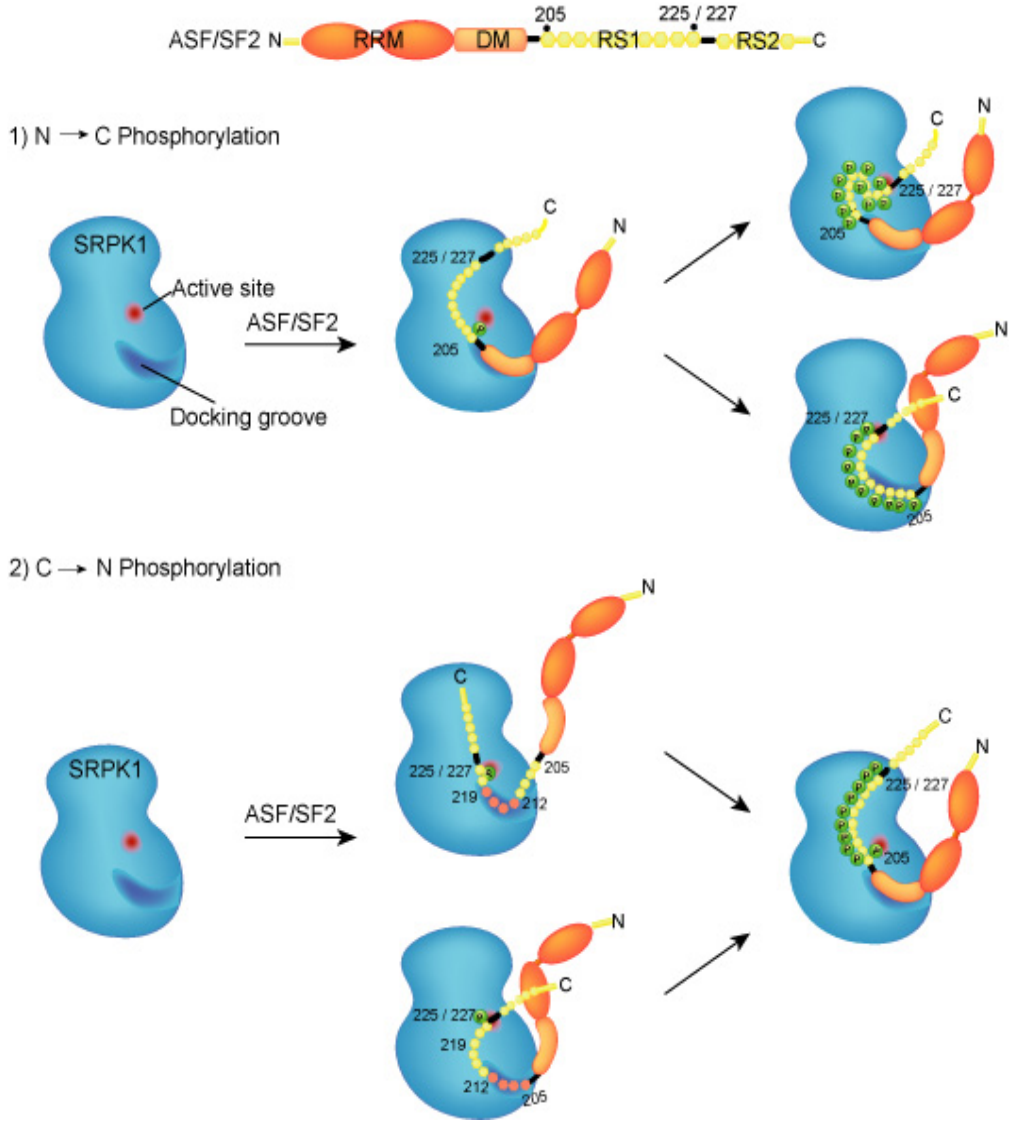

Figure 3.12: Proposed model of unfolding and sliding modes ASF/SF2 for complete phosphorylation at the RS1 domain. The sliding of unfolded ASF/SF2 determines the direction of phosphoryl transfer to the RS1 domain in ASF/SF2. Phosphoryl transfer can occur either from N' to C' direction of RS1 or vice versa. The result described in figure 5 suggests that phosphorylation occurs from the C' to N' direction.

A)

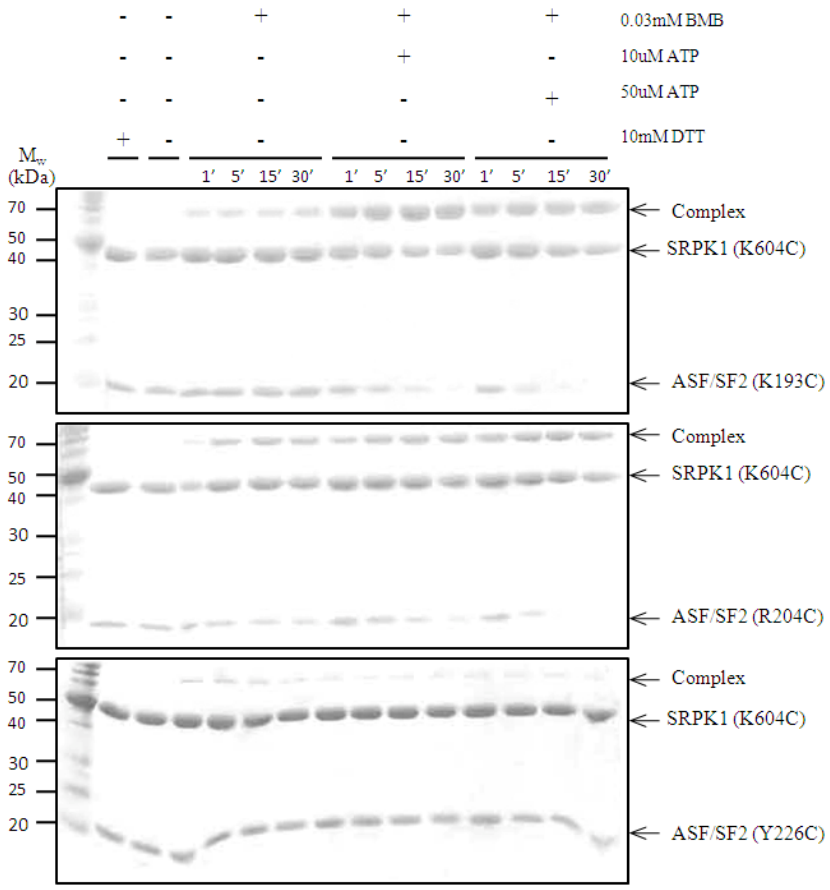

B)

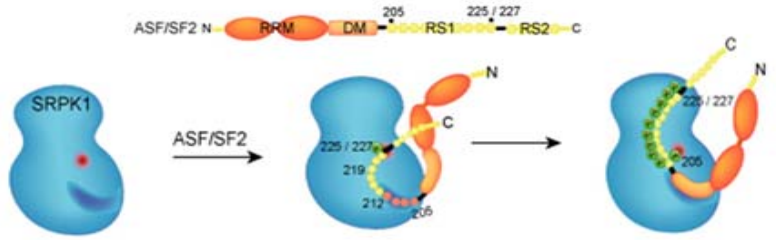

Figure 3.13: Phosphorylation of ASFSF2 RS1 domain by SRPK1 occurs from C'-to-N' direction. A) Crosslinked R204 complex occurs fast in the absence of ATP whereas K193 complex could not be effeciently crosslinked without ATP. The amount of Y226 crosslinked complex remains constant or even diminishes over the course of phosphorylation. B) The summary of direction of phosphorylation of ASF/SF2 by SRPK1.

Many studies showed that many kinase proteins recognize their substrate in a phosphorylation manner; the substrate needs to be primed by upstream kinases (Figure 1.9). In our case, we observe that SRPK primes its own substrate at the RS domain; together with the unfolded RRM and the phospho-RS, the RRM docking motif becomes the next kinase docking substrate. This phosphorylation manner reinforces the processivity of SRPK1 kinase for activation of SR proteins.

Why does SRPK1 phosphorylate ASF/SF2 processively? By exploiting stable binding, SRPK1 ensures the substrate for complete phosphorylation as well as the extent of phosphorylation. SRPK1 phosphorylates approximately 10-12 sites within the first part of the RS domain before ASF/SF2 is released. These sites for phosphorylation requires kinase fidelity and accuracy to prevent different states of phosphorylated substrates. Also, by forming a stable complex with its substrate, SRPK1 can also protect the phosphorylated ASF/SF2 from phosphatase which can also generate different phosphroylated version of ASF/SF2. As mentioned earlier, the phosphorylation state of ASF/SF2 determines its functional activity in splicing and mRNA metabolism; thus, processive phosphorylation is vital step in SR protein regulation.

Figure 3.13A of this chapter is, in part, a reprint of material as it appears in Molecular Cell, 2008, 29, 563-576, Ngo, J.C., Giang, K., Chakrabarti, S., Ma, C.T., Huynh, N., Hagopian, J.C., Dorrestein, P. C., Fu, X.D., Adams, J.A., and Ghosh, G.. The thesis author was the second author of this publication.

CHAPTER IV

PURIFICATION OF WILD TYPE SRPK1

A. Introduction:

SRPK kinases phosphorylate Ser residues in the RS domain in SR proteins at high specificity. SRPK1 is a bipartite kinase, comprising of a kinase core separated by a spacer domain (Figure 1.3 & 1.6). Our laboratory has extensively worked with a catalytically active truncated version of SRPK1, where the short the N-terminal segment and a longer spacer domain were removed. As mentioned previously kinetic and structural characterization of SRPK1 utilized this truncated protein. However, the truncated regions, in particular the spacer domain, have been shown to play important physiological functions such as the regulation of its sub cellular distribution. SRPK1 without the spacer domain is found to accumulate inside the nucleus and cause aggregation of splicing factors, ASF/SF2 (Ding et al., 2006). Therefore, it is essential to carry out comparative characterization of both the full length and truncated SRPK1. For *in vitro* studies, it is important to have clean and active full length SRPK1. I describe here the methods employed to purify full length SRPK1. Two main problems in the purification of SRPK1 full length are the low expression of SRPK1 protein in bacteria and the proteolytic cleavage happening on SRPK1 during 37^{o}C culturing over night. Thus, purification of SRPK1 full length needs to minimize these two problems.

B. Results:

1. Purification of His-SRPK1 from bacteria

SRPK1 levels peak at the early mid-log stage of culturing (Optical Density, OD_{600}= 0.2-0.3). When the bacterial culture grows longer, the level of SRPK1 is reduced. This could be due to overtime accumulation of bacterial proteases during later stage of cell growth and these proteases start to cleave and degrade SRPK1. However, even when purification is done at optimal growth conditions, purity of SRPK1 is low. I found that impurity is not due to unrelated proteins but due to degradation of SRPK1. Based on the size of the cleaved *wt* SRPK1 products suggests that the cleavage occurs somewhere within the spacer region. Moreover, I have not observed degradation of SRPK1 ΔNS3 (Figure 3.6). Thus, the spacer appears to be the target for the protease activity and is responsible for the degradation of the SRPK1full length. In order to reduce the protease activity to SRPK1 full length in cell lysate, we decided to use alkaline pH of 9.5, which is not an optimum pH for proteases to function. The result indicated that SRPK1 full length is cleaner after four steps of purification, namely through: Q-sepharose, S-sepharose, Nickel-NTA, and size-exclusion chromatography (Figure 4.1). Interestingly, we found that SRPK1 did not bind well to Q-sepharose (anion exchange column) at the buffer of pH 9.5 and yet it binds to S-column at a considerable amount despite of the isoelectric point (pI) of SRPK1 being 5.99 (Propagram). This suggests that the acidic residues might be masked in the native protein which prevents its binding to a positively charged matrix.

Since SRPK1 does not bind well Q-Sepharose column at pH 9.5, in our second attempt to purify SRPK1 full length, we decided to reduce the pH of the

A)

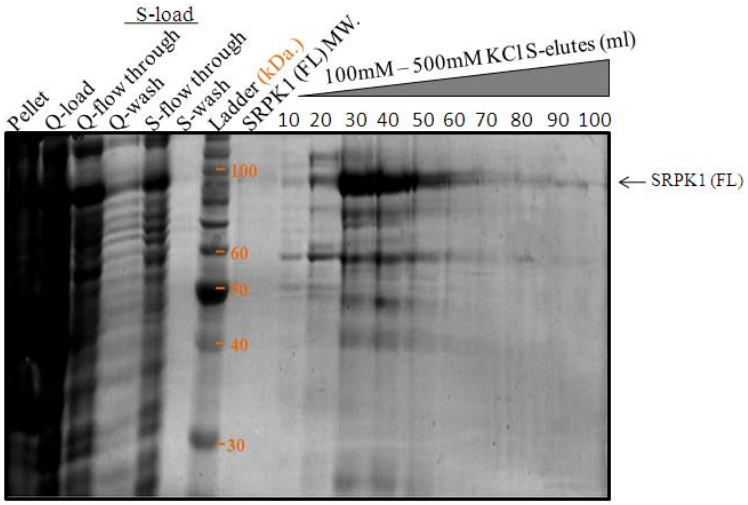

B)

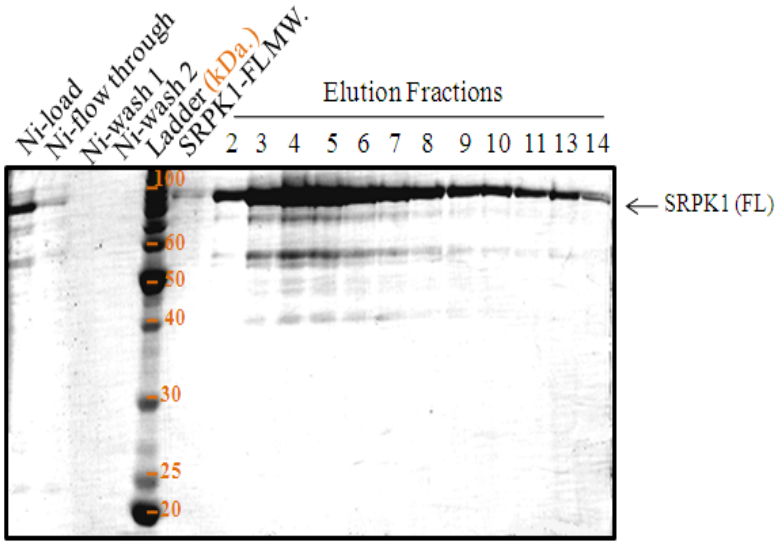

Figure 4.1: Affinity-Column Purification of SRPK1-N' His at pH 9.5.) SRPK1 is purified by Q- and S-sepharose columns. B) SRPK1 has N-terminal His tag. Nickel column is used to further purify SRPK. One notable feature of SRPK1 is that it does not migrate according to its theoretical molecular weight of 75.56 kDa. SRPK1 in SDS-PAGE always migrates at 100kDa. of the molecular weight standard.

A)

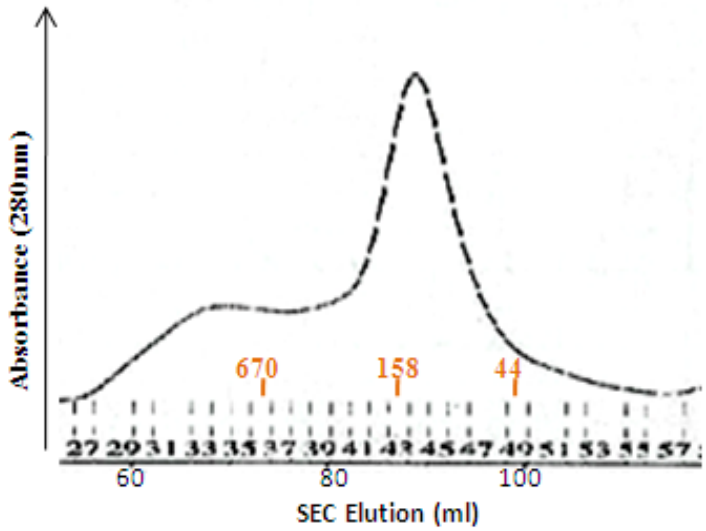

B)

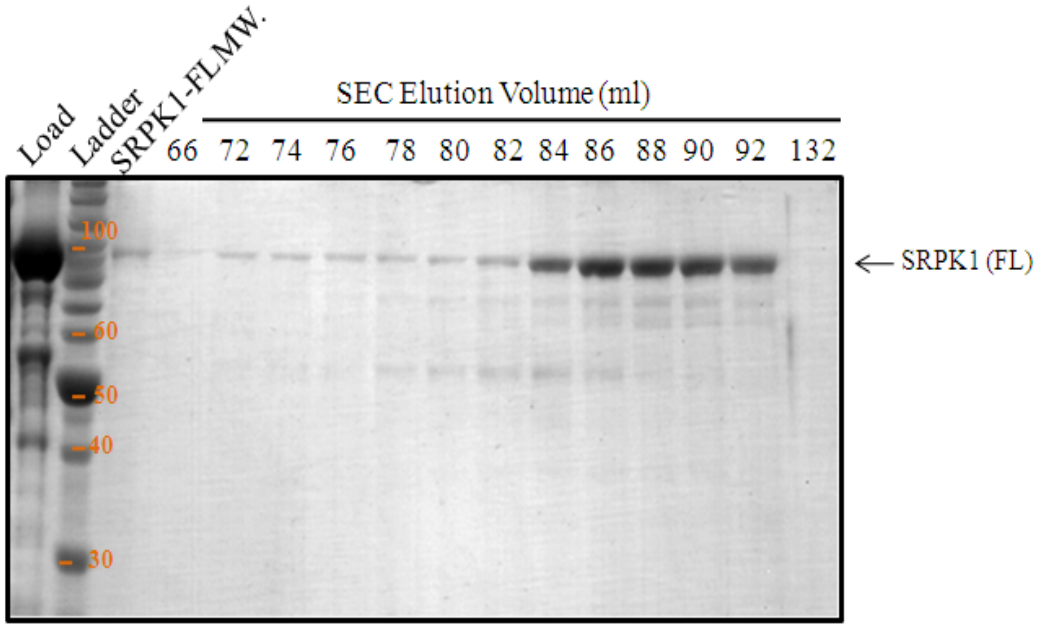

Figure 4.2: Size-exclusion Chromatography of SRPK1-N' His at pH 9.5. A) SRPK1 elution from Hiprep Supedex 200 profile corresponds to the SDS-PAGE analysis (B).

A)

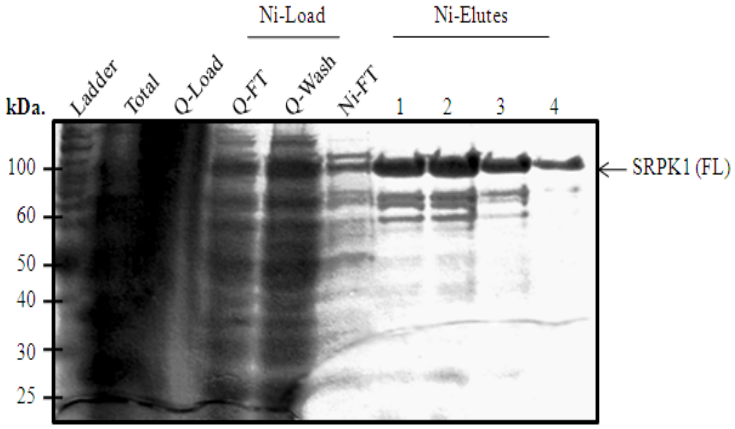

B)

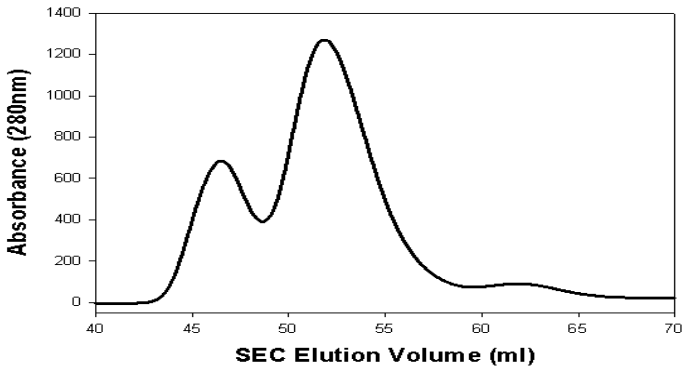

C)

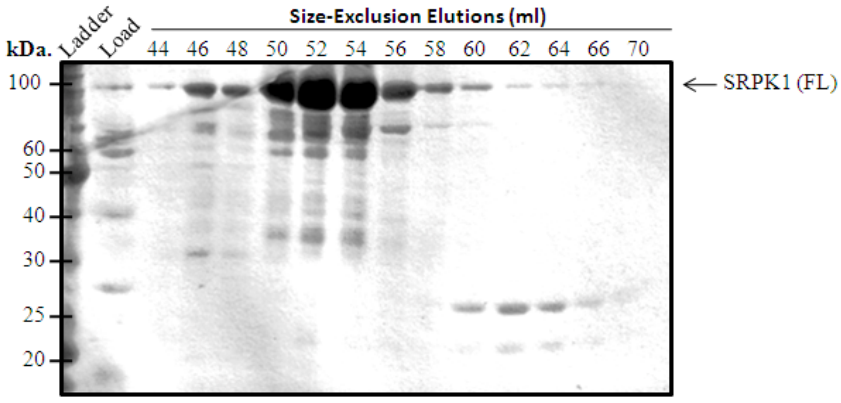

Figure 4.3: Purification of His-SRPK1 at pH 7.5. A. SRPK1 purified from Nickel-column. B. Half of the Nickel elution was used directly in size-exclusion chromatography and the purity is analyzed by SDS-PAGE (C). B & C are designed as method1.

A)

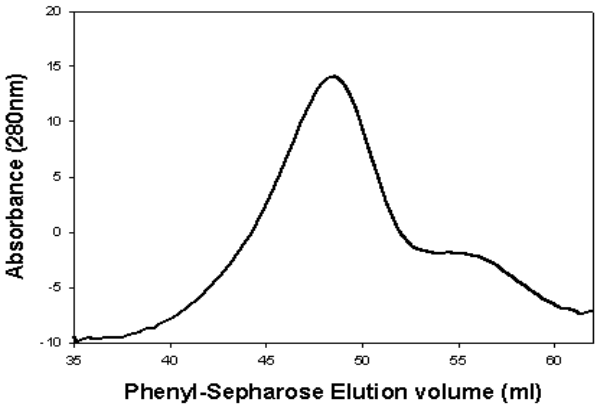

B)

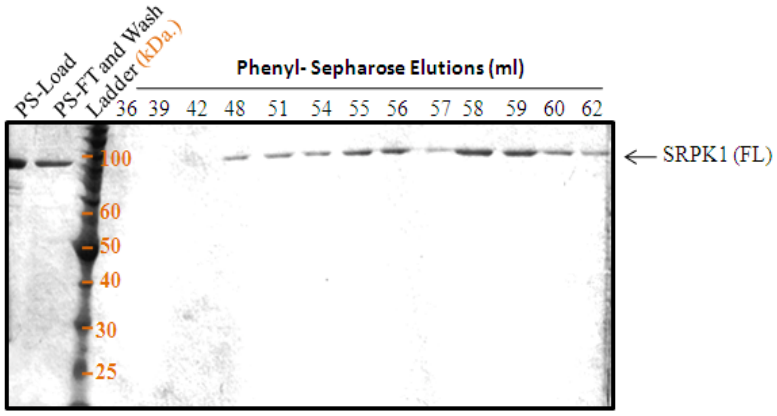

Figure 4.4: Purification of His-SRPK1 by phenyl-sepharose (PS) column. Half the amount of SRPK1 in Nickel-elution was treated with ammonium sulfate to bring the salt concentatration to 2 M. The soluble fraction is used for PS-column (Method 2). The peak fraction (60-90 ml) shows clean SRPK1.

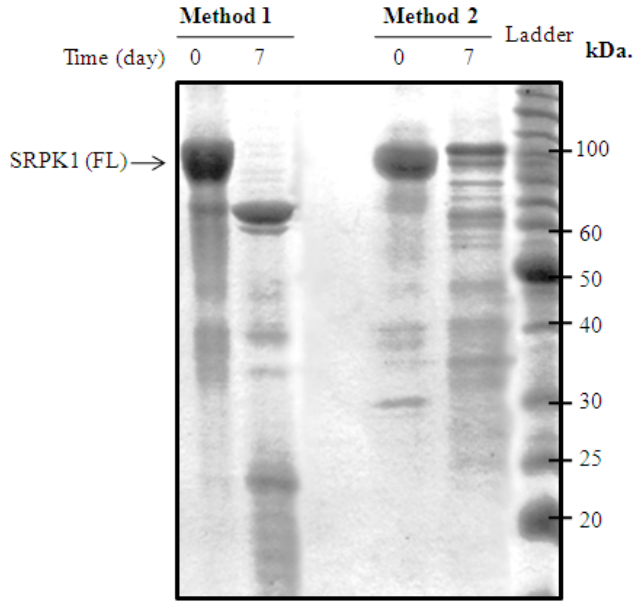

Figure 4.5: SRPK1-His purified from Phenyl-sepharose (PS) column is less degrading. The stability of SRPK1 from two methods (Figure 4.3 & 4.4) were compared by incubation at room temperature for one week.

purification buffer to 7.5 to completely abolish SRPK1 binding to Q-sepharose column. I combined follow-through solution and the wash from Q-sepharose to load onto the Nickel-NTA column. The elution from Nickel-NTA column showed large amount of SRPK1 along with its degradation products as expected (Figure 4.3). Since SRPK1 full length shows high surface of negative and positive charges as it could bind to both Q-sepharose column and S-sepharose column, we decided to use phenyl-sepharose (PS) fast-flow column to purify SRPK1 full length based on its hydrophobicity. SRPK1 shows to tolerate 1.5 M ammonium sufate precipitation (Gui et al., 1994). We loaded SRPK1 at 2M ammonium sulfate (AS) and eluted it by the gradient of 2 M to 50 mM AS salt gradient. SRPK1 eluted at approximately 800 mM AS concentration as highly pure protein (Figure 4.4). I tested protease sensitivity of SRPK1 before and after PS purification step and found that PS-step purified SRPK1 was more stable at room temperature after one week while PS-not bound SRPK1 was completely truncated (Figure 4.5). These results suggested that some small proteases can be removed by PS column chromatography.

2. Purification of His-SRPK1 at pH 7.5 from baculovirus-insect cells

We used similar procedures to purify His-SRPK1 at pH 7.5 from insect cells except that we did not use phenyl-sepharose fast-flow. No degradation product was observed after Nickel purification step (Figure 4.6). We do not know

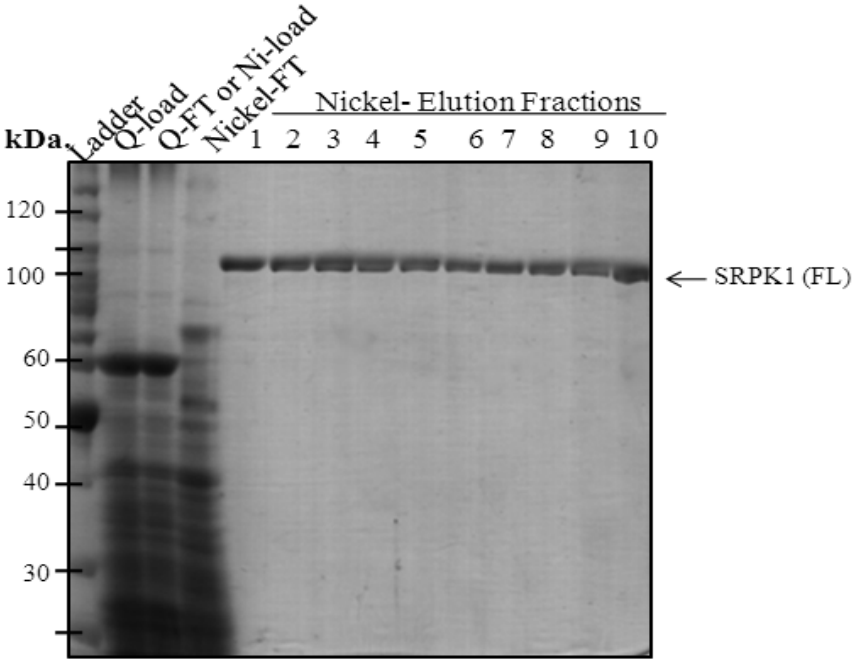

Figure 4.6: Full length SRPK1 is less degradative in insect system. The purification steps involve Q-sepharose column and Nickel-NTA column. The purified SRPK1 full length from insect cells is cleaner after Nickel-column as compared to the purified SRPK1 from *E. coli* cells (figure 4.2).

why the behavior of the same protein derived from two different expression systems is different. One possibility is that proteases present in *E. coli* that can cleave SRPK1 are not present in insect cells. A second reason could be that proper chaperone system maintain the folded state of SRPK1 which prevents the accessibility of proteases. Finally, stability of SRPK1 may require post translational modification which can take place in the insect cell but not in *E. coli*.

C. Discussion:

Our interest is to study the features of SRPK1 full length that regulate its localization and determine its functional stability *in vivo*. Our approach for this study is x-ray crystallization. Our previous laboratory members attempted to crystallize SRPK1 full length with no fruitful result, partly due to unclean SRPK1. SRPK1 full length is 30 KDa larger than ΔNS1 and ΔNS3, that comprise of the kinase core of 43 kDa. with two short stretches of the spacer domain. The molecular weight difference indicates that the spacer domain is almost as big as the kinase core. However, the function of SRPK1 spacer domain is not completely clear. The only evidence about the spacer is that it implicates in SRPK1 subcellular localization since its absence will cause SRPK1 to accumulate in the nucleus (Ding et al., 2006). In addition, it plays a key role in stabilizing SRPK1 full length. Our molecular dynamics simulation studies showed that the stability of full length SRPK1 is independent of ATP whereas the stability of ΔNS1 depends on the presence of ATP (Ngo et al., 2007). The

spacer domain has intriguing functions on the full length SRPK1 but its study as an independent protein is not possible since it is fully unstructured. It might also remain disordered in the full length but the full length can have some compensatory role in stabilizing it as it has on the full length. Thus, our purification of the full length SRPK1 was geared towards reducing proteolytic cleavage and improving SRPK1 yield.

The x-ray structure studies of ΔNS1 and ΔNS3 revealed uneven surface charge distribution in the kinase core with the small lobe and some patches in the large lobe being highly basic (Ngo et al., 2005; Ngo et al., 2007). Despite of its pI of 6.9, only the docking groove and its surrounding show high density of acidic residues. This observation is also confirmed by the fact that ΔNS3 do not bind to Q-sepharose column (Figure 3.6). Similarly, SRPK1 full length with pI of 5.99, does not bind well to the Q-sepharose column at pH 9.5 and 7.5. In contrast, it binds to S-sepharose as the buffer solution being pH of 9.5. Thus, the theoretical pI of SRPK1 is not an accurate reflection of its surface charge. The highly basic surface charge of SRPK1 may serve as interacting surface for other proteins to bind, especially proteases which usually cleave after lysine and arginine residues.

Apart from the unexpected surface charge of SRPK1, an intriguing observation in the size-exclusion chromatography is that SRPK1 appears larger than its theoretical molecular weight. His-SRPK1 full length is 76.5 kDa. However, the apparent molecular weight from the column shows to be 151 kDa,

twice of its actual molecular weight. Two possibilities could be: (1) SRPK1 full length is partially unstructured or (2) SRPK1 is a dimer. In the next chapter, I explored the two possibilities and searched for the biological importance for this unexpected molecular weight of the full length SRPK1.

CHAPTER V

MECHANISM OF SUBCELLULAR LOCALIZATION OF SRPK1

A. Introduction:

It is known that SRPK1 resides mostly in the cytoplasm and only during distinct stages of cell cycle that it localizes to the nucleus. However, recent biochemical fractionation of spliceosome has revealed that both SRPK1 and SRPK2 are present in the spliceosomal complex; SRPK1 during early and SRPK2 during late stages of the spliceosome assembly (Mathew et al., 2008). These results suggest that the distribution of SRPKs might be more dynamic than appreciated earlier. Distribution of SRPKs is expected to be regulated. However, the precise mode of regulation has remained unclear. Several reports have also addressed the regulatory mechanisms of subcellular distributions of SRPK1. It was shown that the spacer domains of these kinases are primarily responsible for their cytoplasmic localization. Until date, the detailed dissection of the spacer domain revealed a highly complex mode in their retention mechanism. The spacer could be divided into three parts and the presence of any two of the three segments could retain SRPKs in the cytoplasm (Ding et al., 2006). This result suggested that no specific sequence within the spacer region serve as a retention signal. Here, I set out to study the role of the spacer domain in the subcellular distribution of SRPK1.

B. Results:

1. Full length SRPK1 is an oligomer: size-exclusion chromatography

In the last step of SRPK1 purification by size-exclusion chromatography, it appeared that full length SRPK1 eluted as a large molecular weight species. This observation led to thorough investigation of the size of full length and truncated SRPK1 proteins by analytical gel filtration column. As shown in Figure 5.2A, SRPK1 elutes as a 151.4 kDa species while the kinase core, SRPK1ΔS, elutes as expected, 52.3 kDa. Similarly, the other kinase core construct, SRPK1ΔNS3 is eluted at the expected size of approximately 44 kDa. Whereas, the spacer-deleted constructs migrate at the expected molecular weight, the full length SRPK1 and the construct with the N-terminal domain deleted show to be approximately twice of their theoretical molecular size by size-exclusoion chromatography (Table 5.1). Thus, the spacer has some role to play in oligomeric state of SRPK1. Two possibilities for the large apparent molecular weight of SRPK1 in the size-exclusion chromatography could be invoked, namely: (1) SRPK1 full length is partially unstructured or (2) it is a dimer.

2. Full length SRPK1 purified from *E. coli* retains constitutive activity

I have further addressed whether the oligomeric state of SRPK1 is derived from protein unfolding/ misfolded structure or from the kinase self-association, using kinase assays as the basis for this study. Kinase is characterized by its catalytic activity in transferring the phosphoryl moiety from ATP to its target

substrate; so, characterizing the kinase activity of SRPK1 would address the status of its kinase fold.

The crystal structure of SRPK1 kinase core, ΔNS3, was solved by Ngo et al.[2005]. ΔNS3 purified from *E. coli* is constitutively active, indicating that the kinase fold of SRPK1 does not require post-translational modification. Also, ΔNS3 construct has a substantial amount of the spacer domain deleted and yet its kinase fold retains all the important features of a kinase (Figure 5.1). Thus, the spacer does not show play a significant role in the kinase activity of SRPK1. The full length SRPK1 purified from *E. coli* is expected to have kinase activity comparable to the one of ΔNS3. The kinase assays show that full length SRPK1 retains high kinetic activity like ΔNS3, suggesting that the kinase core of the full length is well folded (Figure 5.3). Analysis of the secondary structure signature (CD at 222 nm and 208 nm) of the full length protein supports that the full length has the secondary structure signature comparable to that of the kinase core (Figure 5.4). Therefore, the oligomeric state of full length SRPK1 is indicative of SRPK1 self-association rather than its misfolded nature.

3. Spacer of SRPK1 is an oligomer: size-exclusion chromatography

Previous result shows that full length SRPK1 self-associates as a dimer by size-exclusion chromatography and suggests the role of the spacer domain in dimerization of the kinase. I further worked to test if the spacer is an oligomer.

Size-exclusion chromatography shows that His-Spacer migrates approximately three times larger than its expected size (Figure 5.5 & Table 5.1), supporting my observation that the inclusion of the spacer domain mediates dimerization of SRPK1.

Although I have demonstrated that SRPK1 is active, the folding state of the spacer domain is unclear. It is possible that the unfolded spacer domain in full length SRPK1 is responsible for aberrant elution profile. If only the other–full length protein is truly a dimer, the spacer domain is clearly important for the dimer formation as the spacer deleted kinases are monomeric.

4. Full length SRPK1: Pull down assays *in vitro* and *in vivo*

To further examine self-association of SRPK1, GST-pull down assays were employed. To accomplish this, I have generated both poly-histidine and GST fusion SRPK1 and purified them to homogeneity. The result shows that His-SRPK1 binds to GST-SRPK1. The ratio of binding is not 1:1 (Figure 5.6). This could be due to strong self-dimerization of SRPK1 which prevents association of the tagged proteins *in trans*. I also examined self-association of SRPK1 in cells. Flag-SRPK1 and Myc-SRPK1 were coexpressed in HEK-293T cells. Equal expression of both proteins was verified by western blot. Immunoprecipitation soluble extract with anti-Flag antibody followed by WB with anti-Myc antibody

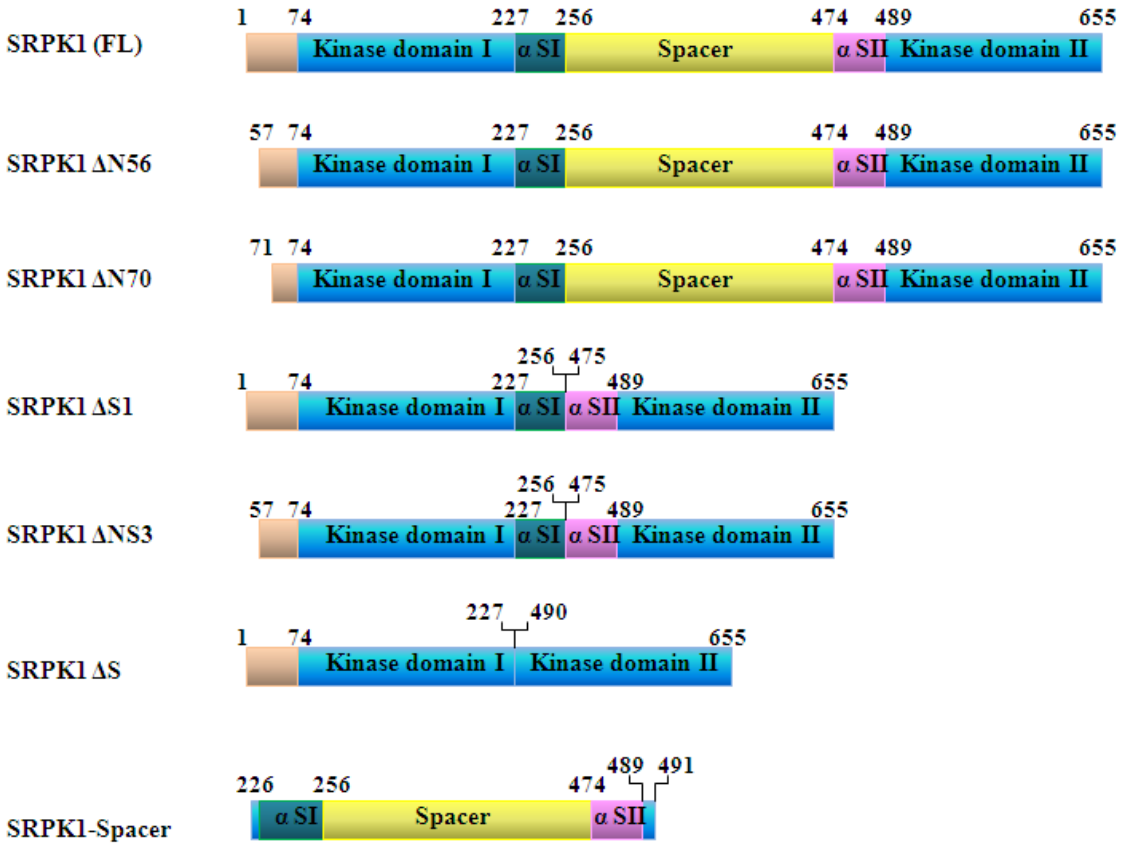

Figure 5.1: Schematic organization of various SRPK1 constructs. SRPK1 is characterized by having its kinase domain of SRPK1 bifurcated by a large spacer domain. Specific function of the spacer is still unknown. The conserved kinase subdomain (shown in blue) defined by Hanks and Quinn (1991) are bifurcated by the spacer region. N- and C-terminal spacer regions are colored in green and pink, respectively.

A)

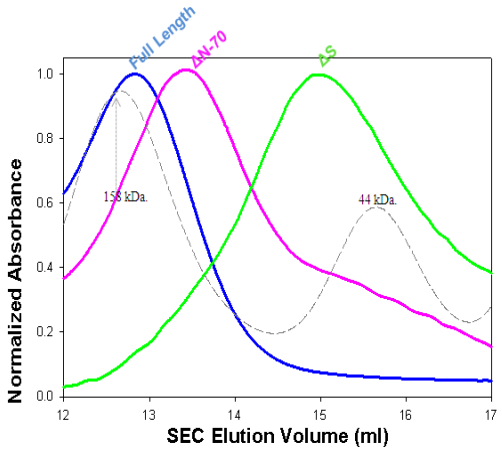

B)

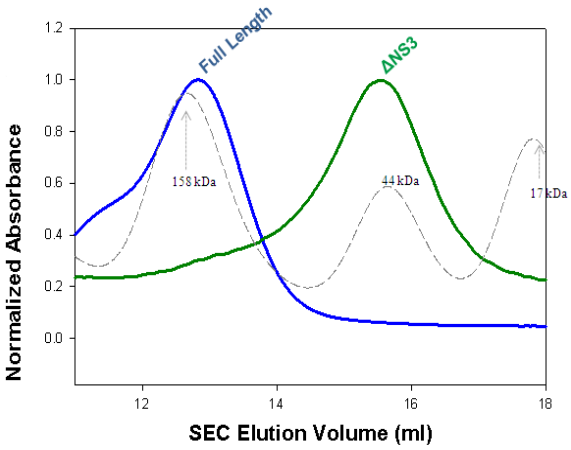

C)

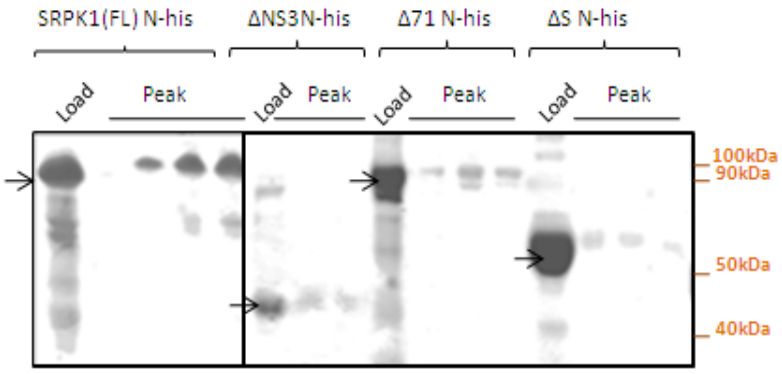

Figure 5.2: Oligomeric state of SRPK1 by size-exclusion chromatography. E. coli–expressed SRPK1 constructs were evaluated by analytical Supedex200 column. A & B) Full length SRPK1of 76.56 kDa. elutes as early as the molecular standard of 158 kDa. while the spacer-deleted constructs, ΔS and ΔNS3, elute as their expected molecular weight. N-terminus deleted constructs, ΔN70, also elutes abnormally higher than its theoretical molecular weight. C) SDS-PAGE analysis was used to examine the purity of the protein elution peak in part B.

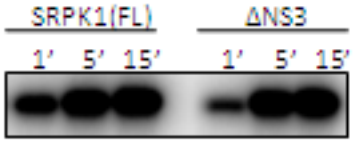

Figure 5.3 Kinase activity of the *E. coli*-expressed full length SRPK1. Full length SRPK1 has kinase activity as comparable as its shorter construct, ΔNS3 does. This proves that the *E. coli* expression system and our purification method for the full length SRPK1 provides well-folded kinase, eliminating the possibility that unfolded SRPK1 elutes at higher molecular weight.

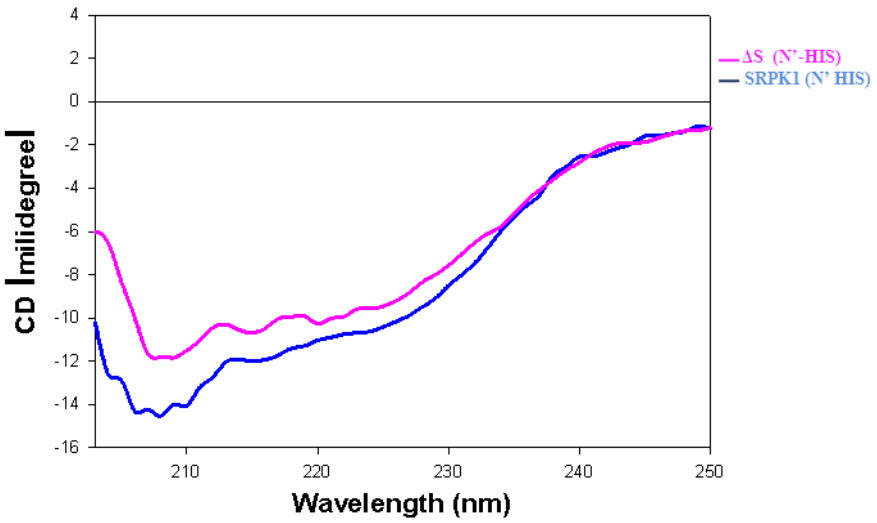

Figure 5.4: Secondary signature of the *E. coli*-expressed SRPK1 constructs. 5 μM of full length and 5uM of ΔS were used to record the seconardy signature by CD spectrophotometer. Two notable deeps are seen at 208 nm and 222 nm, reflecting the α-helical nature of the kinase.

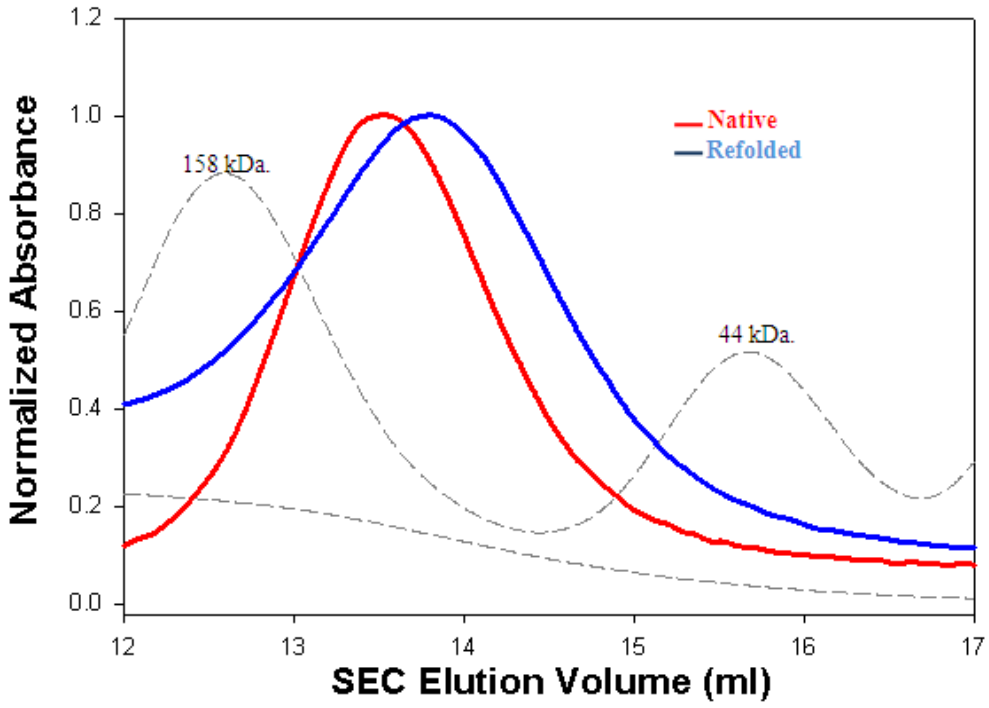

Figure 5.5: Oligomeric nature of SRPK1-Spacer. The apparent of molecular weight of the spacer is determined from two different preparations of His-Spacer. One preparation involves purifying His-Spacer from bacteria in native condition (Chapter 2). The other preparation is to purify His-Spacer in denaturing condition of 6M Urea and then refold it by slow dialysis. The first prepration provides that His-Spacer is a soluble protein and can be purified from the affinity column. The second preparation provides that His-Spacer can be refolded and the refolding process enhances the oligomeric state of SRPK1 leading to its later elution from size-exclusion column.

Table 5.1: Summary table of the apparent size of SRPK1 constructs. Full length SRPK1 in native state appears to be twice as big as its theoretical size, suggesting its native state as a dimer. N-terminus deleted SRPK1 exists as one and a half as its theoretical size but the spacer-deleted spacer SRPK1 migrates at its expected theoretical size. His-Spacer domain shows approximately three times of its expected size. Overall, the result indicates that the spacer domain in SRPK1 mediates in self-dimerization of full length SRPK1.

Proteins	Theoretical MW (Dalton)	Apparent MW (Dalton)	Appt/Thereo
SRPK1 (FL)	76557.9	151459.65	1.98
ΔN70	68670.2	114935.47	1.67
ΔS	48380.8	52321.47	1.08
ΔNS3	44331.1	38113.83	0.86
Spacer-N-his (226-491) Native	31777.8	105733.9	3.3
Spacer-N-his (226-491) Refolded	31777.8	90858.53	2.86

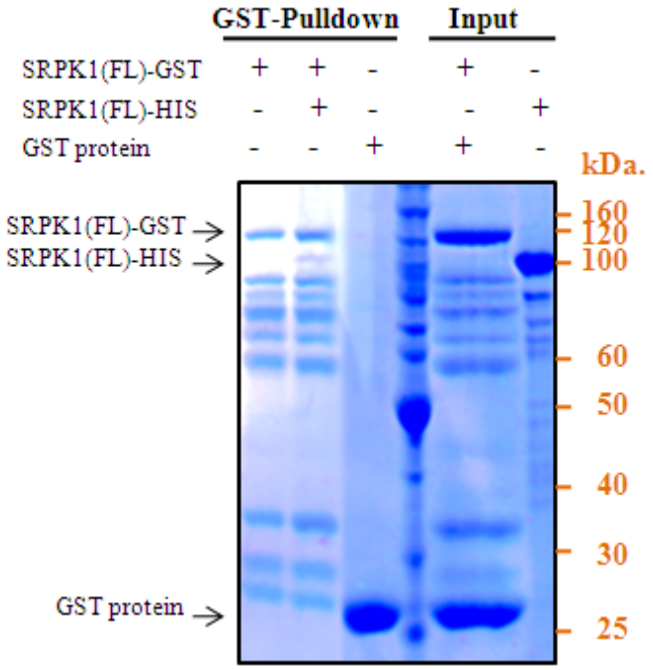

Figure 5.6: SRPK1 self associates *in vitro*. GST Pull down assay was performed to examine in *in-trans* interactions between His-SRPK1 and GST-SRPK1. A small fraction of His-SRPK1 shows to interact with GST-SRPK1.

A)

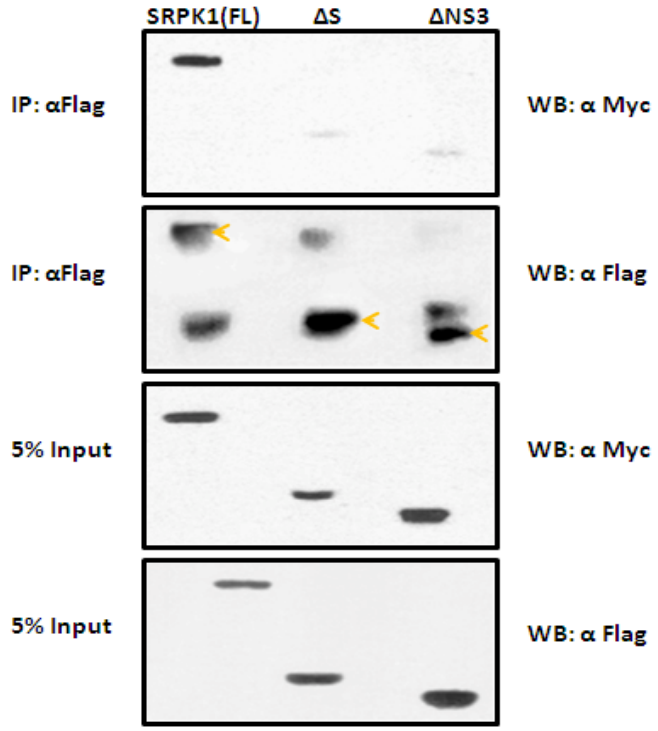

B)

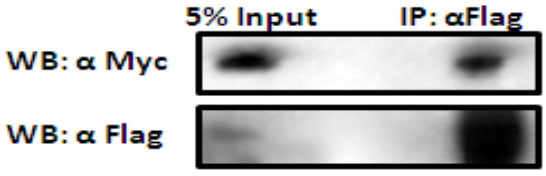

Figure 5.7: Full length SRPK1 self associates *in vivo*. SRPK1 constructs were co-expressed in HEK-293T cells and immunoprecipitation was conducted to examine SRPK1 interaction. Spacer-deleted SRPK1 constructs show poor binding, suggesting that the spacer mediates dimerization of full length SRPK1**.**

showed that these two proteins are associated with each other. These observations support the notion that SRPK1 is a dimer. Co-immunoprecipitation from extracts containing spacer-deleted SRPK1 constructs, SRPK1ΔS and SRPK1ΔNS3 was also performed. These results clearly show that these truncated SRPK1 proteins dimerize poorly (Figure 5.7). Here, I concluded SRPK1 full length to be a dimer and dimerization was primarily mediated by the spacer domain.

5. Spacer domain of SRPK1 self associates *in vivo*:

Previous experiments show that spacer plays a role in self dimerization of SRPK1. Chromatographic data support that spacer is an oligomer (Figure 5.5). To further support the observation about spacer self-association, I co-expressed GST-Spacer and His-Spacer and then performed a GST-pulldown experiment. The result presents that GST-Spacer and His-Spacer interact *in-trans* in *E. coli* system, indicative of self-association of SRPK1-Spacer (Figure 5.8).

6. Dimer SRPK1 and ASF/SF2 interaction

ASF/SF2, a member of SR protein family, is specifically recognized and extensively phosphorylated by SRPK1. I previously modeled the docking interaction between SRPK1 and ASF/SF2 in a sliding ATP-dependent manner.

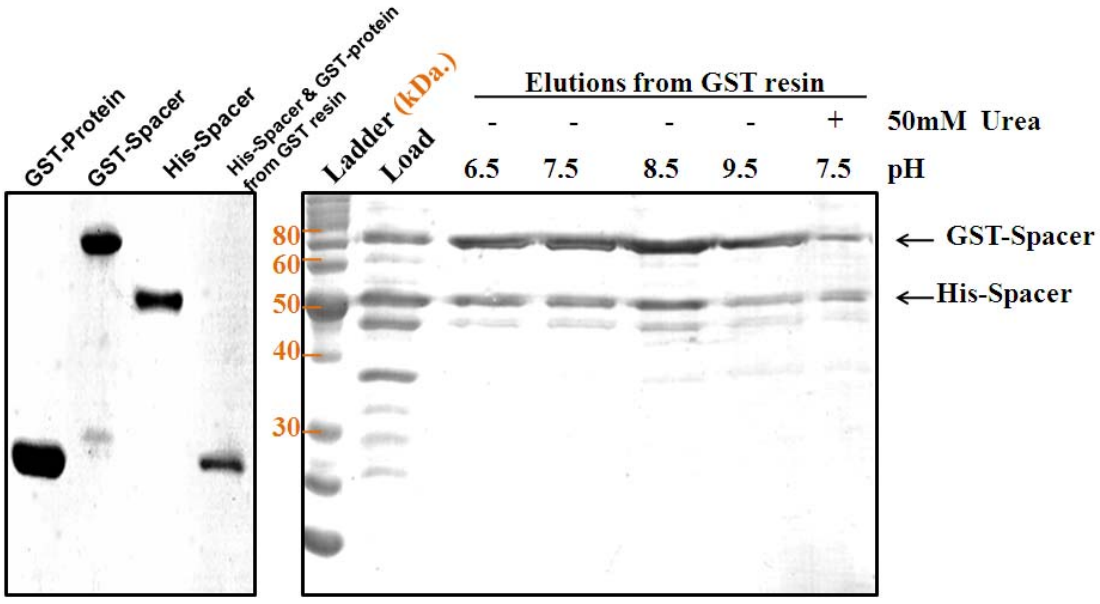

Figure 5.8: Spacer self associates *in vivo*. GST-Spacer and His-Spacer are co-expressed in E. coli and GST Pulldown assay was performed (Right). Each protein in the left gel is purified individually.

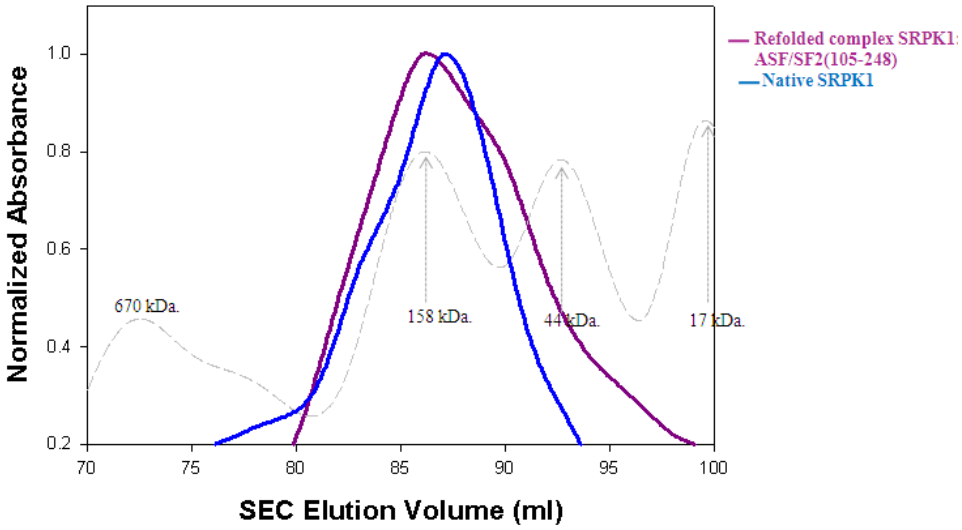

Figure 5.9: Full length SRPK1 exists as a dimer in complex with its substrate, ASF/SF2. Full length SRPK1 and ASF/SF2 (105-248) were refolded together. The complex in size-exclusion chromatography (Hiprep SD 200) showed to migrate as twice as its theoretical molecular weight. The result proves that full length SRPK1 can be refolded with its substrate and it exists as a dimer.

Table 5.2: Summary table of the size analysis for the refolded complex of SRPK1: ASF/SF2. ASF/SF2 (105-248) aggregates when purified alone. The apparent molecular weight of ASF/SF2 was not determined. The analysis suggests that a SRPK1 dimer binds to two ASF/SF2.

Protein	Theoretical MW (Dalton)	Apparent MW (Dalton) by SEC	Appt/Thereo
SRPK1(FL)	76557.9	151459.65	1.98
ASF/SF2 (105-248)	18748.6	Not applicable	
Complex SRPK1: ASF/SF2	95306.5	175478.2	1.84

In the present study, I wanted to see whether full length SRPK1 interacts with ASF/SF2 as a dimer. I refolded 1:1 mixture of SRPK1 and ASF/SF2 by slow dialysis. The refolded sample was then analyzed by size-exclusion chromatography. The size of the SRPK1: ASF/SF2 complex was found to be 175.4 kDa., suggesting that 2:2 ratio of kinase and substrate is present in the complex (Figure 5.9 & Table 5.2). Thus, SRPK1 self-association appears to be the prominent feature of this kinase.

7. Self-dimerization implicates in SRPK1 stability

SRPK1 self-association is observed in both *in vitro* and *in vivo*. Also, substrate-binding is shown to be independent of its dimerization (Figure 5.9 & Table 5.2). Next, I wanted to see whether dimerization played a role in SRPK1 overall functional stability since degradation of SRPK1 is observed in SDS-PAGE analysis. Purified full length SRPK1 always showed degraded products despite of many purification steps and addition of protease inhibitors (Chapter 4). In contrary to the Gaussian elution peak of the full length SRPK1, SDS-PAGE analysis showed that the peak is composed of multiple species which could be the degradation products of SRPK1 (Figure 4.3). The reason for this observation could be that SRPK1 is nicked by proteases during bacteria culturing but self-dimerization stabilizes SRPK1. To test this possibility, I performed limited chymotrysin digestion on the full length SRPK1 and analyzed the digested

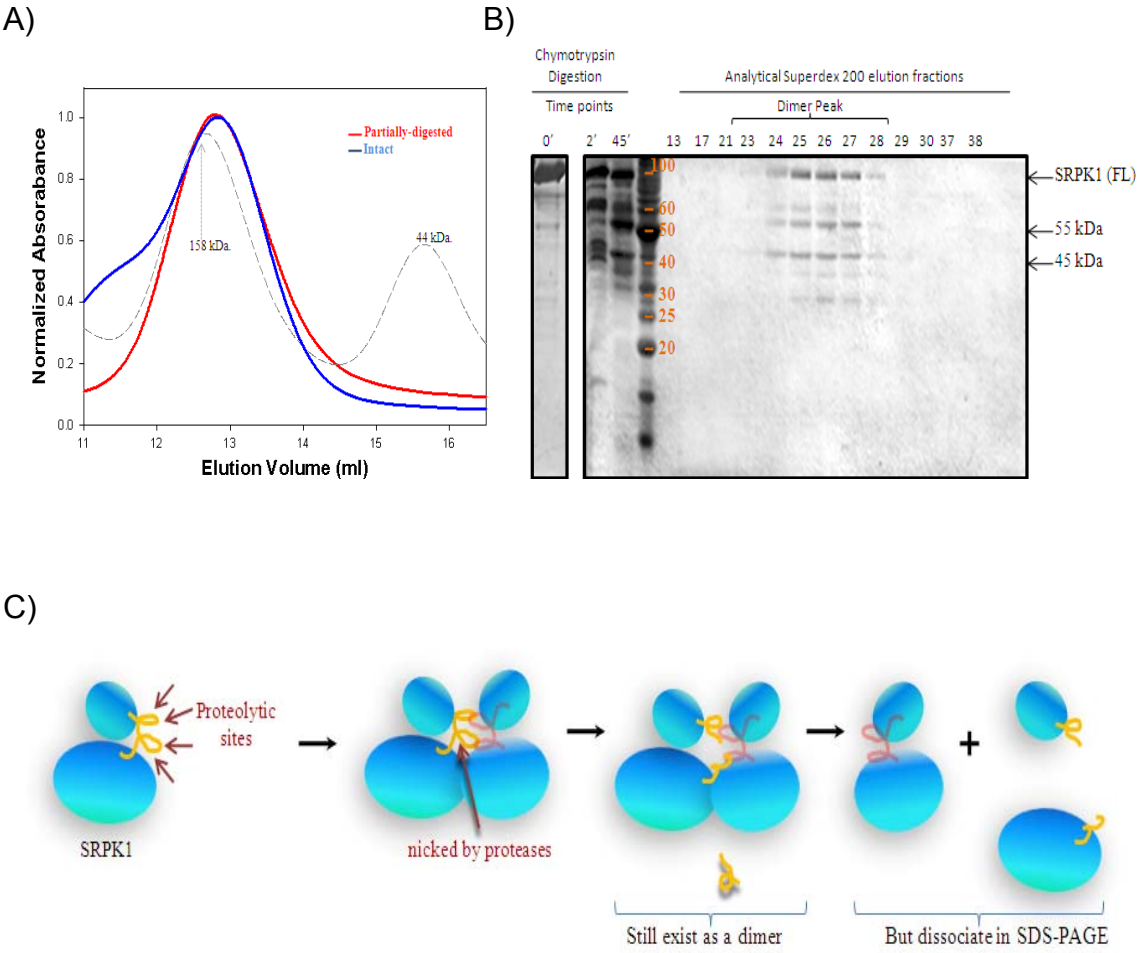

Figure 5.10: SRPK1 remains as a dimer in limited proteolysis. A & B) Purified full length SRPK1 was treated with chymotrypsin for 45 minutes and then subjected to size-exclusion chromatography (SEC), the analytical Supedex200. The partially digested SRPK1 migrates and elutes at the same elution volume as that of the intact full length SRPK1. SDS-PAGE analysis on the partially digested SRPK1 shows that SEC was not able to separate the lower degraded products of SRPK1 from the full length. B) 158 and 44 represents the molecular standard in kDa..The molecular weight (kDa) of the standard is labeled in brown. Each elution fraction is 500 μl; for example fraction 24 corresponds to 12 ml in the chromatographic graph. C) The proposed model for a nicked dimer of SRPK1. *In vivo* SRPK1 dimer is nicked by proteases. Since SRPK1 forms stable homo-dimer, the degraded form of SRPK1 can only be viewed during SDS-PAGE analysis. The model does not propose the structure of SRPK1 dimer.

sample by size-exclusion chromatography and SDS-PAGE. I observed that while the digested sample has the same Gaussian elution peak with the non-digested sample, the digested sample on SDS-PAGE contains multiple degradation products (Figure 5.10). Thus, the dimerization of SRPK1 appears to confer some functional stability to SRPK1 *in vivo*.

8. SRPK1 full length is found abundant in both nucleus and cytoplasm:

Having established that SRPK1 is a dimer, I wanted to investigate if dimerization of SRPK1 was a mechanism of its cytoplasmic retention. Based on literature (Ding et al., 2006) and my previous results, it can be speculated that dimerization through the spacer domain may mask nuclear localization signals of the kinase resulting in its cytoplasmic localization. I wanted to test if localization of endogenous SRPK1 can be modified by overexpression of the spacer domain. Before I conduct this experiment, I wanted to establish the subcellular localization of endogenous SRPK1 in various cell lines. Localization was monitiored by fractionation of the cytoplasm and nucleus (Figure 5.11). Control experiments were performed to check the integrity of the fractionation protocol (Figure 5.12). However, I was surprised to find high level of SRPK1 in the nucleus. I was confronted with the question of how SRPK1 is found abundant in both the compartments and whether self-dimerization as a way to mask localization signal

A) HEK-293T B) HeLa and MEF cells

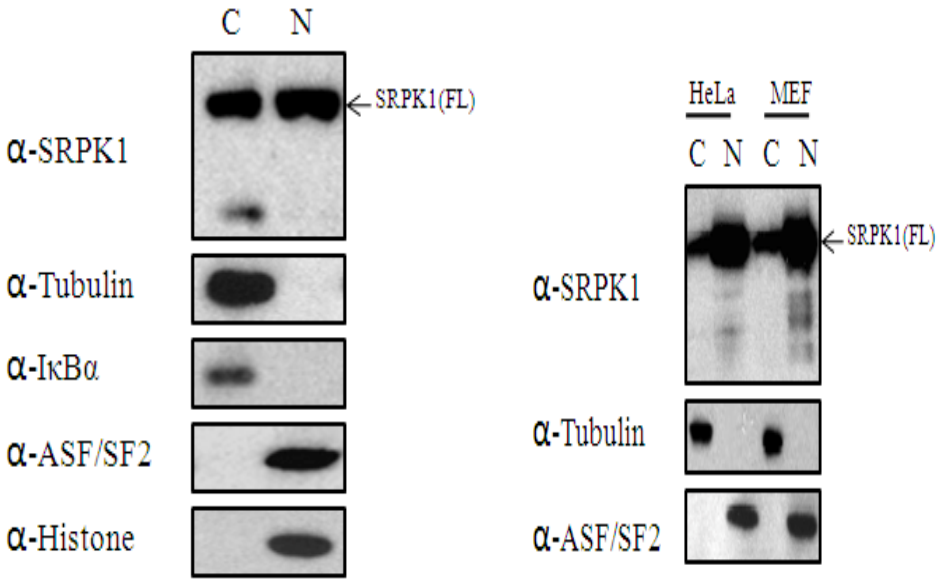

Figure 5.11: SRPK1 is found abundant in the nucleus. A) Nuclear and cytoplasmic fractionation was performed to observe the levels of SRPK1 *in vivo*. Endogenous SRPK1in HEK-293T cells was seen to localize to both cytoplasm and nucleus. B) Endogenous SRPK1 is also present in considerable amount in the nucleus of HeLa cells and MEF cells.

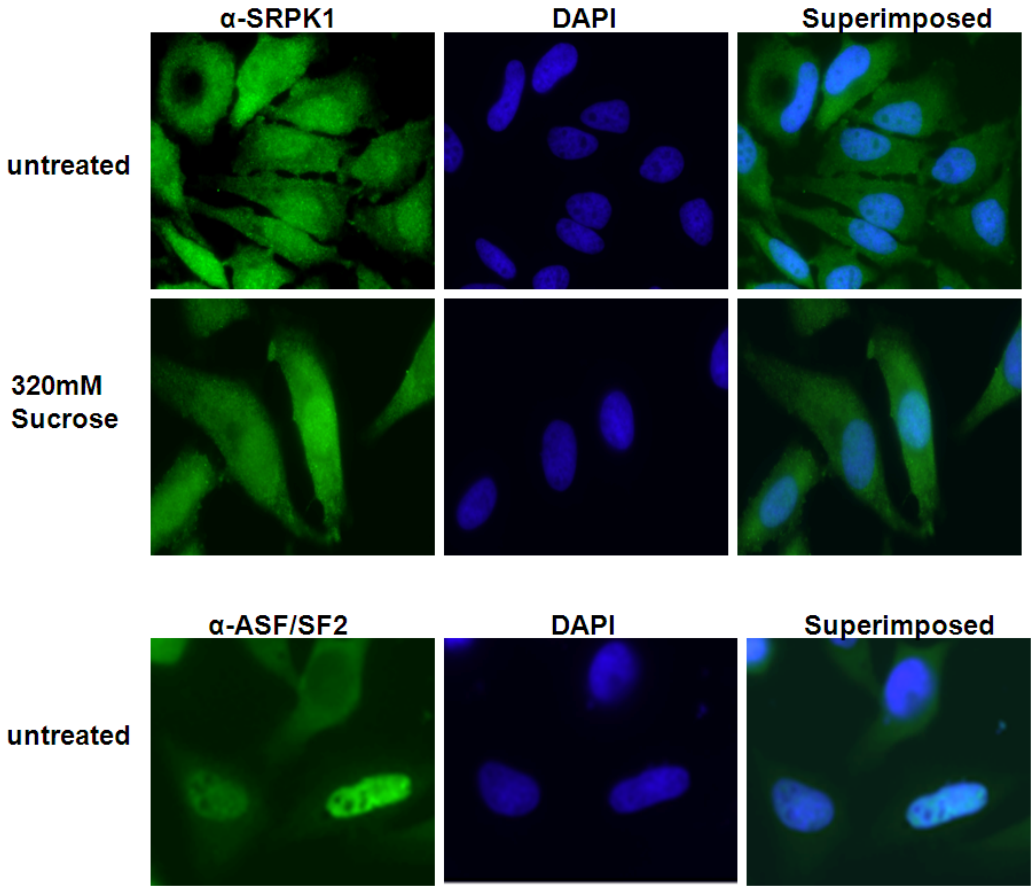

Figure 5.12: SRPK1 subcellular localization. One of the fractionation reagents is sucrose which can create stress to cells. Indirect immunofluorescence was conducted to observe the effect of sucrose to the subcellular localization of SRPK1 (Green fluorescence). The nucleus was labeled by Dapi (blue). Sucrose-treated HeLa cells and untreated cells had similar levels of SRPK1. The immunofluoresence detection of Flag-ASF/SF2 is the control for the nucleus.

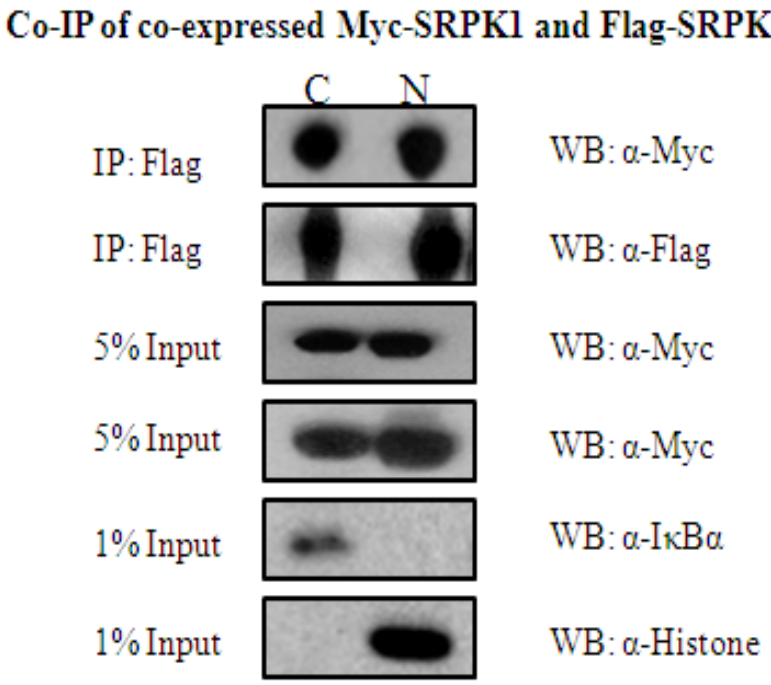

Figure 5.13: SRPK1 exists as a dimer in both nuclear and cytoplasmic compartments. Fractionation of co-expressed Myc-SRPK1 and Flag-SRPK1 was done before co-IP. The result shows that SRPK1dimer was found in both compartments.

is still valid. Co-Immunoprecipitation from each compartment showed that SRPK1 dimer is found in both nucleus and cytoplasm (Figure 5.13).

9. SRPK1-spacer affects subcellular distribution of SRPK1 at a minimal level

My previous data showed that SRPK1 is present in both nucleus and cytoplasm. In addition, SRPK1 self associates in both compartments, suggesting that SRPK1 self-association might not be implicated in SRPK1 subcellular localization. I have observed that self-association of SRPK1 has some implication in SRPK1 functional stability based on the limited chymotrypsin assays. Whether SRPK1 self-association involved in its subcellular localization requires further understanding of the role of spacer. Here, I wanted to address the implication of the spacer domain in SRPK1 on SRPK1 distribution *in vivo*. Since the spacer shows to mediate self-association of SRPK1, I wanted to find what the effect on SRPK1 distribution when the spacer is overexpressed. Fractionation of cytoplasmic and nuclear portions was conducted to observe the level of endogenous SRPK1. In the spacer-transfected cells, endogenous SRPK1 is found to localize in both cytoplasmic and nuclear fractions while the non-transfected cells or empty vector-transfected cells show high level of SRPK1 in the nucleus (Figure 5.14). Thus, it is evident that the spacer does affect the endogenous SRPK1 distribution.

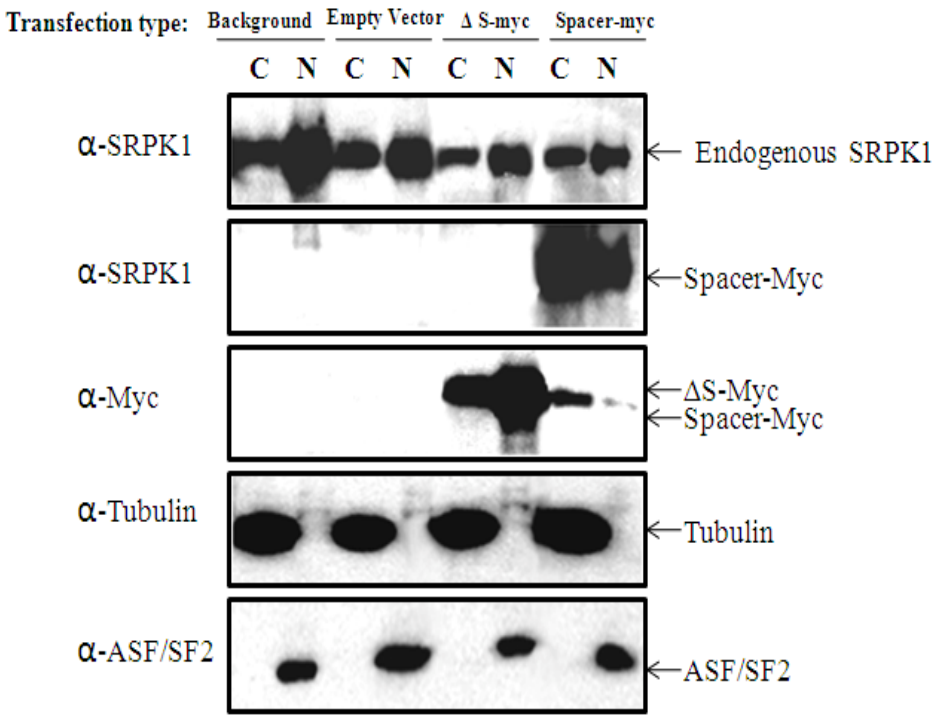

Figure 5.14: Spacer affects subcellular distribution of SRPK1. Fractionation assays: Spacer-overexpressed system showed similar distribution of SRPK1 in the cytoplasm and nucleus. The kinase core, ΔS, was used as control for the effect of the spacer on the distribution of endogenous SRPK1.

10. Interactions between Myc-Spacer and endogenous SRPK1 are not observable:

I have observed that the spacer domain of SRPK1 can affect the subcellular distribution of endogenous SRPK1. My next goal is to examine whether this interaction is transient. I conducted immunoprecipitation of the spacer domain, followed by western blot analysis to see whether the endogenous SRPK1 and spacer bind to each other. However, the interaction is not observable – the spacer domain does not pull down the endogenous SRPK1. Two possible explanations could be that (1) the spacer self-association is more favored and thus interaction between the spacer and full length kinase is a transient process; (2) SRPK1-Spacer alone can not form a stable complex with full length kinase and other parts of SRPK1 are also needed in addition to the spacer to affect subcellular redistribution of SRPK1.

11. C-terminal end of SRPK1 full length might be involved in SRPK1 self dimerization: H-D exchange & MALDI-TOF/TOF.

In order to study the interface of interactions in SRPK1 dimer, I performed H/D exchange on the purified SRPK1 and then analyzed the pepsin-digested fragments of SRPK1 by MALDI-TOF/TOF masspectrometry. Studying well-fragmented sequences by TOF/TOF analysis, I was surprised to find that there was much slower deuterium exchange at the C-terminal end of SRPK1 full length. This indicates that the C-terminal end is highly protected from Deuterium

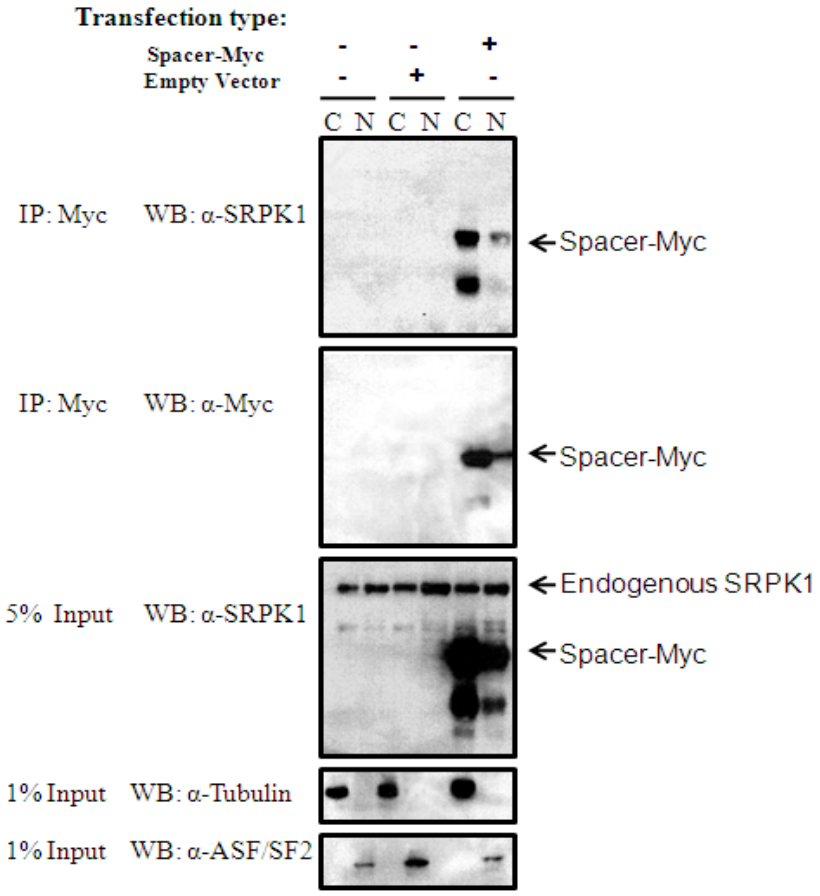

Figure 5.15: Interaction between SRP1 and Spacer. Immunoprecipitation of the Myc-Spacer was performed to observe whether interaction between the spacer and endogenous SRPK1 is observable.

exchange (Figure 5.17). X-ray structure studies of SRPK1ΔNS1 and SRPK1ΔNS3 previously show that the C-terminal segment is not seen to interact with the kinase core and its function and folding is not clear; compared to Sky1p, yeast SRPK1 counter part, which has the C-terminal end involved in stabilizing the kinase core (Ngo et al., 2005). Thus, my mass spectrometry data suggests that the C-terminal end of SRPK1 is protected and probably another element besides the spacer involved in dimerization of SRPK1.

12. SRPK1 binds to Clk/Sty

ClK/Sty is found in the nuclear speckle to regulate SR proteins in a phosphorylation-dependent manner. When Dr. Cho in my laboratory mixed the two kinases with ASF/SF2 for GST pull down assay, she found that the two kinases interact (Figure 5.18A). In order to confirm this observation *in vivo*, I transfected HA-ClK/Sty and perform immunoprecipitation (IP) to see if transfected Clk/Sty can be precipitated with endogenous SRPK1. The result showed that they do bind but the background of detection is too strong to make a definite conclusion (Figure 5.18B). However, when I co-transfected Clk/Sty with SRPK1 full length for co-IP, I found the strong interaction between SRPK1 and Clk/Sty (Figure 5.18C). On the other hand, co-IP on the co-transfected Clk/Sty and ΔS showed no interaction between these twokinases. As previously discussed that the spacer and the C-terminal end are important for the dimerization of SRPK1, here, I found that the spacer is also important for SRPK1

A)

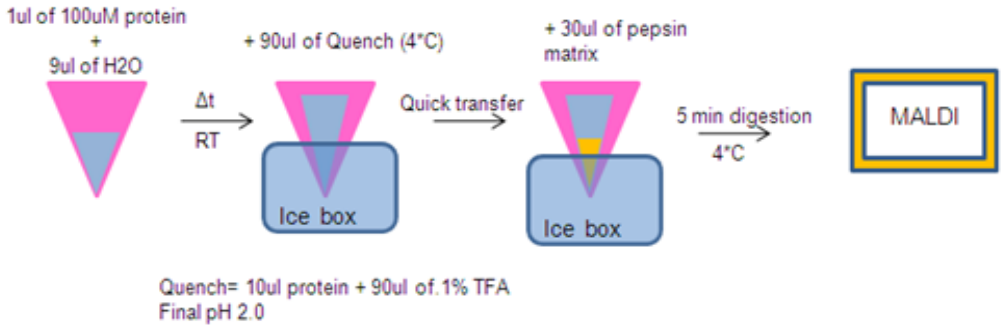

B)

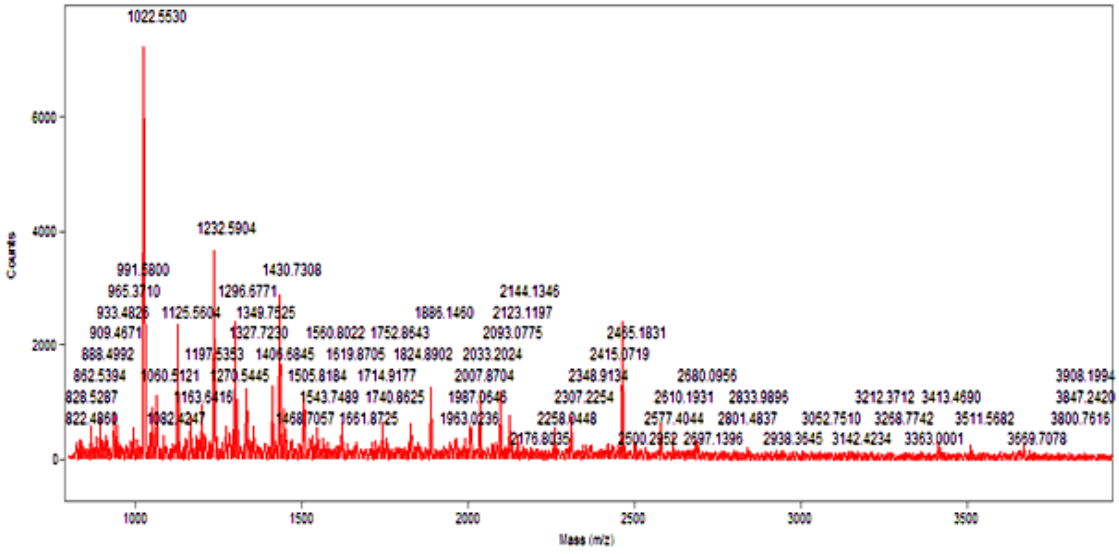

Figure 5.16: Peptide mass fingerprint of a mixture of peptic digests of full length SRPK1. A) a summary of preparation before proteo fly; in place of Deuterium exchange, the first step is D_2O instead of H_2O. B) SRPK1 is incubated at room temperature before being subjecting to the pepsin digestion. This is the proteo profile of full length of SRPK1 without Deuterium exchange.

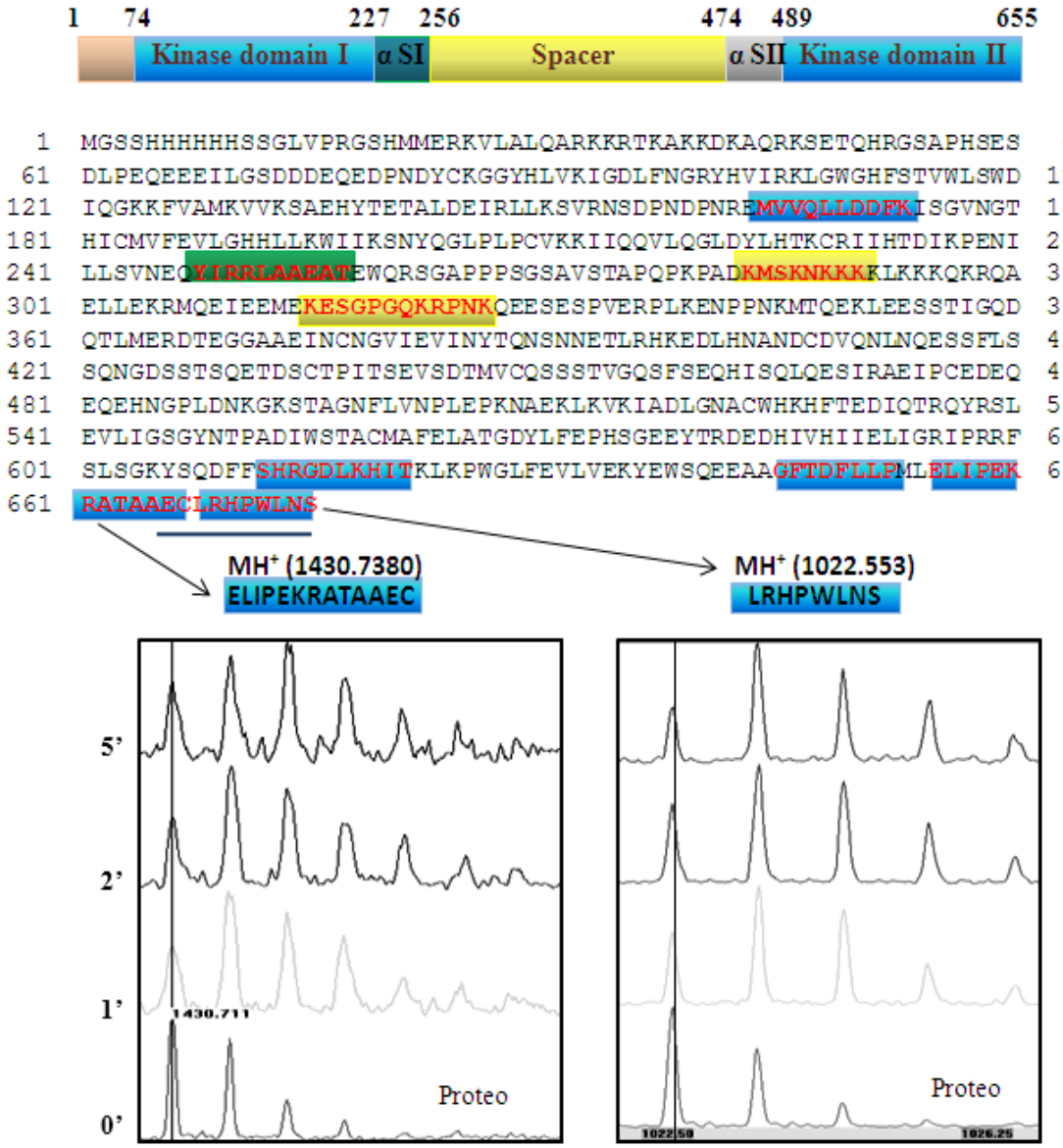

Figure 5.17: H/D exchange reveals the protected C'-end of full length SRPK1. H/D exchange was performed at room temperature and quenched at specific time-points of 1, 2, and 5 minutes before pepsin digestion. Proteo fragments at each timepoints were analyzed by MALDI for H/D exchange. Color-coded fragments in the above sequence indicates well-sequenced fragments by MALDI TOF/TOF. The result showed that while other fragments exchanged with deuterium after 1 minute , the C'-end of SRPK1 was resistant to deuterium exchange up to 5 minutes. The black underline in the above sequence indicates another possible proteo fragment identified by MALDI TOF/TOF.

to interact with other protein kinases such as Clk/Sty. Whether binding to Clk/Sty or other nuclear biomolecules help to retain the kinase in the nucleus is currently studied.

C. Discussion:

SRPK1 regulates SR protein localization and trafficking in a phosphorylation-dependent manner; it is found mostly in the cytoplasm and stays there until the signal of mitosis allows it to migrate to the nucleus. Nuclear accumulation of SRPK1 ΔS can cause SR protein to aggregate (Ding et al., 2006). What factors retain SRPK1 in the cytoplasm are not known.

By size-exclusion chromatography, we found that full length SRPK1 is a dimer and ΔS is a monomer. This data is further supported by GST-pulldown assays and co-immunoprecipitation. Thus, I established that SRPK1 is a dimer and the spacer domain mediates the dimerization of SRPK1. Since the spacer-deleted SRPK1 localizes to the nucleus and it is a monomer, this information suggests that the spacer has the localization signal that allows the full length to be a dimer as well as keeps the full length in the cytoplasm. Having proven SRPK1 as being a dimer, I hypothesized that dimerization of SRPK1 is a key mechanism in SRPK1 subcellular distribution.

However, I could not capture interaction between SRPK1 and its spacer domain by immunoprecipitation. This suggests that the spacer is not the only element for SRPK1 dimerization; other parts of the kinase in addition to the

A)

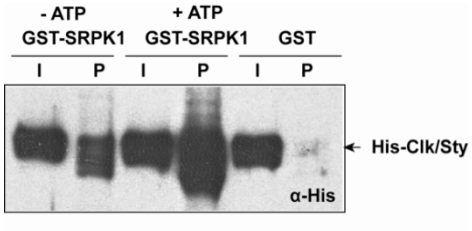

B)

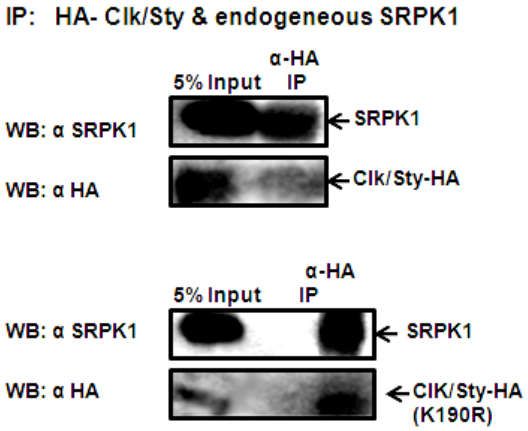

C)

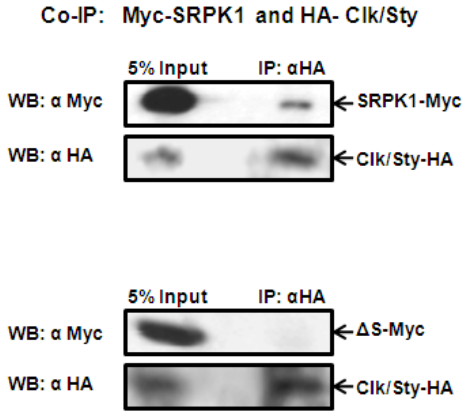

Figure 5.18: SRPK1 binds to Clk/Sty *in vivo*. A) GST-pull down assays between GST-SRPK1(fl) and His-Clk/Sty were done at two conditions, with and without ATP (The experiment was done by Dr. Cho); the experiment shows that ATP enhances the interaction between SRPK1 and Clk/Sty. B) Immuno-precipitation of transfected Clk/Sty-HA shows that some small amount of Clk/Sty interact with SRPK1. The inactive Clk/Sty interacts with SRPK1 better. C) Co-IP of CLK/STY-HA and SRPK1-Myc showed strong ineraction between Clk/Sty. However, the spacer-deleted SRPK1 ΔS does not interact with Clk/Sty.

spacer are also involved to stabilize the dimer form. The N-terminal domain (residue 1-70) can also mediate the dimerization of SRPK1 since ΔN70 shows to have apparent molecular weight less than two fold of the expected molecular weight by size exclusion chromatography. H/D exchange experiment is also employed to study the interacting interface of SRPK1 dimer and it further supports the unstructured nature of the spacer of SRPK1 which has high deuterium exchange in spacer domain. Because MALDI TOF/TOF analysis only provides a few fragmentation sequences for the spacer domain, I could not locate the interacting surface of the dimer for the time being. However, one interesting result from MALDI-TOF/TOF and H/D exchange experiments is that the amide hydrogens in the C-terminal end of SRPK1 are highly protected from the deuterium exchange. How this site is resistant to deuterium exchange after 5 minutes incubation with D_2O is not clear. Deletion analysis of the C-terminal end of SRPK1 is not advisable since the C-terminal end constitutes the second domain of the kinase fold. Since H/D exchange takes place under native conditions in which at any instant of time, the equilibrium is always toward the folded state and only a very small fraction exists in the unfolded state (Eyles et al., 2004, Mandell et al., 2005, Domon et al. 2006, Mukherjee et al., 2007), it is possible that C-terminal end of SRPK1 is protected by being involved in dimerization of SRPK1.

It is more surprising to find that SRPK1 is abundant in both nucleus and cytoplasm by fractionation assays. Many studies have shown the cytoplasmic localization of SRPK1 (Koizumi et al., 1999) and nuclear localization during the

G_2 –M phase (Ding et al., 2006). In this chapter, I have shown that SRPK1 is distributed in the nucleus and the cytoplasm to a similar extent. To test the validity of my fractionation method, I also viewed the integrity of the nucleus at the first step of cytoplasmic separation by indirection immunofluorescence. The nucleus stained by DAPI clearly retained normal physiological feature as cells without fractionation treatment. Since SRPK1 is found distributive in both nucleus and cytoplasm, I could not find the correlation between the dimerization and the subcellular location of SRPK1. Dimerization of SRPK1 is seen prominently in both nucleus and cytoplasm by co-IP experiments. Probably, SRPK remains in its dimeric form in both of the compartments. What is the role of dimerization then? At this stage it is unclear what the role of the dimer is. We observed that more degraded products of SRPK1 are in the cytoplasm by immunodetection on the fractionation contents, mainly due to more proteases found in the cytoplasm. Limited chymotrypsin analysis further supports that SRPK1 retains its dimeric state even when it is nicked *in vivo.* Thus, my experiments show that dimerization may differentially regulate the stability to SRPK1 in the cytoplasm and nucleus.

I further observed that full length SRPK1 interacts with Clk/Sty while the spacer-deleted SRPK1 fails to bind to Clk/Sty, an exclusive nuclear kinase. Hence, it is probable that the spacer can mediate SRPK1 nuclear localization by interacting with Clk/Sty.

My results on dimerization and interaction between SRPK1 and Clk/Sty suggest that the retention elements for SRPK1 can be derived from interacting

with its partners [self-dimerization] or other biomolecules such as Clk/Sty. Interactions between SRPK1 and LaminB Receptors, an integral protein in the inner nuclear membrane (Nikolakaki et al. 1996, Papoutsopoulou et al. 1999, Nikolakaki et al. 2001) has been recorded and probably another possible way to keep SRPK1 in the nucleus.

REFERENCES

Alahari, S. K., Schmidt, H., and Kaufer, N. F. (1993). The fission yeast prp4+ gene involved in pre-mRNA splicing codes for a predicted serine/threonine kinase and is essential for growth. Nucleic Acids Res *21*, 4079-4083.

Alvarez, M., Estivill, X., and de la Luna, S. (2003). DYRK1A accumulates in splicing speckles through a novel targeting signal and induces speckle disassembly. J Cell Sci *116*, 3099-3107.

Aubol, B. E., Chakrabarti, S., Ngo, J., Shaffer, J., Nolen, B., Fu, X. D., Ghosh, G., and Adams, J. A. (2003). Processive phosphorylation of alternative splicing factor/splicing factor 2. Proc Natl Acad Sci U S A *100*, 12601-12606.

Ben-David, Y., Letwin, K., Tannock, L., Bernstein, A., and Pawson, T. (1991). A mammalian protein kinase with potential for serine/threonine and tyrosine phosphorylation is related to cell cycle regulators. Embo J *10*, 317-325.

Britten, R. J., and Davidson, E. H. (1969). Gene regulation for higher cells: a theory. Science *165*, 349-357.

Casar, B., Pinto, A., and Crespo, P. (2008). Essential role of ERK dimers in the activation of cytoplasmic but not nuclear substrates by ERK-scaffold complexes. Mol Cell *31*, 708-721.

Chiara, M. D., Palandjian, L., Feld Kramer, R., and Reed, R. (1997). Evidence that U5 snRNP recognizes the 3' splice site for catalytic step II in mammals. Embo J *16*, 4746-4759.

Colwill, K., Feng, L. L., Yeakley, J. M., Gish, G. D., Caceres, J. F., Pawson, T., and Fu, X. D. (1996a). SRPK1 and Clk/Sty protein kinases show distinct substrate specificities for serine/arginine-rich splicing factors. J Biol Chem *271*, 24569-24575.

Colwill, K., Pawson, T., Andrews, B., Prasad, J., Manley, J. L., Bell, J. C., and Duncan, P. I. (1996b). The Clk/Sty protein kinase phosphorylates SR splicing factors and regulates their intranuclear distribution. Embo J *15*, 265-275.

de Graaf, K., Hekerman, P., Spelten, O., Herrmann, A., Packman, L. C., Bussow, K., Muller-Newen, G., and Becker, W. (2004). Characterization of cyclin L2, a novel cyclin with an arginine/serine-rich domain: phosphorylation by DYRK1A and colocalization with splicing factors. J Biol Chem *279*, 4612-4624.

Ding, J. H., Zhong, X. Y., Hagopian, J. C., Cruz, M. M., Ghosh, G., Feramisco, J., Adams, J. A., and Fu, X. D. (2006). Regulated cellular partitioning of SR protein-specific kinases in mammalian cells. Mol Biol Cell *17*, 876-885.

Domon, B., and Aebersold, R. (2006). Mass spectrometry and protein analysis. Science *312*, 212-217.

Duncan, P. I., Stojdl, D. F., Marius, R. M., and Bell, J. C. (1997). In vivo regulation of alternative pre-mRNA splicing by the Clk1 protein kinase. Mol Cell Biol *17*, 5996-6001.

Duncan, P. I., Stojdl, D. F., Marius, R. M., Scheit, K. H., and Bell, J. C. (1998). The Clk2 and Clk3 dual-specificity protein kinases regulate the intranuclear distribution of SR proteins and influence pre-mRNA splicing. Exp Cell Res *241*, 300-308.

Eyles, S. J., and Kaltashov, I. A. (2004). Methods to study protein dynamics and folding by mass spectrometry. Methods *34*, 88-99.

Frame, S., Cohen, P., and Biondi, R. M. (2001). A common phosphate binding site explains the unique substrate specificity of GSK3 and its inactivation by phosphorylation. Mol Cell *7*, 1321-1327.

Fu, X. D. (1995). The superfamily of arginine/serine-rich splicing factors. Rna *1*, 663-680.

Graveley, B. R. (2000). Sorting out the complexity of SR protein functions. Rna *6*, 1197-1211.

Gui, J. F., Lane, W. S., and Fu, X. D. (1994). A serine kinase regulates intracellular localization of splicing factors in the cell cycle. Nature *369*, 678-682.

Hayes, G. M., Carrigan, P. E., Beck, A. M., and Miller, L. J. (2006). Targeting the RNA splicing machinery as a novel treatment strategy for pancreatic carcinoma. Cancer Res *66*, 3819-3827.

Howell, B. W., Afar, D. E., Lew, J., Douville, E. M., Icely, P. L., Gray, D. A., and Bell, J. C. (1991). STY, a tyrosine-phosphorylating enzyme with sequence homology to serine/threonine kinases. Mol Cell Biol *11*, 568-572.

Huang, Y., and Steitz, J. A. (2005). SRprises along a messenger's journey. Mol Cell *17*, 613-615.

Huse, M., and Kuriyan, J. (2002). The conformational plasticity of protein kinases. Cell *109*, 275-282.

Jang, S. W., Yang, S. J., Ehlen, A., Dong, S., Khoury, H., Chen, J., Persson, J. L., and Ye, K. (2008). Serine/arginine protein-specific kinase 2 promotes

leukemia cell proliferation by phosphorylating acinus and regulating cyclin A1. Cancer Res *68*, 4559-4570.
Johnson, J. M., Castle, J., Garrett-Engele, P., Kan, Z., Loerch, P. M., Armour, C. D., Santos, R., Schadt, E. E., Stoughton, R., and Shoemaker, D. D. (2003). Genome-wide survey of human alternative pre-mRNA splicing with exon junction microarrays. Science *302*, 2141-2144.

Johnson, K. W., and Smith, K. A. (1991). Molecular cloning of a novel human cdc2/CDC28-like protein kinase. J Biol Chem *266*, 3402-3407.

Koizumi, J., Okamoto, Y., Onogi, H., Mayeda, A., Krainer, A. R., and Hagiwara, M. (1999). The subcellular localization of SF2/ASF is regulated by direct interaction with SR protein kinases (SRPKs). J Biol Chem *274*, 11125-11131.

Kuroyanagi, N., Onogi, H., Wakabayashi, T., and Hagiwara, M. (1998). Novel SR-protein-specific kinase, SRPK2, disassembles nuclear speckles. Biochem Biophys Res Commun *242*, 357-364.

Lavigueur, A., La Branche, H., Kornblihtt, A. R., and Chabot, B. (1993). A splicing enhancer in the human fibronectin alternate ED1 exon interacts with SR proteins and stimulates U2 snRNP binding. Genes Dev *7*, 2405-2417.

Lin, S., Xiao, R., Sun, P., Xu, X., and Fu, X. D. (2005). Dephosphorylation-dependent sorting of SR splicing factors during mRNP maturation. Mol Cell *20*, 413-425.

Ma, C. T., Velazquez-Dones, A., Hagopian, J. C., Ghosh, G., Fu, X. D., and Adams, J. A. (2008). Ordered multi-site phosphorylation of the splicing factor ASF/SF2 by SRPK1. J Mol Biol *376*, 55-68.

Mandell, J. G., Baerga-Ortiz, A., Croy, C. H., Falick, A. M., and Komives, E. A. (2005). Application of amide proton exchange mass spectrometry for the study of protein-protein interactions. Curr Protoc Protein Sci *Chapter 20*, Unit20 29.

Manley, J. L., and Tacke, R. (1996). SR proteins and splicing control. Genes Dev *10*, 1569-1579.

Marianayagam, N. J., Sunde, M., and Matthews, J. M. (2004). The power of two: protein dimerization in biology. Trends Biochem Sci *29*, 618-625.

Mathew, S., George, S. P., Wang, Y., Siddiqui, M. R., Srinivasan, K., Tan, L., and Khurana, S. (2008). Potential molecular mechanism for c-Src kinase-mediated regulation of intestinal cell migration. J Biol Chem *283*, 22709-22722.

Matthews, J. M., and Visvader, J. E. (2003). LIM-domain-binding protein 1: a multifunctional cofactor that interacts with diverse proteins. EMBO Rep *4*, 1132-1137.

Mukherjee, S., Mohan, P. M., Kuchroo, K., and Chary, K. V. (2007). Energetics of the native energy landscape of a two-domain calcium sensor protein: distinct folding features of the two domains. Biochemistry *46*, 9911-9919.

Nakagawa, O., Arnold, M., Nakagawa, M., Hamada, H., Shelton, J. M., Kusano, H., Harris, T. M., Childs, G., Campbell, K. P., Richardson, J. A.*, et al.* (2005).

Centronuclear myopathy in mice lacking a novel muscle-specific protein kinase transcriptionally regulated by MEF2. Genes Dev *19*, 2066-2077.

Ngo, J. C., Chakrabarti, S., Ding, J. H., Velazquez-Dones, A., Nolen, B., Aubol, B. E., Adams, J. A., Fu, X. D., and Ghosh, G. (2005). Interplay between SRPK and Clk/Sty kinases in phosphorylation of the splicing factor ASF/SF2 is regulated by a docking motif in ASF/SF2. Mol Cell *20*, 77-89.

Ngo, J. C., Gullingsrud, J., Giang, K., Yeh, M. J., Fu, X. D., Adams, J. A., McCammon, J. A., and Ghosh, G. (2007). SR protein kinase 1 is resilient to inactivation. Structure *15*, 123-133.

Nikolakaki, E., Kohen, R., Hartmann, A. M., Stamm, S., Georgatsou, E., and Giannakouros, T. (2001). Cloning and characterization of an alternatively spliced form of SR protein kinase 1 that interacts specifically with scaffold attachment factor-B. J Biol Chem *276*, 40175-40182.

Nikolakaki, E., Simos, G., Georgatos, S. D., and Giannakouros, T. (1996). A nuclear envelope-associated kinase phosphorylates arginine-serine motifs and modulates interactions between the lamin B receptor and other nuclear proteins. J Biol Chem *271*, 8365-8372.

Nolen, B., Yun, C. Y., Wong, C. F., McCammon, J. A., Fu, X. D., and Ghosh, G. (2001). The structure of Sky1p reveals a novel mechanism for constitutive activity. Nat Struct Biol *8*, 176-183.

Papoutsopoulou, S., Nikolakaki, E., and Giannakouros, T. (1999). SRPK1 and LBR protein kinases show identical substrate specificities. Biochem Biophys Res Commun *255*, 602-607.

Prasad, J., Colwill, K., Pawson, T., and Manley, J. L. (1999). The protein kinase Clk/Sty directly modulates SR protein activity: both hyper- and hypophosphorylation inhibit splicing. Mol Cell Biol *19*, 6991-7000.

Remenyi, A., Good, M. C., and Lim, W. A. (2006). Docking interactions in protein kinase and phosphatase networks. Curr Opin Struct Biol *16*, 676-685.

Rossi, F., Labourier, E., Forne, T., Divita, G., Derancourt, J., Riou, J. F., Antoine, E., Cathala, G., Brunel, C., and Tazi, J. (1996). Specific phosphorylation of SR proteins by mammalian DNA topoisomerase I. Nature *381*, 80-82.

Sanford, J. R., Gray, N. K., Beckmann, K., and Caceres, J. F. (2004). A novel role for shuttling SR proteins in mRNA translation. Genes Dev *18*, 755-768.

Sun, Q., Hampson, R. K., and Rottman, F. M. (1993). In vitro analysis of bovine growth hormone pre-mRNA alternative splicing. Involvement of exon sequences and trans-acting factor(s). J Biol Chem *268*, 15659-15666.

Taft, R. J., Pheasant, M., and Mattick, J. S. (2007). The relationship between non-protein-coding DNA and eukaryotic complexity. Bioessays *29*, 288-299.

Tian, M., and Maniatis, T. (1993). A splicing enhancer complex controls alternative splicing of doublesex pre-mRNA. Cell *74*, 105-114.

Velazquez-Dones, A., Hagopian, J. C., Ma, C. T., Zhong, X. Y., Zhou, H., Ghosh, G., Fu, X. D., and Adams, J. A. (2005). Mass spectrometric and kinetic analysis of ASF/SF2 phosphorylation by SRPK1 and Clk/Sty. J Biol Chem *280*, 41761-41768.

Wang, H. Y., Lin, W., Dyck, J. A., Yeakley, J. M., Songyang, Z., Cantley, L. C., and Fu, X. D. (1998). SRPK2: a differentially expressed SR protein-specific kinase involved in mediating the interaction and localization of pre-mRNA splicing factors in mammalian cells. J Cell Biol *140*, 737-750.

Wu, J. Y., and Maniatis, T. (1993). Specific interactions between proteins implicated in splice site selection and regulated alternative splicing. Cell *75*, 1061-1070.

Xiao, S. H., and Manley, J. L. (1997). Phosphorylation of the ASF/SF2 RS domain affects both protein-protein and protein-RNA interactions and is necessary for splicing. Genes Dev *11*, 334-344.

Zahler, A. M. (2001). Tale of a tail kinase. Nat Struct Biol *8*, 104-106.

Zahler, A. M., Neugebauer, K. M., Lane, W. S., and Roth, M. B. (1993). Distinct functions of SR proteins in alternative pre-mRNA splicing. Science *260*, 219-222.

Zuckerkandl, E. (2002). Why so many noncoding nucleotides? The eukaryote genome as an epigenetic machine. Genetica *115*, 105-129.

APPENDIX

Primer List

Constructs		Primer (5' to 3')
ASF/SF2 K193C	Top	TACATCCGGGTTTGTGTTGATGGGCCC
	Bottom	GGGCCCATCAACACAAACCCGGATGTA
ASF/SF2 R204C	Top	CCAAGTTATGGGTGCTCTCGATCT
	Bottom	AGATCGAGAGCACCCATAACTTGG
ASF/SF2 Y226C	Top	AGGAGTCGCAGTTGCTCCCCAAGGAGAAGC
	Bottom	GCTTCTCCTTGGGGAGCAACTGCGACTCCT
ASF/SF2 R243C	Top	CCCGTCATAGCTGTTCTCGCTCTCGTACA
	Bottom	TGTACGAGAGCGAGAACAGCTATGACGGG
SRPK1 full length in pFAST	Top	CCG GAA TTC ATGGAGCGGAAAGTGCTTGCGCTCCAGG
	Bottom	ATA AGA ATG CGG CCG CTT AGG AGT TAA GCC AAG GGT GCC GGAG
SRPK1 full length in pβActin-Flag	Top	GGAATTC CAT ATG GAGCGGAAAGTGCTTGCGCTCCAGG
	Bottom	ATA AGA ATG CGG CCG CTT AGG AGT TAA GCC AAG GGT GCC GGAG
SRPK1 full length in pGEX 4T2	Top	CCG GAA TTC ATGGAGCGGAAAGTGCTTGCGCTCCAGG
	Bottom	ATA AGA ATG CGG CCG CTT AGG AGT TAA GCC AAG GGT GCC GGAG
SRPK1-Δ56 in pβActin-Flag	Top	CTTAT GGCC ATG GAG GCC ATG GATCCTAATGATTATTGTAAAGGAGGTTATCATCTTGTG
	Bottom	ATA AGA ATG CGG CCG CTT AGG AGT TAA GCC AAG GGT GCC GGAG
SRPK1-Δ56 in pCMV-Myc	Top	GGGAATTC CAT ATG GATCCTAATGATTATTGTAAAGGAGGTTATCATCTTGTG
	Bottom	ATA AGA ATG CGG CCG CTT AGG AGT TAA GCC AAG GGT GCC GGAG
SRPK1-ΔS in pβActin-Flag	Top	GGAATTC CAT ATG GAGCGGAAAGTGCTTGCGCTCCAGG
	Bottom	ATA AGA ATG CGG CCG CTT AGG AGT TAA GCC AAG GGT GCC GGAG
SRPK1-ΔS in pCMV-Myc	Top	CTTAT GGCC ATG GAG GCC ATG GAGCGGAAAGTGCTTGCGCTCCAGG
	Bottom	ATA AGA ATG CGG CCG CTT AGG AGT TAA GCC AAG GGT GCC GGAG

SRPK1-ΔS in pET 15b	Top	GGAATTC CAT ATG GAGCGGAAAGTGCTTGCGCTCCAGG
	Bottom	GAAGGATCCCTAGGAGTTAAGCCAAGG
SRPK1-ΔNS3 in pβActin-Flag	Top	GGGAATTC CAT ATG GATCCTAATGATTATTGTAAAGGAGGTTATCATCTTGTG
	Bottom	ATA AGA ATG CGG CCG CTT AGG AGT TAA GCC AAG GGT GCC GGAG
SRPK1-ΔNS3 in pCMV-Myc	Top	CTTAT GGCC ATG GAG GCC ATG GATCCTAATGATTATTGTAAAGGAGGTTATCATCTTGTG
	Bottom	ATA AGA ATG CGG CCG CTT AGG AGT TAA GCC AAG GGT GCC GGAG
SRPK1-Spacer (225-475) in pCMV-Myc	Top	CTTAT GGCC ATG GAG GCC ATG CAGTACATTCGGAGGCTGGCTG
	Bottom	ATAGTTTAGCGGCCGCTCAGAGCTTTTCTGCATTTTTTGGCTC
SRPK1 C63S	Top	GC AGC CAT ATG GAC CCT AAT GAT TAT AGT AAA GGA GGT TAT
	Bottom	ATA ACC TCC TTT ACT ATA ATC ATT AGG GTC CAT ATG GCT GC
SRPK1 K604C	Top	ATCACGAAGCTGTGTCCTTGGGGCCTT
	Bottom	AAGGCCCCAAGGACACAGCTTCGTGAT